DETERMINATION OF A_0 FOR AXIALLY SYMMETRIC MOLECULES

Thesis for the Degree of Ph. D.

MICHIGAN STATE UNIVERSITY

THOMAS L. BARNETT

1967

This is to certify that the

thesis entitled

Determination of A_o for Axially

Symmetric Molecules

presented by

Thomas L. Barnett

has been accepted towards fulfillment
of the requirements for

Ph. D. degree in Physics

T. H. Edwards
Major professor

Date May 15, 1967

O-169

ABSTRACT

DETERMINATION OF A_o FOR AXIALLY SYMMETRIC MOLECULES

by Thomas L. Barnett

A new method is developed for determination of accurate values of the molecular constant A_o for axially symmetric molecules by simultaneously analyzing a degenerate fundamental band and its first overtone. In particular, the method is developed for a simultaneous fit of the ν_4 and $2\nu_4$ bands of a methyl halide. [$A_o = h/(8\pi^2 c I_o^A)$, where I_o^A is principal moment of inertia of the molecule about its axis of symmetry in the ground vibrational state. Accurate values of I_o^A are necessary to determine the structures of these molecules.]

The development of this new method begins from the Amat-Nielsen generalized frequency expression, listed here complete through third order and containing many fourth-order terms. This expression is then specialized to forms appropriate to individual least squares fits of the ν_4 and $2\nu_4$ bands, and simultaneous fits of the ν_4 and $2\nu_4$ bands.

This method of determining A_o has been successfully applied through least squares computer analyses to high-resolution spectra of the methyl halides and similar molecules. The excellent value of $A_o = 5.1291 \pm 0.0009$ cm^{-1} obtained for methyl bromide seems to clearly demonstrate the superiority of this method over previous methods of determining A_o. Analyses of the other molecules of the

same type (methyl iodide, methyl chloride, methyl fluoride, methyl cyanide, and singly-deuterated methane) led to less precise values of A_o, mostly because of perturbations occuring in one or both of the bands involved.

"Ground state" and "substitution" structures are calculated for methyl bromide, making use of the excellent value of A_o obtained here. The results are discussed in light of theoretical predictions by Kraitchman and Costain.

DETERMINATION OF A_o FOR AXIALLY SYMMETRIC MOLECULES

by

Thomas Leslie Barnett

A THESIS

Submitted to
Michigan State University
in partial fulfillment of the requirements
for the degree of

DOCTOR OF PHILOSOPHY

Department of Physics

1967

J46071
9-26-67

TO MY WIFE

MARY

ACKNOWLEDGMENT

I wish to thank Dr. T. H. Edwards for his encouragement and many helpful suggestions throughout my research. Our many discussions have guided and shaped this work to a large extent. I wish to also thank Dr. P. M. Parker for various discussions, as well as for an excellent course on the theoretical aspects of molecular spectroscopy. I am indebted to Dr. R. S. Schwendeman of the M. S. U. Department of Chemistry for several very valuable discussions concerning the problems involved in the determination of molecular structures. I would like to acknowledge the useful suggestions, help, advice, etc. throughout my years here from my co-workers Kent Moncur, Lewis Snyder, Mel Olman, and Don Keck. In particular, I wish to express a special appreciation to Don Keck for the numerous times he has helped me in aligning and adjusting the spectrometer, in which he often did most of the work with whatever assistance I could offer.

I am very much indebted to the M. S. U. Computer Center for the use throughout my research of their C. D. C. 3600 computer, without which none of the analyses would have been possible. And finally, I wish to expressly thank the National Science Foundation for their generous support of our research.

TABLE OF CONTENTS

LIST OF TABLES

LIST OF FIGURES

LIST OF APPENDICES

INTRODUCTION

The methyl halides have been the subject of many investigations in molecular spectroscopy over the years. Herzberg (1) summarizes the situation up to 1945, and many papers on the methyl halides can be found in the literature subsequent to this date. From the viewpoint of infrared molecular spectroscopy these molecules have many attractive features, being polyatomic (five atoms), but having a three-fold axis of symmetry (see Fig. 1). The presence of this symmetry axis greatly simplifies the theory and to some extent the experimental treatment, but introduces some problems unique to such "axially symmetric" molecules.

One persistent problem has been the difficulty in determining accurate values of the molecular parameter A_o [$= h/(8\pi^2 c I_o^A)$, where I_o^A is the principal moment of inertia of the molecule about its symmetry axis in its ground vibrational state]. It has long been known that a perpendicular band of an axially symmetric molecule cannot be solved for the value of A_o alone, but rather for only a numerical value which represents A_o plus the coefficient of a first-order vibration-rotation interaction term. Heretofore, methods of determining A_o for axially symmetric molecules have lacked precision, or directness, or both.

In this thesis a new method, permitting the determination of A_o directly from infrared spectra, is described and applied. The method consists of making a simultaneous analysis of two or more suitably related

Fig. 1 Definition of Rotational Constants

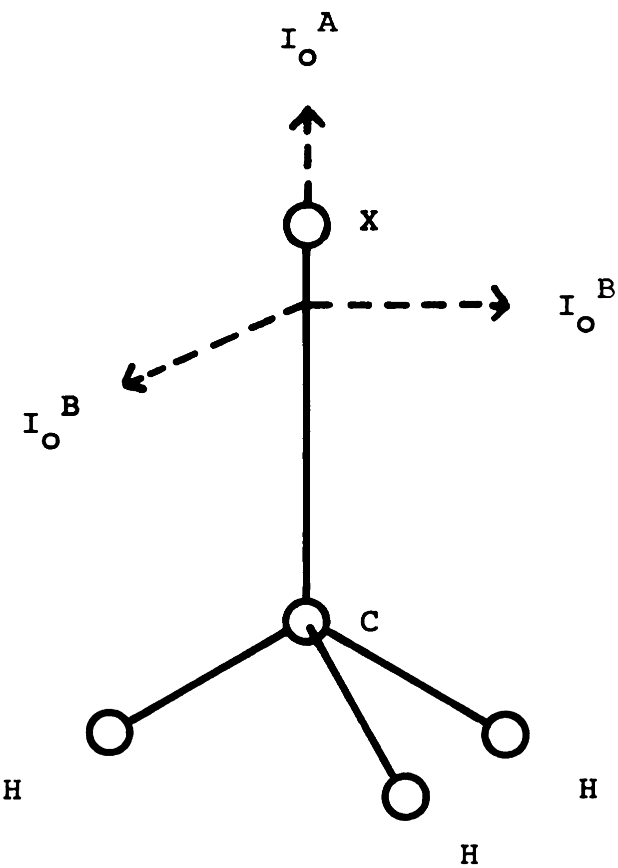

$$A_o = \frac{h}{8\pi^2 c I_o^A}, \qquad B_o = \frac{h}{8\pi^2 c I_o^B}$$

$$A_{[v]} = A_e - \sum_{s=1}^{6} \alpha_s^A (v_s + g_s/2)$$

$$B_{[v]} = B_e - \sum_{s=1}^{6} \alpha_s^B (v_s + g_s/2)$$

$$A_o = A_{[v]} \quad \text{for all } v_s = 0$$

$$B_o = B_{[v]} \quad \text{for all } v_s = 0$$

vibration-rotation bands by means of least squares fitting on a large, high speed digital computer. Chapter I contains an outline of the procedure used by Nielsen, Amat, et al. (2) in obtaining the generalized fourth-order quantum mechanical hamiltonian for a vibrating and rotating symmetric top molecule. In Chapter II the fourth-order symmetric top energies are tabulated along with the classical interpretations of the various terms. The generalized frequency expression, representing any symmetric top vibration-rotation transition from the ground vibrational state to an upper vibrational state, is also listed. In Chapter III the generalized frequency expression is specialized to single-band frequency expressions suitable for computer analyses of the methyl halide ν_4 and $2\nu_4$ bands. The reasons for A_o not being obtainable from a single-band analysis are discussed in detail. The new method of obtaining A_o is described in Chapter IV. Frequency expressions appropriate for simultaneous least squares fits of ν_4 and $2\nu_4$, and of $\nu_3+\nu_4$ and $2\nu_4$, are given.

Chapter V contains a general discussion of the least squares procedure as applied to our problems and comments upon the statistical considerations, including the use of simultaneous confidence intervals. The experimental procedures used to obtain the spectra and extract the transition frequencies are the subject of Chapter VI. Chapters VII, VIII, IX, and X contain the results of single-band and simultaneous analyses of CH_3Br, CH_3I, CH_3F, and CH_3CN respectively. Chapters XI and XII present the results of the less complete analyses of CH_3Cl and CH_3D. A general discussion is given in Chapter XIII concerning the problems involved in calculating structures from the measured values of A_o and B_o for the methyl halides. Calculations of the "ground state" and "substitution" structures for CH_3Br are reported and discussed. The Conclusion sums up the main results and attempts to assess the value of this work and the importance of obtaining accurate values of A_o for the methyl halides and other symmetric top molecules.

CHAPTER I

GENERAL FOURTH-ORDER HAMILTONIAN

The general fourth-order hamiltonian for a molecule undergoing vibration and rotation has been developed by Nielsen, Amat, et al. (2). A very brief summary of their procedure follows.

One begins with the Darling-Dennison quantum mechanical hamiltonian (3)

$$\underline{H} = 1/2[\mu^{1/4}\sum_{\alpha\beta}(P_\alpha - p_\alpha)\mu_{\alpha\beta}\mu^{-1/2}(P_\beta - p_\beta)\mu^{1/4}$$
$$+ \mu^{1/4}\sum_{s\sigma}p_{s\sigma}{}^*\mu^{-1/2}p_{s\sigma}{}^*\mu^{1/4}] + V,$$

where

α and β	range over the principal axes x, y, z;
s	ranges over the set of normal coordinates necessary to represent the normal modes of the molecule;
σ	ranges over only the components of doubly-degenerate normal coordinate pairs (σ = 1 or 2);
P_α	represents the α-component of the total angular momentum of the molecule;
p_α	represents the α-component of the internal angular momentum of the molecule;
$p_{s\sigma}{}^*$	represents the momentum conjugate to the normal coordinate $Q_{s\sigma}$;
V	represents the potential energy of the molecule;

$\mu_{\alpha\beta} = (I_{\gamma\gamma}{}'I_{\alpha\beta}{}' + I_{\alpha\gamma}{}'I_{\gamma\beta}{}')\mu;$

$\mu_{\alpha\alpha} = (I_{\beta\beta}{}'I_{\gamma\gamma}{}' - I_{\beta\gamma}{}'^2)\mu;$

$$\mu^{-1} = \begin{vmatrix} I_{xx}' & -I_{xy}' & -I_{xz}' \\ -I_{xy}' & I_{yy}' & -I_{yz}' \\ -I_{xz}' & -I_{yz}' & I_{zz}' \end{vmatrix}$$

$$I_{\alpha\alpha}' = I_{\alpha\alpha}^{e} + \sum_{s\sigma} a_{s\sigma}^{\alpha\alpha} Q_{s\sigma} + \sum_{s\sigma s'\sigma'} A'^{\alpha\alpha}_{s\sigma s'\sigma'} Q_{s\sigma} Q_{s'\sigma'};$$

$$I_{\alpha\beta}' = I_{\alpha\beta}^{e} - \sum_{s\sigma} a_{s\sigma}^{\alpha\beta} Q_{s\sigma} - \sum_{s\sigma s'\sigma'} A'^{\alpha\beta}_{s\sigma s'\sigma'} Q_{s\sigma} Q_{s'\sigma'};$$

and since the principal axes of inertia are used as the molecular base framework ($I_{\alpha\beta}^{e} = \delta_{\alpha\beta} I_{\alpha\alpha}^{e}$) then $a_{s\sigma}^{\alpha\beta}$ and $A'^{\alpha\beta}_{s\sigma s'\sigma'}$ are constants of the molecule.

The Darling-Dennison hamiltonian, $\underline{H}$, is diagonal in J (the total angular momentum is necessarily conserved) but may, in general, contain terms off-diagonal in the quantum numbers v_s, ℓ_t, and K (see Table I for definitions of these symbols). Here, only axially symmetric molecules will be considered.

This hamiltonian is not directly solvable, hence a perturbation treatment of the problem is called for. It is assumed that $\underline{H}$ can be expressed in a power series expansion, as a sum of terms of rapidly decreasing magnitude, viz.,

$$\underline{H} = H_0 + H_1 + H_2 + H_3 + H_4 + \ldots$$

with $H_0 \gg H_1 \gg H_2 \gg H_3 \gg H_4 \gg \ldots.$

In the power series expansion of the hamiltonian, $\underline{H}$, in terms of the normal coordinates, the zero-order term, H_0, is the hamiltonian representing a harmonic oscillator plus a rigid rotor. It is diagonal in all quantum numbers

Table I Definition of Symbols

v_s	-	vibrational quantum number representing s-th vibrational mode
ℓ_t	-	second vibrational quantum number for doubly-degenerate normal modes; associated with internal vibrational angular momentum
J	-	rotational quantum number associated with total angular momentum
K	-	rotational quantum number for axially symmetric molecules associated with component of total angular momentum along symmetry axis

and is exactly solvable. Classically, the higher order terms will represent corrections to the rigid rotor-harmonic oscillator model, such as centrifugal distortion due to rotation, anharmonicities in the vibrations, and interactions between vibration and rotation.

The perturbation treatment is carried out by means of contact transformations on $\underline{H}$. The first contact transformation on $\underline{H}$, yielding

$$h' = H_0 + h_1' + h_2' + h_3' + h_4' + \ldots,$$

is chosen such that H_0 is left unchanged but H_1 is diagonalized with respect to v_s in the representation which diagonalizes H_0. This leaves the hamiltonian actually diagonal through first order with respect to all the quantum numbers (J, K, v_s, and ℓ_t). In the absence of any accidental resonance, the energy of an axially symmetric molecule through third order is obtained from the diagonal elements of $(H_0 + h_1' + h_2' + h_3')$. The off-diagonal terms from h_2' will not contribute to the energy before fourth order, and those off-diagonal in h_3' will not contribute before sixth order.

The second contact transformation, operating on h', is chosen so as to leave H_0 and h_1' unchanged, while diagonalizing h_2' with respect to v_s in the zero-order representation (the representation in which H_0 is diagonal). The twice-transformed hamiltonian,

$$h^{\dagger} = H_0 + h_1' + h_2^{\dagger} + h_3^{\dagger} + h_4^{\dagger} + \ldots,$$

is diagonal in all quantum numbers through h_1', and diagonal with respect to v_s through $h_2^\dagger$, but may have terms off-diagonal with respect to K and ℓ_t in $h_2^\dagger$, and off-diagonal with respect to v_s, ℓ_t, and K in $h_3^\dagger$ and $h_4^\dagger$.

It should be sufficient, in the absence of any accidental resonance, to obtain an "exact" representation of the energy to third order from the diagonal elements of $h^\dagger$ through $h_3^\dagger$, plus a partial fourth-order contribution to the energy from the diagonal elements of $h_4^\dagger$.

CHAPTER II

SYMMETRIC TOP ENERGIES AND GENERALIZED

FREQUENCY EXPRESSION

I. Energy Expression

In general, the symmetric top energy eigenvalues are obtained by solving the secular determinant

$$\det[\ \langle J,K,\ldots,v_s,\ldots,\ell_t,\ldots|\ h^\dagger\ |J,K',\ldots,v_s',\ldots,\ell_t',\ldots\rangle - (\delta_{KK'},\ldots,\delta_{v_s v_s'},\ldots,\delta_{\ell_t \ell_t'},\ldots)\ E_{VR}\ ] = 0.$$

To obtain the energies completely through third order and partially through fourth order, one needs only the diagonal elements of $(H_0 + h_1' + h_2^\dagger + h_3^\dagger + h_4^\dagger)$, viz.,

$$\det[\ \langle J,K,\ldots,v_s,\ldots,\ell_t,\ldots|(H_0 + h_1' + h_2^\dagger + h_3^\dagger + h_4^\dagger)|J,K,\ldots,v_s,\ldots,\ell_t,\ldots\rangle - E_{VR}\ ] = 0.$$

The elements of the general twice-transformed hamiltonian, as developed by Nielsen, Amat, et al. (2), and their contributions to the symmetric top energies are given in Table II. [Note that in Table II and subsequent expressions "s" runs over all the normal modes of vibration, "n" runs over only non-degenerate modes, and "t" runs over only degenerate modes.]

Table III contains the entire energy expression for a symmetric top molecule, complete through third order and containing the diagonal fourth order contributions. The classical interpretation of each term is noted in Table IV. Actually, it is doubtful that the third and fourth order terms can be assigned any classical significance.

Table II Elements of Hamiltonian Matrix and Corresponding Energy Terms

$$H_o = 1/2\sum_\alpha P_\alpha{}^2/I_\alpha + \hbar/2\sum_{s\sigma}\lambda_s^{1/2}(p_{s\sigma}{}^2/h^2+q_{s\sigma}{}^2)$$

$$E_o = B_eJ(J+1) + (A_e-B_e)K^2 + \sum_s\omega_s(v_s+g_s/2)$$

$$h_1' = 1/2\sum_\alpha\sum_{ab}{}^\alpha(1)Y_a{}^b(q_ap_b+p_bq_a)P_\alpha$$

$$E_1 = -2A_e\sum_t\zeta_t{}^z\ell_tK$$

$$h_{21}' = \sum_{\alpha\beta\gamma\delta}{}^{\alpha\beta\gamma\delta}(2)YP_\alpha P_\beta P_\gamma P_\delta$$

$$E_{21} = -D_e^JJ^2(J+1)^2 - D_e^{JK}K^2J(J+1) - D_e^KK^4$$

$$h_{22}' = \sum_{\alpha\beta}\sum_{\substack{ab\\a\leq b}}[{}^{\alpha\beta}(2)Y^{ab}p_ap_b+{}^{\alpha\beta}(2)Y_{ab}q_aq_b]P_\alpha P_\beta$$

$$E_{22} = -\sum_s\alpha_s^B(v_s+g_s/2)J(J+1) - \sum_s(\alpha_s^A-\alpha_s^B)(v_s+g_s/2)K^2$$

$$h_{23}' = \sum_{\substack{ab\ \ cd\\a\leq b,c\leq d}}[(2)Y_{ab}^{cd}]1/2(q_aq_bp_cp_d+p_cp_dq_aq_b) + \sum_{\substack{abcd\\a\leq b\leq c\leq d}}[(2)Y_{abcd}]q_aq_bq_cq_d$$

$$E_{23} = \sum_{\substack{ss'\\s\leq s'}}x_{ss'}(v_s+g_s/2)(v_{s'}+g_{s'}/2) + \sum_{\substack{tt'\\t\leq t'}}x_{\ell_t\ell_{t'}}\ell_t\ell_{t'}$$

$$h_{31}' = \sum_{\alpha\beta\gamma}\sum_{ab}[{}^{\alpha\beta\gamma}(3)Y_a{}^b]1/2(q_ap_b+p_bq_a)P_\alpha P_\beta P_\gamma$$

$$E_{31} = \sum_t\eta_t^J\ell_tJ(J+1)K$$

$$h_{32}' = \sum_\alpha\sum_{\substack{abcd\\b\leq c\leq d}}[{}^\alpha(3)Y_a^{bcd}]1/2(q_ap_bp_cp_d+p_bp_cp_dq_a)P_\alpha + \sum_\alpha\sum_{\substack{abcd\\a\leq b\leq c}}[{}^\alpha(3)Y_{abc}^d]1/2(q_aq_bq_cp_d+p_dq_aq_bq_c)P_\alpha$$

$$E_{32} = \sum_t\eta_t^K\ell_tK^3 + \sum_t[\eta_t+\sum_s\eta_{t,s}(v_s+g_s/2)]\ell_tK$$

$$h_{41}{}^{\dagger} = \sum_{\alpha\beta\gamma\delta}\sum_{\substack{ab\\ a\leq b}}[{}^{\alpha\beta\gamma\delta}(4)Z_{ab}q_aq_b + {}^{\alpha\beta\gamma\delta}(4)Z^{ab}p_ap_b]P_\alpha P_\beta P_\gamma P_\delta$$

$$E_{41} = \sum_s \beta_s^J(v_s+g_s/2)J^2(J+1)^2 + \sum_s \beta_s^{JK}(v_s+g_s/2)K^2J(J+1) + \sum_s \beta_s^K(v_s+g_s/2)K^4$$

$$h_{42}{}^{\dagger} = \sum_{\alpha\beta}\{\sum_{\substack{abcd\\ a\leq b\leq c\leq d}}[{}^{\alpha\beta}(4)Z_{abcd}q_aq_bq_cq_d + {}^{\alpha\beta}(4)Z^{abcd}p_ap_bp_cp_d] + \sum_{\substack{abcd\\ a\leq b,c\leq d}} {}^{\alpha\beta}(4)Z_{ab}^{cd}1/2(q_aq_bp_cp_d+p_cp_dq_aq_b) + {}^{\alpha\beta}(4)Z\}P_\alpha P_\beta$$

$$E_{42} = \{\sum_{\substack{ss'\\ s\leq s'}}\gamma_{ss'}^B(v_s+g_s/2)(v_{s'}+g_{s'}/2) + \sum_{\substack{tt'\\ t\leq t'}}\gamma_{\ell_t\ell_{t'}}\ell_t\ell_{t'} + \Delta B_e\}[J(J+1)-K^2] + \{\sum_{\substack{ss'\\ s\leq s'}}\gamma_{ss'}^A(v_s+g_s/2)(v_{s'}+g_{s'}/2) + \sum_{\substack{tt'\\ t\leq t'}}\gamma_{\ell_t\ell_{t'}}\ell_t\ell_{t'} + \Delta A_e\}K^2$$

$$h_{43}{}^{\dagger} = \sum_{\alpha\beta\gamma\delta\varepsilon\eta} {}^{\alpha\beta\gamma\delta\varepsilon\eta}(4)ZP_\alpha P_\beta P_\gamma P_\delta P_\varepsilon P_\eta$$

$$E_{43} = H_o^J J^3(J+1)^3 + H_o^{JK}K^2J^2(J+1)^2 + H_o^{KJ}K^4J(J+1) + H_o^K K^6$$

$$h_{44}{}^{\dagger} = \sum_{abcdef}[(4)Z_{abcdef}q_aq_bq_cq_dq_eq_f + (4)Z^{abcdef}p_ap_bp_cp_dp_ep_f] + \sum_{abcdef}[(4)Z_{abcd}^{ef}1/2(q_aq_bq_cq_dp_ep_f+p_ep_fq_aq_bq_cq_d) + (4)Z_{ef}^{abcd}1/2(p_ap_bp_cp_dq_eq_f+q_eq_fp_ap_bp_cp_d)] + \sum_{\substack{ab\\ a\leq b}}[(4)Z_{ab}q_aq_b + (4)Z^{ab}p_ap_b]$$

$$E_{44} = \sum_{\substack{ss's''\\ s\leq s'\leq s''}} y_{ss's''}(v_s+g_s/2)(v_{s'}+g_{s'}/2)(v_{s''}+g_{s''}/2) + \sum_{\substack{stt'\\ t\leq t'}} y_{s\ell_t\ell_{t'}}(v_s+g_s/2)\ell_t\ell_{t'} + \sum_s \Delta\omega_s(v_s+g_s/2)$$

Table III Symmetric Top Energy Expression through Fourth Order

$$E_{VR} =$$

$$\sum_s \omega_s(v_s+g_s/2) + \sum_s \Delta\omega_s(v_s+g_s/2) +$$

$$\sum_{\substack{ss' \\ s\le s'}} x_{ss'}(v_s+g_s/2)(v_{s'}+g_{s'}/2) + \sum_{\substack{tt' \\ t\le t'}} x_{\ell_t\ell_{t'}}\ell_t\ell_{t'} +$$

$$\sum_{\substack{ss's'' \\ s\le s'\le s''}} y_{ss's''}(v_s+g_s/2)(v_{s'}+g_{s'}/2)(v_{s''}+g_{s''}/2) +$$

$$\sum_{\substack{stt' \\ t\le t'}} y_{s\ell_t\ell_{t'}}\ell_t\ell_{t'}(v_s+g_s/2) +$$

$$A_eK + B_e[J(J+1) - K^2] +$$

$$[-2A_e\sum_t \zeta_t^z\ell_t + \sum_t\{\eta_t + \sum_s \eta_{t,s}(v_s+g_s/2)\}\ \ell_t]\ K +$$

$$- D_e^J J^2(J+1)^2 - D_e^{JK}K^2J(J+1) - D_e^K K^4 +$$

$$- \sum_s \alpha_s^A(v_s+g_s/2)K^2 - \sum_s \alpha_s^B(v_s+g_s/2)[J(J+1) - K^2] +$$

$$\sum_t \eta_t^J\ell_tJ(J+1)K + \sum_t \eta_t^K\ell_tK^3 +$$

$$\sum_s \beta_s^J(v_s+g_s/2)J^2(J+1)^2 + \sum_s \beta_s^{JK}(v_s+g_s/2)K^2J(J+1) +$$

$$\sum_s \beta_s^K(v_s+g_s/2)K^4 +$$

$$[\sum_{\substack{ss' \\ s\le s'}} \gamma_{ss'}^A(v_s+g_s/2)(v_{s'}+g_{s'}/2) + \sum_{\substack{tt' \\ t\le t'}} \gamma_{\ell_t\ell_{t'}}\ell_t\ell_{t'}]\ K^2 +$$

$$[\sum_{\substack{ss' \\ s\le s'}} \gamma_{ss'}^B(v_s+g_s/2)(v_{s'}+g_{s'}/2)$$

$$+ \sum_{\substack{tt' \\ t\le t'}} \gamma_{\ell_t\ell_{t'}}\ell_t\ell_{t'}][J(J+1) - K^2] +$$

$$H_o^J J^3(J+1)^3 + H_o^{JK}K^2J^2(J+1)^2 + H_o^{KJ}K^4J(J+1) + H_o^K K^6$$

Table IV Classical Interpretation of Energy Terms

Constants involved in energy terms	Classical interpretation of energy term
ω_s	harmonic oscillator energy
$\Delta\omega_s$	fourth-order correction to harmonic oscillator energy having same quantum dependence
$x_{ss'}$, $x_{\ell_t \ell_{t'}}$	first-anharmonic corrections
$y_{ss's''}$, $y_{s\ell_t \ell_{t'}}$	second-anharmonic corrections
A_e, B_e	rigid rotor energies of molecule in equilibrium configuration
$A_e \sum_t \zeta_t^z$	Coriolis term - first-order term representing vibration-rotation interaction
η_t, $\eta_{t,s}$	third-order vibration-rotation correction to Coriolis term
D_e^J, D_e^{JK}, D_e^K	centrifugal distortion corrections to rigid rotor energies
α_s^A, α_s^B	corrections to A_e and B_e in excited vibrational states
η_t^J, η_t^K	third-order vibration-rotation interaction terms
β_s^J, β_s^{JK}, β_s^K	corrections to D_e^J, D_e^{JK}, and D_e^K in excited vibrational states
$\gamma_{ss'}^A$, $\gamma_{\ell_t \ell_{t'}}^A$	fourth-order corrections to α_s^A
$\gamma_{ss'}^B$, $\gamma_{\ell_t \ell_{t'}}^B$	fourth-order corrections to α_s^B
H_o^J, H_o^{JK}, H_o^{KJ}, H_o^K	fourth-order centrifugal distortion corrections

II. Frequency Expression

In our work we are solely concerned with transitions in absorption which take the molecule from a level within the rotational fine structure superimposed upon the ground vibrational state (all $v_s = 0$) to a level within the rotational fine structure superimposed upon an upper vibrational state (one or more $v_s \neq 0$). To obtain the frequency expression representing a general transition of this sort, one subtracts the energy expression representing the ground state from that representing the upper state. It is desireable to have an expression general enough to represent all possible transitions between the rotational fine structure levels superimposed upon the ground and upper vibrational states. In the ground vibrational state $v_s = 0$ for all "s"; $\ell_t = 0$ for all values of "t" since the ground state is non-degenerate; J and K represent the ground state quantum numbers associated with the total angular momentum and its component along the symmetry axis respectively. In the upper vibrational state one or more of the v_s are non-zero; the ℓ_t corresponding to those v_s which are non-zero for degenerate modes are themselves non-zero; $J + \Delta J$ and $K + \Delta K$ represent the upper state values of the J and K quantum numbers.

Table V lists the generalized frequency expression representing a general vibration-rotation transition from the ground state to any upper vibrational state, assuming negligible inversion probability and the absence of

Table V Amat-Nielsen Generalized Frequency Expression

$$(v_n, v_{n+1}, \ldots, v_t, \Delta\ell_t, v_{t+1}, \Delta\ell_{t+1}, \ldots)^{\Delta K}\Delta J_K(J) =$$

$$\sum_s (\omega_s + \Delta\omega_s) v_s +$$

$$\sum_s \sum_{s'}{}_{s \le s'} x_{ss'} [(v_s+g_s/2)(v_{s'}+g_{s'}/2) - g_s g_{s'}/4] +$$

$$\sum_t \sum_{t'}{}_{t \le t'} x_{\ell_t \ell_{t'}} \Delta\ell_t \Delta\ell_{t'} +$$

$$\sum_s \sum_{s'} \sum_{s''}{}_{s \le s' \le s''} y_{ss's''} [(v_s+g_s/2)(v_{s'}+g_{s'}/2)(v_{s''}+g_{s''}/2) - g_s g_{s'} g_{s''}/8] +$$

$$\sum_s \sum_t \sum_{t'}{}_{t \le t'} y_{s\ell_t \ell_{t'}} (v_s+g_s/2) \Delta\ell_t \Delta\ell_{t'} +$$

$$A_o [(K+\Delta K)^2 - K^2] +$$

$$B_o [(J+\Delta J)(J+1+\Delta J) - J(J+1) - (K+\Delta K)^2 + K^2] +$$

$$[-2A_e \sum_t \zeta_t{}^z \Delta\ell_t + \sum_t \{\eta_t + \sum_s \eta_{ts}(v_s+g_s/2)\}\Delta\ell_t][K+\Delta K] +$$

$$-D_o{}^J [(J+\Delta J)^2 (J+1+\Delta J)^2 - J^2 (J+1)^2] +$$

$$-D_o^{JK} [(K+\Delta K)^2 (J+\Delta J)(J+1+\Delta J) - K^2 J(J+1)] +$$

$$-D_o{}^K [(K+\Delta K)^4 - K^4] +$$

$$[-\sum_s \alpha_s{}^A v_s + \sum_s \sum_{s'}{}_{s \le s'} \gamma_{ss'}^A (v_s v_{s'} + v_s g_{s'}/2 + v_{s'} g_s/2)$$
$$+ \sum_t \sum_{t'}{}_{t \le t'} \gamma_{\ell_t \ell_{t'}}^A \Delta\ell_t \Delta\ell_{t'}] [(K+\Delta K)^2] +$$

$$[-\sum_s \alpha_s{}^B v_s + \sum_s \sum_{s'}{}_{s \le s'} \gamma_{ss'}^B (v_s v_{s'} + v_s g_{s'}/2 + v_{s'} g_s/2)$$
$$+ \sum_t \sum_{t'}{}_{t \le t'} \gamma_{\ell_t \ell_{t'}}^B \Delta\ell_t \Delta\ell_{t'}] [(J+\Delta J)(J+1+\Delta J) - (K+\Delta K)^2] +$$

$$\sum_t \eta_t{}^J \Delta\ell_t [(K+\Delta K)(J+\Delta J)(J+1+\Delta J)] +$$

$$\sum_t \eta_t{}^K \Delta\ell_t [(K+\Delta K)^3] +$$

$$\sum_s \beta_s{}^J v_s [(J+\Delta J)^2 (J+1+\Delta J)^2] +$$

$$\sum_s \beta_s^{JK} v_s [(K+\Delta K)^2 (J+\Delta J)(J+1+\Delta J)] +$$

$$\sum_s \beta_s{}^K v_s [(K+\Delta K)^4] +$$

$$H_o^{J}[(J+\Delta J)^3(J+1+\Delta J)^3-J^3(J+1)^3] +$$
$$H_o^{JK}[(K+\Delta K)^2(J+\Delta J)^2(J+1+\Delta J)^2-K^2J^2(J+1)^2] +$$
$$H_o^{KJ}[(K+\Delta K)^4(J+\Delta J)(J+1+\Delta J)-K^4J(J+1)] +$$
$$H_o^{K}[(K+\Delta K)^6-K^6]$$

any accidental resonances. With the proper selection rules this expression should represent vibration-rotation spectra, Raman spectra, electric field-induced spectra, microwave spectra, etc. Note the following substitutions:

$$A_o = A_e - \sum_s \alpha_s^A (g_s/2) + \sum_{s \leq s'} \gamma_{ss'}^A (g_s g_{s'}/4),$$

$$B_o = B_e - \sum_s \alpha_s^B (g_s/2) + \sum_{s \leq s'} \gamma_{ss'}^B (g_s g_{s'}/4),$$

$$D_o^m = D_e^m - \sum_s \beta_s^m (g_s/2), \quad m = J,\ JK,\ K,$$

which were made by way of grouping together all the terms which have exactly the same quantum dependences.

A diagram, taken from Ref. (1), of the observed frequencies of the various methyl halide fundamentals is shown in Fig. 2. The band $2\nu_5$ is also shown as a dashed line because this band is in Fermi resonance with ν_1. The unperturbed position of ν_1 would be between the indicated positions of $2\nu_5$ and ν_1.

The atomic motions involved in the normal vibrations of a CH_3X molecule are indicated in Fig. 3. This diagram is also taken from Ref. (1).

Schematically, one may consider that superimposed upon the vibrational energy levels are rotational energy levels - rigid rotor levels corrected by higher order effects. Splendid diagrams are given on p. 28 of Ref. (1) for non-degenerate states and on p. 404 of Ref. (1) for degenerate states split by the Coriolis interaction.

A vibration-rotation band may be represented schematically as the set of allowed transitions from the

Fig. 2 Methyl Halide Fundamental Vibration Frequencies

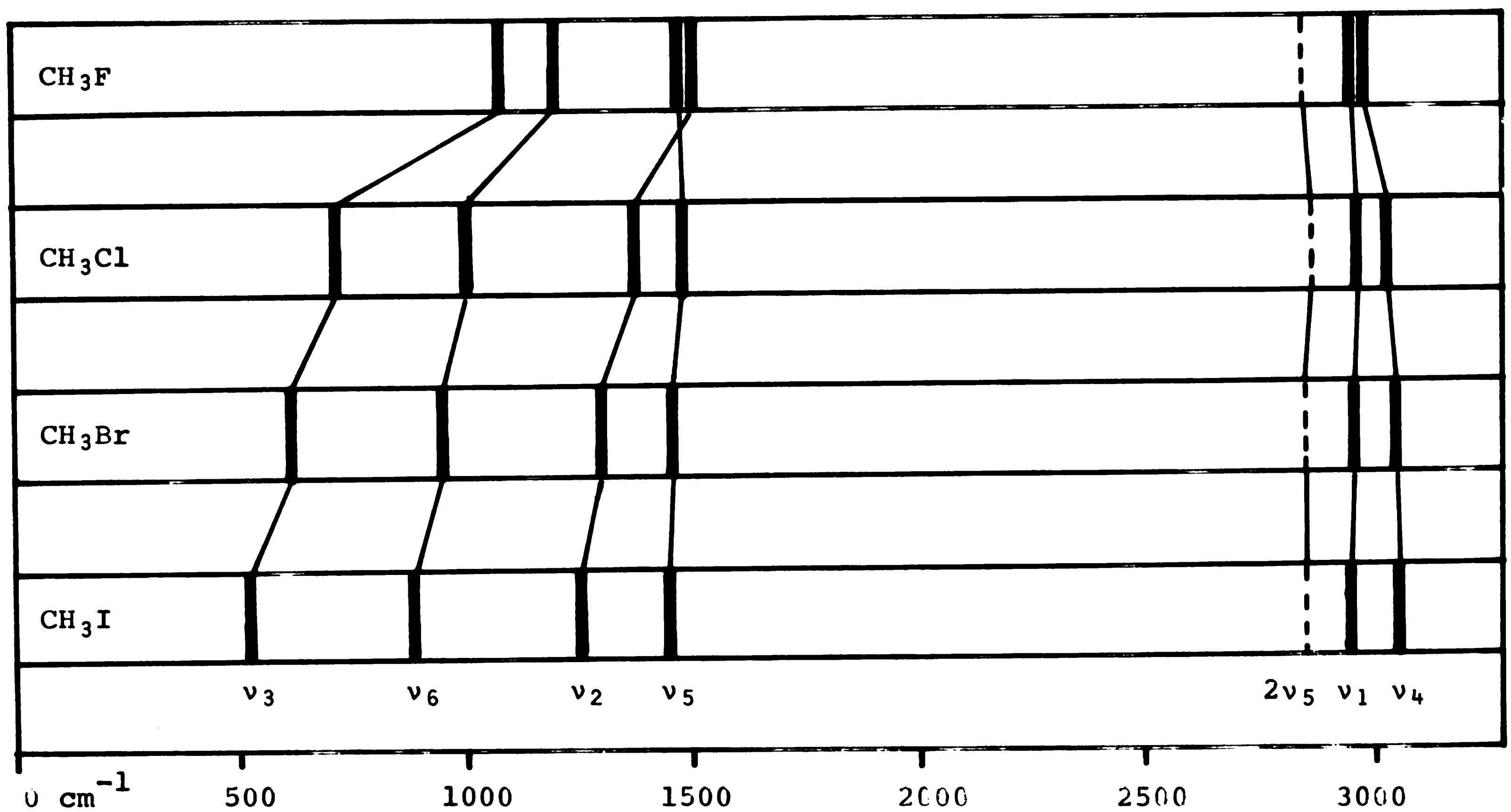

Fig. 3 CH_3X Normal Modes

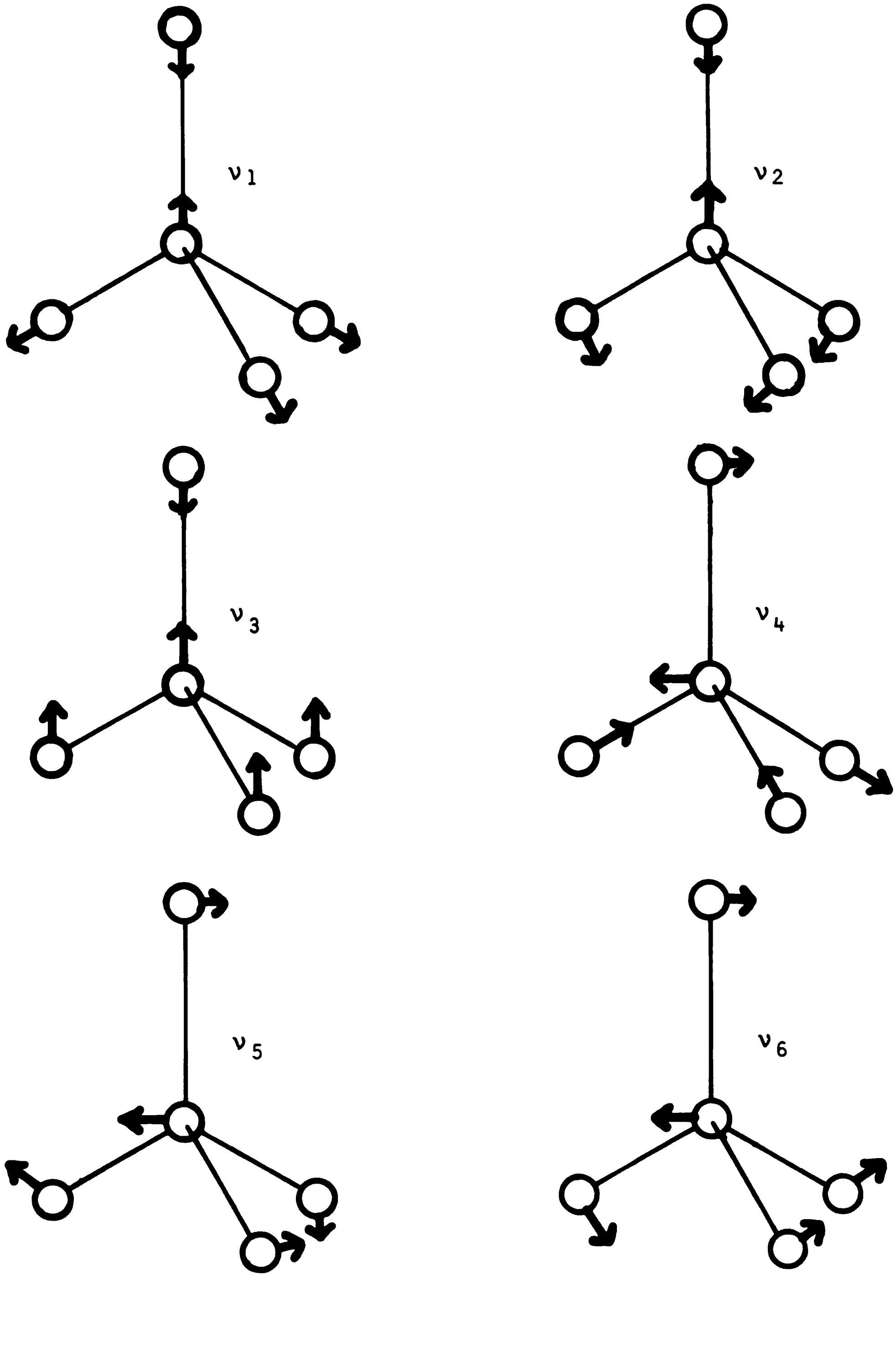

rotational levels within the ground vibrational state up to rotational levels within the upper vibrational state. A parallel band consists of transitions from a non-degenerate ground state to a non-degenerate upper state; a perpendicular band consists of transitions from a non-degenerate ground state to a degenerate upper state.

Infrared vibration-rotation spectra are described by the electric dipole selection rules on Δv_s, $\Delta \ell_t$, ΔJ, and ΔK. For a pure harmonic oscillator the allowed electric dipole selection rule on the vibrational quantum number is $\Delta v_s = \pm 1$. The presence of electrical or mechanical anharmonicity permits, in general, $\Delta v_s = \pm 1, \pm 2, \pm 3, \ldots$, but with greatly reduced intensity relative to the fundamentals. Of course, for transitions in absorption only positive Δv_s exist. The selection rule on $\Delta \ell_t$ for a particular band can be obtained from Amat's Rule (4). Discussion of this will be deferred until Chapter III. We shall merely note here that for a parallel band $\Delta \ell_t = 0$, and for a perpendicular band $\Delta \ell \neq 0$ in general. The dipole selection rules on ΔJ and ΔK are:

Parallel band

$\Delta K = 0$

$\Delta J = 0, \pm 1$ ($\Delta J \neq 0$ when $J = 0$);

Perpendicular band

$\Delta K = \pm 1$

$\Delta J = 0, \pm 1$.

CHAPTER III

SINGLE-BAND FREQUENCY EXPRESSION

Let us consider the analysis of a single band of a methyl halide molecule. Analyzing a band consists of determining the best set of estimators of the coefficients involved in the frequency expression appropriate to that band. These coefficients are molecular constants or linear combinations of molecular constants. This can be done in a relatively crude manner with graphs [see Ref. (5)], or in a much more sophisticated and precise manner by means of a least squares computer fit.

In general, the frequency expression listed in Table V cannot be used directly in the analysis of a band. A primary requirement in either a graphical or least squares analysis is that all the terms in the frequency expression be linearly independent of one another. This means that if X_1, X_2, ..., X_n represent the quantum dependences of the various terms, it must <u>not</u> be possible to represent any X_i in the form

$$X_i = aX_1 + bX_2 + \ldots + eX_{i-1} + fX_{i+1} + \ldots + mX_n.$$

Consider the specific case of the ν_4 band of a methyl halide molecule. This represents a degenerate carbon-hydrogen stretching mode. The methyl halide molecule has six normal modes of vibration, of which three, ν_1, ν_2, and ν_3, are non-degenerate, and three, ν_4, ν_5, and ν_6, are degenerate. In the case of ν_4, $\Delta v_4 = 1$ and $\Delta v_i = 0$ for $i = 1, 2, 3, 5,$ and 6. The ΔK and ΔJ selection rules are those appropriate to a perpendicular band, viz.,

$\Delta K = \pm 1,$

$\Delta J = 0, \pm 1.$

The selection rule on $\Delta\ell_4$ is given by Amat's Rule as described below. In general, Amat's Rule places restrictions on the allowed values of $\Delta\ell_4$ such that

$$\Delta K - \sum_t \Delta\ell_t = \pm 3p, \quad p = 0, 1, 2, \ldots.$$

There is a restriction on the possible values of ℓ_t in the state v_t,

$$|\ \ell_t\ | = v_t, v_t \pm 2, \ldots,$$

or, since $\Delta v_t = v_t$ and $\Delta\ell_t = \ell_t$ for a transition originating in the ground vibrational state,

$$|\ \Delta\ell_t\ | = \Delta v_t, \Delta v_t \pm 2, \ldots.$$

Since $\Delta v_4 = 1$ is the only non-zero Δv_s for ν_4, one has the two conditions on $\Delta\ell_4$:

1. $\Delta K - \Delta\ell_4 = \pm 3p, \quad p = 0, 1, 2, \ldots$
2. $|\ \Delta\ell_4\ | = 1, 3, \ldots.$

Since $\Delta K = \pm 1$, the only solution possible is

$$\pm 1 - \Delta\ell_4 = 0 \quad \text{or}$$

$$\Delta\ell_4 = \Delta K.$$

When $\Delta\ell_4 = \Delta K$ is substituted into the frequency expression obtained by specializing Table V to the ν_4 band, several terms are found to be linearly dependent. In particular, the Coriolis term splits into a constant term plus a term with the same quantum dependence as A_o, viz.,

$$[-2A_e\zeta_4^z + \eta_4 + 2\eta_{44}][\Delta\ell_4(K + \Delta K)] =$$

$$[-2A_e\zeta_4{}^z + \eta_4 + 2\eta_{44}][\Delta K(K + \Delta K)] =$$
$$[-A_e\zeta_4{}^z + 1/2\ \eta_4 + \eta_{44}][(\Delta K)^2]$$
$$+ [-A_e\zeta_4{}^z + 1/2\ \eta_4 + \eta_{44}][(K + \Delta K)^2 - K^2].$$

In the same manner the $\eta_4{}^K$ term, with quantum dependence $[\Delta\ell_4(K + \Delta K)^3]$, is linearly dependent upon several other terms and is treated in a similar manner, viz.,

$$\eta_4{}^K[\Delta\ell_4(K + \Delta K)^3] = \eta_4{}^K[\Delta K(K + \Delta K)^3] =$$
$$\eta_4{}^K[\Delta K(K^3 + 3K^2\Delta K + 3K\Delta K^2 + \Delta K^3)] =$$
$$1/4\ \eta_4{}^K[(K + \Delta K)^4 - K^4] \quad \text{same quantum dep. as } -D_o{}^K$$
$$+ 3/2\ \eta_4{}^K[(K + \Delta K)^2] \quad \text{same quantum dep. as } -\alpha_4{}^A$$
$$- 1/2\ \eta_4{}^K[(K + \Delta K)^2 - K^2] \quad \text{same quantum dep. as } A_o$$
$$- 1/4\ \eta_4{}^K \quad \text{same quantum dep. as } \nu_o.$$

The final frequency expression, suitable for a least squares computer fit of ν_4 (with $k = 1$), is given in Table VI. Note, in particular, that A_o cannot be obtained alone from such a single-band analysis. The sum $(A_o - A_e\zeta_4{}^z + 1/2\eta_4 + \eta_{44} - 1/2\eta_4{}^K)$ is obtained as the coefficient of $[(K + \Delta K)^2 - K^2]$. The third-order η terms are probably quite small, however the Coriolis coefficient, $A_e\zeta_4{}^z$, is certainly not negligible compared to A_o. Unless $\zeta_4{}^z$ can be estimated accurately by some other means, such as calculating it theoretically, the value of A_o cannot be accurately determined. A similar thing happens in the case of several other terms for which the estimator of the coefficient obtained from a least squares fit represents a sum of several individual molecular parameters.

It should be noted that the expression in Table VI

Table VI Frequency Expression Suitable for Single-Band Fit of ν_4 or $2\nu_4$.

$$
\begin{aligned}
{}^{\Delta K}\Delta J_K(J) - \{ & B_o[(J+\Delta J)(J+1+\Delta J)-J(J+1) - (K+\Delta K)^2+K^2] \\
& -D_o^{\,J}[(J+\Delta J)^2(J+1+\Delta J)^2-J^2(J+1)^2] \\
& -D_o^{JK}[(K+\Delta K)^2(J+\Delta J)(J+1+\Delta J)-K^2J(J+1)]\} \quad =
\end{aligned}
$$

$$
\begin{bmatrix} \nu_o(\nu_4) & \text{or} \\ \nu_o(2\nu_4 \perp) & \text{or} \\ \nu_o(2\nu_4 \parallel) & \end{bmatrix} \text{as appropriate} - [k(\Delta K)^2(A_e\zeta_4^{\,z}-1/4\eta_4^{\,K})] +
$$

$$
\begin{aligned}
& [A_o - kA_e\zeta_4^{\,z} - 1/2k\eta_4^{\,K}][(K+\Delta K)^2-K^2] + \\
& [-D_o^{\,K} - 1/4k\eta_4^{\,K}][(K+\Delta K)^4-K^4] + \\
& [-\alpha_4^{\,A} + 3/2k\eta_4^{\,K}][(\Delta v_4)(K+\Delta K)^2] + \\
& [-\alpha_4^{\,B}][(\Delta v_4)\{(J+\Delta J)(J+1+\Delta J) - (K+\Delta K)^2\}] + \\
& [\eta_4^{\,J}][(k\Delta K)(K+\Delta K)(J+\Delta J)(J+1+\Delta J)] + \\
& [\beta_4^{\,J}][(\Delta v_4)(J+\Delta J)^2(J+1+\Delta J)^2] + \\
& [\beta_4^{JK}][(\Delta v_4)(K+\Delta K)^2(J+\Delta J)(J+1+\Delta J)] + \\
& [\beta_4^{\,K}][(\Delta v_4)(K+\Delta K)^4] + \\
& [H_o^{\,J}][(J+\Delta J)^3(J+1+\Delta J)^3-J^3(J+1)^3] + \\
& [H_o^{JK}][(K+\Delta K)^2(J+\Delta J)^2(J+1+\Delta J)^2-K^2J^2(J+1)^2] + \\
& [H_o^{KJ}][(K+\Delta K)^4(J+\Delta J)(J+1+\Delta J)-K^4J(J+1)] + \\
& [H_o^{\,K}][(K+\Delta K)^6-K^6]
\end{aligned}
$$

Set $k = 1$ for the ν_4 band, $k = -2$ for the $2\nu_4$ band.

---

is only one of several equivalent frequency expressions which could be written, even after the linear dependences have been removed. It happens to be the one most convenient for our purposes.

Consider now a single-band fit of the $2\nu_4$ band of a methyl halide. In this case the selection rule on $\Delta\ell_4$ is obtained from Amat's Rule in the following manner. For $2\nu_4$, $\Delta v_4 = 2$ and $\Delta v_i = 0$ for i = 1, 2, 3, 5, and 6. The two conditions on $\Delta\ell_4$ are

1. $\Delta K - \Delta\ell_4 = \pm 3p, \quad p = 0, 1, 2, \ldots,$
2. $|\Delta\ell_4| = 0, 2, 4, \ldots.$

Two solutions are possible, a perpendicular component ($\Delta K = \pm 1$):

$$\pm 1 - \Delta\ell_4 = \pm 3 \quad (p = 1) \quad \text{or}$$

$$-\Delta\ell_4 = \pm 2,$$

and a parallel component ($\Delta K = 0$):

$$0 - \Delta\ell_4 = 0 \quad (p = 0) \quad \text{or}$$

$$\Delta\ell_4 = 0.$$

Both of these can be represented as a general selection rule for the $2\nu_4$ band:

$$\Delta\ell_4 = -2\Delta K.$$

In the same manner as for ν_4, the Coriolis term splits into a constant term plus a term with the same quantum dependence as A_o, viz.,

$$[-2A_e\zeta_4{}^z + \eta_4 + 3\eta_{44}][\Delta\ell_4(K + \Delta K)] =$$

$$[-2A_e\zeta_4{}^z + \eta_4 + 3\eta_{44}][-2\Delta K(K + \Delta K)] =$$

$$[2A_e\zeta_4{}^z - \eta_4 - 3\eta_{44}][(\Delta K)^2]$$

$$+ [2A_e\zeta_4{}^z - \eta_4 - 3\eta_{44}][(K + \Delta K)^2 - K^2].$$

Similarly for $\eta_4{}^K$:

$$\eta_4{}^K[\Delta\ell_4(K + \Delta K)^3] \;=\; -2\eta_4{}^K[\Delta K(K + \Delta K)^3] \;=$$

$- 1/2\ \eta_4{}^K[(K + \Delta K)^4 - K^4]$ same quantum dep. as $-D_o{}^K$

$- 3\ \eta_4{}^K[(K + \Delta K)^2]$ same quantum dep. as $-2\alpha_4{}^A$

$+ \eta_4{}^K[(K + \Delta K)^2 - K^2]$ same quantum dep. as A_o

$+ 1/2\ \eta_4{}^K$ same quantum dep. as ν_o.

The frequency expression appropriate for a single-band fit of $2\nu_4$ (with $k = -2$) is listed in Table VI. The quantity A_o cannot be obtained alone, but rather only the linear combination $(A_o + 2A_e\zeta_4{}^z - \eta_4 - 3\eta_{44} + \eta_4{}^K)$.

CHAPTER IV

SIMULTANEOUS FREQUENCY EXPRESSION

It was pointed out in Chapter III that for any single band, the fact that $\Delta\ell_t$ is proportional to ΔK means that the Coriolis term is necessarily linearly dependent upon the A_o term, so that one can obtain from a least squares fit only a numerical value for a linear combination of the two coefficients. The key to obtaining accurate values of the individual molecular constants, however, is the fact that the constant of proportionality for overtone bands is different from that for fundamentals, viz., $\Delta\ell_4 = \Delta K$ for ν_4 and $\Delta\ell_4 = -2\Delta K$ for $2\nu_4$. If the transition frequencies of ν_4 and $2\nu_4$ are fit simultaneously to an expression general enough to represent both bands, the fact that $\Delta\ell_4$ takes on different values for the two bands introduces an extra variable into the quantum dependence of the Coriolis term. In other words, the term $[(K + \Delta K)^2 - K^2]$ is now linearly independent of $[(\Delta\ell_4)(K + \Delta K)]$. A least squares simultaneous fit of the data of the two bands will yield individual values of A_o and the Coriolis coefficient. Similarly, $\eta_4{}^K$ is also linearly independent of the other terms in this case.

Table VII gives a frequency expression suitable for a simultaneous least squares fit of ν_4 and $2\nu_4$. It is assumed that values of Δv_4 and $\Delta\ell_4$ will be input for each transition, along with ΔK, ΔJ, K, J, the frequency of the transition, and the weight assigned to it. Again, it should

Table VII Frequency Expression for Simultaneous Fit of ν_4 and $2\nu_4$.

$$
\begin{aligned}
{}^{\Delta K}\Delta J_K(J) - \{ & B_o[(J+\Delta J)(J+1+\Delta J)-J(J+1)-(K+\Delta K)^2+K^2] \\
& -D_o^J[(J+\Delta J)^2(J+1+\Delta J)^2-J^2(J+1)^2] \\
& -D_o^{JK}[(K+\Delta K)^2(J+\Delta J)(J+1+\Delta J)-K^2J(J+1)]\} \quad =
\end{aligned}
$$

$$
\begin{bmatrix} \nu_o(\nu_4) & \text{or} \\ \nu_o(2\nu_4 \perp) & \text{or} \\ \nu_o(2\nu_4 \parallel) & \end{bmatrix} \quad \text{as appropriate} \quad +
$$

$$
\begin{aligned}
& [A_o][(K+\Delta K)^2-K^2] \; + \\
& [-2A_e\zeta_4{}^z+\eta_4][(\Delta\ell_4)(K+\Delta K)] \; + \\
& [-D_o{}^K][(K+\Delta K)^4-K^4] \; + \\
& [-\alpha_4{}^A][(\Delta v_4)(K+\Delta K)^2] \; + \\
& [\eta_4{}^K][(\Delta\ell_4)(K+\Delta K)^3] \; + \\
& [\beta_4{}^K][(\Delta v_4)(K+\Delta K)^4] \; + \\
& [H_o{}^K][(K+\Delta K)^6-K^6] \; + \\
& [-\alpha_4{}^B][(\Delta v_4)\{(J+\Delta J)(J+1+\Delta J)-(K+\Delta K)^2\}] \; + \\
& [\eta_4{}^J][(\Delta\ell_4)(K+\Delta K)(J+\Delta J)(J+1+\Delta J)] \; + \\
& [\beta_4{}^J][(\Delta v_4)(J+\Delta J)^2(J+1+\Delta J)^2] \; + \\
& [\beta_4^{JK}][(\Delta v_4)(K+\Delta K)^2(J+\Delta J)(J+1+\Delta J)] \; + \\
& [H_o{}^J][(J+\Delta J)^3(J+1+\Delta J)^3-J^3(J+1)^3] \; + \\
& [H_o^{JK}][(K+\Delta K)^2(J+\Delta J)^2(J+1+\Delta J)^2-K^2J^2(J+1)^2] \; + \\
& [H_o^{KJ}][(K+\Delta K)^4(J+\Delta J)(J+1+\Delta J)-K^4J(J+1)] \; + \\
& \qquad [\eta_{44}][(\Delta v_4+1)(\Delta\ell_4)(K+\Delta K)] \; + \\
& \qquad [\gamma_{44}^A][(\Delta v_4)(\Delta v_4+2)(K+\Delta K)^2] \; + \\
& \qquad [\gamma_{\ell_4\ell_4}^A][(\Delta\ell_4)^2(K+\Delta K)^2] \; + \\
& \qquad [\gamma_{44}^B][(\Delta v_4)(\Delta v_4+2)\{(J+\Delta J)(J+1+\Delta J)-(K+\Delta K)^2\}] \; + \\
& \qquad [\gamma_{\ell_4\ell_4}^B][(\Delta\ell_4)^2\{(J+\Delta J)(J+1+\Delta J)-(K+\Delta K)^2\}]
\end{aligned}
$$

be noted that this is not the only possible form of a valid expression. It happens to be the one most convenient for us, however, and it is the one which was used in the analyses.

It may be noted that it would be also possible to obtain a value of A_o and the Coriolis coefficient by analyzing ν_4 and $2\nu_4$ individually and then combining the results. From a least squares fit of ν_4 to the formula of Table VI (with k = 1) one obtains a numerical value for the quantity $(A_o - A_e\zeta_4{}^z + \ldots)$, and from a fit of $2\nu_4$ to the formula of Table VI (with k = -2), a numerical value of $(A_o + 2A_e\zeta_4{}^z + \ldots)$. Then if the η terms are neglected, one can solve the two equations for values of A_o and $A_e\zeta_4{}^z$.

However, the method of simultaneously analyzing ν_4 and $2\nu_4$ is definitely superior to that of analyzing the two bands individually and combining the results. First, confidence intervals (statistical limits of accuracy; explained in detail later) are obtained for the individual quantities A_o and $(A_e\zeta_4{}^z - 1/2\eta_4)$ from a simultaneous fit. From individual fits of ν_4 and $2\nu_4$, confidence intervals are obtained for the quantities $(A_o - A_e\zeta_4{}^z + \ldots)$ and $(A_o + 2A_e\zeta_4{}^z + \ldots)$ respectively. It is not at all apparent how one goes about determining from these the confidence intervals on the individual quantities. Secondly, the simultaneous analysis method is superior because of the mathematical nature of the least squares fitting process. A least squares fit will obtain the best possible fit of the given data to the given equation. The "best" fit is defined as that fit (set of estimators of the coefficients) for which the weighted sum of the squares of the deviations, (ν_{obs} - ν_{calc}), is a minimum. This does not necessarily ensure the "physically best" fit, however. If the data is less than perfect, the fit may yield a biased set of estimators. The advantage of the simultaneous fit is that the computer is forced to select the one set of estimators of the coefficients which best represents both bands. Single-band analyses yield a set of estimators of the appropriate coefficients for each band. In the case of one band being perturbed, those estimators which are directly comparable between the bands, e. g., α_4^B, may be considerably different. Such a discrepancy is obvious only for those coefficients which are the same for both bands, but some or all of the rest are likely to be adversely affected since the entire set of estimators is adjusted in obtaining the "best" fit. This is obviously a bad state of affairs since the molecular parameters are constants of the molecule and not merely of the band.

If both bands are relatively unperturbed a simultaneous fit is the best procedure because individual values of A_o and $(A_e\zeta_4^z - 1/2\eta_4)$ are obtained, the single set of estimators of the coefficients is obtained from about twice the amount of data involved in a single-band fit, and confidence intervals are obtained for the individual molecular constants. The values of the molecular constants thus obtained should be closer to the "true" values than those of either band alone. If one band is considerably perturbed it may be desireable to determine the values of some of the coefficients from a single-band fit of the good band. These coefficients would then be held constant in the simultaneous fit. A simultaneous fit of the good band plus the "unperturbed" parts of the poorer one should yield the best estimate of A_o and the other parameters available from the data. If, say, ν_4 were the good band and $2\nu_4$ the perturbed band, single-band fits would yield a very good value of $(A_o - A_e\zeta_4^z + \ldots)$ and probably a quite poor value of $(A_o + 2A_e\zeta_4^z + \ldots)$. A value of A_o determined from these would be rather untrustworthy. In a simultaneous fit, however, the data of the good band, which is predominant both in quantity and statistical weight, is likely to "hold in line" the unperturbed data of the poorer band and force it to fit reasonably well. The value of A_o obtained from such a fit, although somewhat uncertain in precision, is probably the best that can be obtained from the given data.

All too often it happens that one of the bands is quite badly perturbed. One must treat each case on its own merits. If enough unperturbed lines of the poorer band can be identified, a simultaneous fit can probably be made. The results will be less precise than one would wish, but will be of some value. If the band is too badly perturbed the results will be so untrustworthy as to be nearly worthless.

If one is lucky a substitute band may be available to replace the badly perturbed band. This was the case for methyl fluoride, as described in Chapter IX. The ν_4 band appeared to be quite badly perturbed, while the $2\nu_4$ band did not seem too bad. Fortunately, the data from $\nu_3 + \nu_4$ of methyl fluoride was available from a recent thesis by W. E. Blass (7). The $\nu_3 + \nu_4$ and $2\nu_4$ bands could be fit simultaneously to obtain A_o, $A_e\zeta_4{}^z + \ldots$, and the other molecular constants. For future reference, the frequency expression appropriate to this fit is listed in Table VIII. It is generally not too difficult to obtain a substitute for a perturbed ν_4. Any band of the type $\nu_n + \nu_4$, where ν_n represents a non-degenerate transition, will do nearly as well. It is likely to be very difficult, however, to obtain a substitute for a perturbed $2\nu_4$. A band of the type $\nu_n + 2\nu_4$ would do quite well. However, such bands seem to be so weak that it is a very difficult matter to obtain an acceptable high-resolution spectrum.

There exist a few other methods by which values of A_o have been or can be determined. Two important methods are described in some detail in Appendix I. The first is the zeta-sum method. This is the method by which nearly all previous values of A_o have been estimated for the methyl halides. The principles behind this method and its application are discussed in Appendix Ia. A comparison of our method with the zeta-sum method is presented below, since we feel that our values represent a considerable improvement over those determined from zeta-sums.

A second method which shows great promise is

Table VIII Frequency Expression for Simultaneous Fit of $\nu_3 + \nu_4$ and $2\nu_4$.

$$
\begin{aligned}
{}^{\Delta K}\Delta J_{K}(J) - \{ & B_o[(J+\Delta J)(J+1+\Delta J)-J(J+1)-(K+\Delta K)^2+K^2] \\
& -D_o^{J}[(J+\Delta J)^2(J+1+\Delta J)^2-J^2(J+1)^2] \\
& -D_o^{JK}[(K+\Delta K)^2(J+\Delta J)(J+1+\Delta J) \ -K^2J(J+1)]\} \quad =
\end{aligned}
$$

$$
\begin{bmatrix} \nu_o(\nu_3+\nu_4) & \text{or} \\ \nu_o(2\nu_4 \perp) & \text{or} \\ \nu_o(2\nu_4 \|) & \end{bmatrix} \text{ as appropriate } +
$$

$$
\begin{aligned}
& [A_o][(K+\Delta K)^2-K^2] + \\
& [-2A_e\zeta_4^{z}+\eta_4][(\Delta\ell_4)(K+\Delta K)] + \\
& [-D_o^{K}][(K+\Delta K)^4-K^4] + \\
& [\eta_4^{K}][(\Delta\ell_4)(K+\Delta K)^3] + \\
& [H_o^{K}][(K+\Delta K)^6-K^6] + \\
& [\eta_4^{J}][(\Delta\ell_4)(K+\Delta K)(J+\Delta J)(J+1+\Delta J)] + \\
& [H_o^{J}][(J+\Delta J)^3(J+1+\Delta J)^3-J^3(J+1)^3] + \\
& [H_o^{JK}][(K+\Delta K)^2(J+\Delta J)^2(J+1+\Delta J)^2-K^2J^2(J+1)^2] + \\
& [H_o^{KJ}][(K+\Delta K)^4(J+\Delta J)(J+1+\Delta J)-K^4J(J+1)] +
\end{aligned}
$$

$$
\begin{bmatrix} [(-\alpha_4^{A}) \text{ from } 2\nu_4] \text{ or} \\ [(-\alpha_3^{A}-\alpha_4^{A}) \text{ from } \nu_3+\nu_4] \end{bmatrix} \times [(\Delta v_4)(K+\Delta K)^2] +
$$

$$
\begin{bmatrix} [(-\alpha_4^{B}) \text{ from } 2\nu_4] \text{ or} \\ [(-\alpha_3^{B}-\alpha_4^{B}) \text{ from } \nu_3+\nu_4] \end{bmatrix} \times [(\Delta v_4)\{(J+\Delta J)(J+1+\Delta J)-(K+\Delta K)^2\}] +
$$

$$
\begin{bmatrix} [(\beta_4^{J}) \text{ from } 2\nu_4] \text{ or} \\ [(\beta_3^{J}+\beta_4^{J}) \text{ from } \nu_3+\nu_4] \end{bmatrix} \times [(\Delta v_4)(J+\Delta J)^2(J+1+\Delta J)^2] +
$$

$$
\begin{bmatrix} [(\beta_4^{JK}) \text{ from } 2\nu_4] \text{ or} \\ [(\beta_3^{JK}+\beta_4^{JK}) \text{ from } \nu_3+\nu_4] \end{bmatrix} \times [(\Delta v_4)(K+\Delta K)^2(J+\Delta J)(J+1+\Delta J)] +
$$

$$
\begin{bmatrix} [(\beta_4^{K}) \text{ from } 2\nu_4] \text{ or} \\ [(\beta_3^{K}+\beta_4^{K}) \text{ from } \nu_3+\nu_4] \end{bmatrix} \times [(\Delta v_4)(K+\Delta K)^4].
$$

Raman spectroscopy. As shown in Appendix Ib, it is possible to determine A_o directly from a full Raman spectrum of a symmetric top molecule. For the Raman ν_4 band the permitted selection rules are $\Delta K = \pm 1, \pm 2$, $\Delta J = 0, \pm 1, \pm 2$. The $\Delta \ell_4$ selection rules are found to be $\Delta \ell_4 = \Delta K$ for transitions with $\Delta K = \pm 1$, and $\Delta \ell_4 = -1/2\ \Delta K$ for transitions with $\Delta K = \pm 2$. Because of this fact, the Coriolis term is linearly independent of the A_o term, and the coefficients can be obtained individually in the same manner as for the simultaneous fit. In fact, the frequency formula of Table VII should apply to such a Raman analysis with the exception that only one vibrational constant (ν_o) is obtained. With the advent of the laser as a source, Raman spectroscopy has received new life and has the potential of eventually surpassing infrared spectroscopy in many areas.

A third method of determining A_o in certain very special cases is that applied by Maki and Hexter (8). They obtained an estimate of A_o for CH_3I from a study of the Coriolis resonance between the $K = 4, -\ell$ levels of $\nu_3 + \nu_6$ and the $K = 3, +\ell$ levels of ν_5. These bands were already known to be in Fermi resonance. This method is obviously of limited applicability and is probably of limited accuracy.

In the following section the zeta-sum method is compared with our method. The methods and variants listed below are ordered, in our opinion, from the least accurate to the most accurate presently available.

1. Application of the zeta-sum rule to Q-branch analyses of ν_4, ν_5, and ν_6 using Q-branch maxima (most previous values of A_o seem to have been determined in this manner).
2. Application of the zeta-sum rule to Q-branch analyses of ν_4, ν_5, and ν_6 using the leading edges of the Q-branches.
3. Application of the zeta-sum rule to Q-branch analyses of ν_4, ν_5, and ν_6 using subband origins.
4. Application of the zeta-sum rule after full single-band analyses of the rotational fine structure of ν_4, ν_5, and ν_6.
5. Solution for A_o from numerical values of $(A_o - A_e\zeta_4{}^z + \ldots)$ and $(A_o + 2A_e\zeta_4{}^z + \ldots)$ obtained from Q-branch analysis of ν_4 and $2\nu_4$.
6. Solution for A_o from numerical values of $(A_o - A_e\zeta_4{}^z + \ldots)$ and $(A_o + 2A_e\zeta_4{}^z + \ldots)$ obtained from single-band fits of resolved rotational fine structure of ν_4 and $2\nu_4$.
7. Determination of A_o from simultaneous fit of resolved rotational fine structure of ν_4 and $2\nu_4$.

A Q-branch analysis means a fit of the observed frequencies of the wide unresolved Q-branches to the formula [see Ref. (5)]

$$\nu_o(Q_K) = [\nu_o + A'(1-2\zeta) - B'] \pm 2[A'(1-\zeta) - B']K + [(A' - B') - (A'' - B'')]K^2.$$

This formula, as taken from Ref. (5), is written in the older notation of A" and B" representing the lower state constants and A' and B' the upper state constants. However, an equivalent expression can be easily obtained by specializing Table V to the desired band with $\Delta K = \pm 1$, $\Delta J = 0$, and J = constant.

In the past, most Q-branch analyses seem to have been done using the maxima of the Q-branches. Since the Q-branches are wide ($\sim 1\ cm^{-1}$) and sometimes irregularly shaped, determination of the positions of the maxima is a process of somewhat limited accuracy. Any perturbations present may give anomalous intensity distributions in the Q-branches or shift the maxima. Furthermore, even in the ideal case, the maxima of the Q-branches occur at different values of J for different Q-branches, whereas the formula was set up for constant J.

A slightly better procedure would be to use the sharp leading edges of the Q-branches. While the leading edges still represent varying J-values, they are often easier to measure and should suffer less from intensity anomalies.

A Q-branch analysis should be done in the manner described by Brown and Edwards (9). In this more refined method, the true subband origins (for $J = 0$) are found by graphing or fitting the ${}^{R}R_K(J)$, ${}^{R}P_K(J)$, ${}^{P}R_K(J)$, and/or ${}^{P}P_K(J)$ lines subband by subband. Q-branch fits using these subband origins should yield the best results available from this sort of procedure.

If one has the rotational fine structure resolved in the ν_4, ν_5, and ν_6 bands, however, it is rather pointless to make a Q-branch analysis. If one has access to a good sized computer it is much more fruitful to make single-band frequency analyses of each band. Then the zeta-sum rule can be applied to the results of these fits. Applied in this manner, the zeta-sum rule should yield reasonably good values of A_o.

If large computer facilities are not available, Q-branch fits of the subband origins for ν_4 and $2\nu_4$ will yield numerical values of $(A_o - A_e\zeta_4{}^z + \ldots)$ and $(A_o + 2A_e\zeta_4{}^z + \ldots)$ respectively. These can be solved for A_o and $A_e\zeta_4{}^z$.

The methods of obtaining A_o and $A_e\zeta_4{}^z$ from combined single-band fits and from simultaneous fits of ν_4 and $2\nu_4$ have been discussed in detail in the first part of this chapter. The advantages of using the simultaneous analysis method have also been discussed in detail.

CHAPTER V

LEAST SQUARES ANALYSIS OF THE DATA

The first part of this chapter contains a description of the mathematics involved in the least squares method. This is taken mainly from Hildebrand's "Introduction to Numerical Analysis" (10).

Assume we have available a set of numerical values, $f(x_i) \equiv f_i$, taken at various discrete values of variable x, x_i, over a particular region. Suppose we have reason to believe that a function, y(x), of a chosen general series form should closely approximate the "true" function, $f(x_i)$, over this region. In general, y(x) will have the form

$$y(x) = \sum_{k=0}^{n} a_k \, \phi_k(x),$$

where the $\phi_k(x)$ are (n+1) known, appropriately chosen functions, linearly independent of one another, and the a_k are (n+1) constants which are to be determined. We wish to obtain the set of constants, a_k, which gives the best possible agreement (according to a chosen criterion) between y(x) and the set $f(x_i)$ over the given region.

Suppose we define the "deviation" or "residual" at any point, x_i, as

$$f(x_i) - y(x_i) \equiv f(x_i) - \sum_{k=0}^{n} a_k \, \phi_k(x_i).$$

The least squares criterion for the "best possible fit" is that the weighted sum of the squares of the deviations should be a minimum, viz.,

$$\sum_{i=1}^{N} w(x_i)[f(x_i) - \sum_{k=0}^{n} a_k \, \phi_k(x_i)]^2 = \text{minimum},$$

where N is the number of sets of data.

This imposes the conditions

$$\frac{\partial}{\partial a_r} \{ \sum_{i=1}^{N} w(x_i)[f(x_i) - \sum_{k=0}^{n} a_k \phi_k(x_i)]^2 \} = 0,$$

for $r = 0, 1, \ldots, n$, or

$$\sum_{i=1}^{N} w(x_i) \phi_r(x_i)[f(x_i) - \sum_{k=0}^{n} a_k \phi_k(x_i)] = 0.$$

These are the normal equations, $(n+1)$ simultaneous linear equations in the $(n+1)$ unknown quantities $a_0, a_1, \ldots, a_n$.

The formation of the set of normal equations is illustrated below for a very simple example. Suppose the equation

$$y = A + Bx + Cz$$

is thought to adequately represent a physical process for which N sets of data, f_i, have been taken, each with weight w_i, at points (x_i, z_i). It should be noted that variables x and z can be quite general. For example, z might represent x^2, sin x, etc., or might represent a function of a different variable, such as z'^3, tan z', $e^{z'}$, etc.

In terms of the previous notation, $y_i = y(x_i,z_i)$, $f_i = f(x_i,z_i)$, $\phi_1 = 1$, $\phi_2 = x$, $\phi_3 = z$. The set of normal equations (three equations in three unknowns) is

1. $A\sum_{i=1}^{N}w_i + B\sum_{i=1}^{N}w_i x_i + C\sum_{i=1}^{N}w_i z_i = \sum_{i=1}^{N}w_i f_i,$
2. $A\sum_{i=1}^{N}w_1 x_i + B\sum_{i=1}^{N}w_i x_i{}^2 + C\sum_{i=1}^{N}w_i x_i z_i = \sum_{i=1}^{N}w_i x_i f_i,$
3. $A\sum_{i=1}^{N}w_i z_i + B\sum_{i=1}^{N}w_i x_i z_i + C\sum_{i=1}^{N}w_i z_i{}^2 = \sum_{i=1}^{N}w_i z_i f_i.$

Since x_i, z_i, f_i, and w_i are all known (observed) quantities, the sums $\sum_{i=1}^{N}w_i x_i z_i$, etc. are known constant quantities. The set of three equations in three unknowns, A, B, and C, can be solved for these quantities.

Suppose now that the frequency expression of

Table VII is to be fit by least squares. Identifying terms with those in the previous definition, $y = \sum_{k=0}^{n} a_k \phi_k$, one has the set of terms listed in Table IX. In principle, the normal equations are formed in the same manner as for the simple case just illustrated. In practice, a computer is necessary to handle the sheer mass of calculations.

In solving these normal equations for large numbers of coefficients a computer is even more necessary. In addition, the direct method of substituting equations into one another becomes so complicated and inefficient that the more general and more powerful methods of numerical matrix inversion must be used.

The set of normal equations,

$$\sum_{k=0}^{n} a_k [\sum_{i=1}^{N} w(x_i)\phi_r(x_i)\phi_k(x_i)] = [\sum_{i=1}^{N} w(x_i)\phi_r(x_i)f(x_i)],$$

with r = 0, 1, ..., n, can be represented as a matrix equation

$$\underline{M}\ \underline{A} = \underline{N},$$

where

$$\underline{M} = \begin{bmatrix} M_{00} & M_{01} & \cdots & M_{0n} \\ M_{10} & M_{11} & \cdots & M_{1n} \\ \cdots & \cdots & \cdots & \cdots \\ M_{n0} & M_{n1} & \cdots & M_{nn} \end{bmatrix}$$

$$M_{rk} = \sum_{i=1}^{N} w(x_i)\phi_r(x_i)\phi_k(x_i), \quad r,k = 0, 1, \ldots, n,$$

$$\underline{N} = \begin{bmatrix} N_0 \\ N_1 \\ \cdot\cdot \\ N_n \end{bmatrix}$$

$$N_r = \sum_{i=1}^{N} w(x_i)\phi_r(x_i)f(x_i), \quad r = 0, 1, \ldots, n,$$

Table IX Normal Equation Terms

Coefficient	Quantum Dependence
$a_0 = \nu_o$	$\phi_0 = 1.0$
$a_1 = A_o$	$\phi_1 = [(K+\Delta K)^2 - K^2]$
$a_2 = [-2A_e\zeta_4{}^z + \eta_4]$	$\phi_2 = [(\Delta \ell_4)(K+\Delta K)]$
$a_3 = [-D_o{}^K]$	$\phi_3 = [(K+\Delta K)^4 - K^4]$
$a_4 = [-\alpha_4{}^A]$	$\phi_4 = [(\Delta v_4)(K+\Delta K)^2]$
$a_5 = \eta_4{}^K$	$\phi_5 = [(\Delta \ell_4)(K+\Delta K)^3]$
$a_6 = \beta_4{}^K$	$\phi_6 = [(\Delta v_4)(K+\Delta K)^4]$
$a_7 = H_o{}^K$	$\phi_7 = [(K+\Delta K)^6 - K^6]$
$a_8 = [-\alpha_4{}^B]$	$\phi_8 = [(\Delta v_4)\{(J+\Delta J)(J+1+\Delta J) - (K+\Delta K)^2\}]$
$a_9 = \eta_4{}^J$	$\phi_9 = [(\Delta \ell_4)(J+\Delta J)(J+1+\Delta J)(K+\Delta K)]$
$a_{10} = \beta_4{}^J$	$\phi_{10} = [(\Delta v_4)(J+\Delta J)^2(J+1+\Delta J)^2]$
$a_{11} = \beta_4^{JK}$	$\phi_{11} = [(\Delta v_4)(K+\Delta K)^2(J+\Delta J)(J+1+\Delta J)]$
$a_{12} = H_o{}^J$	$\phi_{12} = [(J+\Delta J)^3(J+1+\Delta J)^3 - J^3(J+1)^3]$
$a_{13} = H_o^{JK}$	$\phi_{13} = [(K+\Delta K)^2(J+\Delta J)^2(J+1+\Delta J)^2 - K^2J^2(J+1)^2]$
$a_{14} = H_o^{KJ}$	$\phi_{14} = [(K+\Delta K)^4(J+\Delta J)(J+1+\Delta J) - K^4J(J+1)]$

$$
\begin{aligned}
f_i = {}^{\Delta K}\Delta J_K(J) - \{ & B_o[(J+\Delta J)(J+1+\Delta J) - J(J+1) - (K+\Delta K)^2 + K^2] \\
& - D_o{}^J[(J+\Delta J)^2(J+1+\Delta J)^2 - J^2(J+1)^2] \\
& - D_o^{JK}[(K+\Delta K)^2(J+\Delta J)(J+1+\Delta J) - K^2J(J+1)]\}
\end{aligned}
$$

$$\underline{A} = \begin{bmatrix} a_0 \\ a_1 \\ \cdot\cdot \\ a_n \end{bmatrix} .$$

The solution, obtained by inverting $\underline{M}$, is

$$\underline{A} = \underline{M}^{-1}\underline{N}.$$

This gives the set of coefficients, a_k, as a column vector, $\underline{A}$.

Many kinds of matrix inversion techniques are available. Most computer installations will have library routines. The various methods will not be discussed here. Some may be more efficient than others in a given case, but most will be suitable as long as they are mathematically accurate.

The remainder of this chapter is concerned with the application of least squares fitting methods to the data for the ν_4 and $2\nu_4$ bands of a methyl halide molecule. For a simultaneous least squares fit of ν_4 and $2\nu_4$ each set of data, representing one transition, will consist of Δv_4 (= 1 for ν_4, 2 for $2\nu_4$), ΔK, ΔJ, K, J, ν_{obs} (the observed frequency of the line), and w (the weight assigned to the line). There will be as many sets of data as lines in the fit. We shall assume that the frequencies of the transitions have been measured and are known.

The least squares fits were performed on the Michigan State University Control Data 3600 computer using the program FALSTAF (<u>F</u>requency <u>A</u>nalysis by <u>L</u>east <u>S</u>quares <u>T</u>o

All-powerful Formula). We obtained the basic least squares program from Dale Fimple of Sandia Corporation. It was written by M. A. Efroyemson of Esso Research and Engineering Company and is described in "Mathematical Methods for Digital Computers" (11). Input and output sections were rewritten to accept the data in a more convenient format and print out the quantities of interest to us. The program was also double-precisioned to handle large numbers with more accuracy. The FALSTAF program is listed in Appendix II.

The results of a typical least squares fit are composed of three main parts: (1) the estimators of the coefficients, (2) the predicted frequencies, and (3) the various statistical quantities. As discussed previously, the estimators of the coefficients represent the best values (in a least squares sense) of the molecular constants, or combinations of them, which are available from the data. The calculated or predicted frequencies are obtained from the coefficients just found. Other lines, not already included in the data, can be calculated, then found in the spectrum, and finally added to the data in a new fit. Generally, after each fit a "predicted spectrum" is calculated, in other words, the ΔK and ΔJ quantities are allowed to take on their permitted values and all transition frequencies are calculated on the basis of the previously determined coefficients up to specified maximum values of K and J.

From our standpoint, the most important statistical quantities are the standard deviation of the fit and the simultaneous confidence intervals on the coefficients. If there are N observations (line frequencies in the data list) and p coefficients to be determined, the weighted standard deviation of the fit is

$$s = [N/(N-p)\sum_{i=1}^{N} w_i(\Delta\nu_i)^2]^{1/2},$$

where $\Delta\nu_i = (\nu_{obs})_i - (\nu_{calc})_i$. The main value of this statistical quantity is that it serves as a criterion of "goodness" of the fit and as a comparison with other fits.

If M_{ii}^{-1} is the diagonal element, corresponding to the coefficient a_i, of the inverse of the normal equation matrix, then the standard error associated with a_i is

$$\psi(a_i) = s^2 M_{ii}^{-1}.$$

The simultaneous confidence interval corresponding to a_i is defined as $[\pm S\psi(a_i)]$, where $S = pF_\alpha(p, N-p)$, and the $F_\alpha(p, N-p)$ are tabulated values of the F-distribution (<u>12</u>, <u>13</u>). The value of the coefficient and its simultaneous confidence interval are then written $[a_i \pm S\psi(a_i)]$. The interpretation of the simultaneous confidence interval is that if the data in the fit is considered to be one sampling of a normally-distributed infinite population of similar sets of data, then the probability that all of the quantities $[a_i \pm S\psi(a_i)]$ will include the "true" value of a_i is $(1 - \alpha)$.

CHAPTER VI

METHODS OF OBTAINING AND TREATING SPECTRA

The spectra of the methyl halides and related molecules were obtained on the Michigan State University high-resolution infrared vacuum recording spectrometer. This spectrometer, which employs an f/5 Pfund-Littrow monochromator of focal length approximately one meter, has been described in detail elsewhere (14, 15, 16).

The source generally used for the $2\nu_4$ spectra near 6000 cm^{-1} was a commercial 300w zirconium lamp. These lamps could not be used in the ν_4 region near 3000 cm^{-1} because the glass envelope cut off about half of the energy. A new zirconium arc source was built, having a water-cooled brass housing and a sapphire window. It used the electrodes taken from old 300w zirconium arcs. All ν_4 spectra and some of the $2\nu_4$ spectra were obtained using this source.

The foreoptics leading into the spectrometer consisted of an all-mirror system. The infrared energy from the source (along with the visible radiation) was sent through an 80 cm long multiple traverse cell containing the gas under study. The number of traversals could be varied so as to optimize conditions among pressure, path length, and output energy. The spectrometer contained two Bausch and Lomb "certified precision" eschelette gratings, a 600 line/mm 212mm×158mm grating blazed at 1.6μ, and a 300 line/mm 254mm×128mm grating blazed at 5μ. These were mounted back-to-back on a worm gear-driven turntable and could be switched with relative ease. The spectrometer was normally used in "single-pass" configuration, in which the light struck the grating only once. It could be adjusted, however, to be used in "double-pass" configuration in which the light diffracted from the grating was intercepted and sent back to the grating for a second diffraction. This greatly increased the resolution, but reduced the available energy, especially for the calibration "fringes". Thus, double-passing was useful only in certain regions of the spectrum.

The infrared output energy was measured with Eastman-Kodak lead sulphide detectors, P-type for ν_4 and N-type for $2\nu_4$. These were cooled to -196°C by means of a liquid nitrogen bath. The infrared beam was chopped at 90 cycles/sec. The lead sulphide detector output was amplified by a Tektronix Type 122 preamplifier followed by a phase-sensitive amplifier. The amplifier output was recorded as one trace on a Leeds and Northrop Model G two-pen recorder.

The second pen of the recorder traced the "fringes." These were Edser-Butler bands of visible light in the higher orders of the grating, detected with an RCA 1P21 or selected 931A photomultiplier. The fringe trace (lower trace in Fig. 4) served as a frequency "ruler" to calibrate the spectrum since the fringes are equally spaced in frequency. Our calibration methods have already been described in "Wavelength Standards in the Infrared" (17) and will be described in more detail below.

The pens were first aligned parallel to the ver-

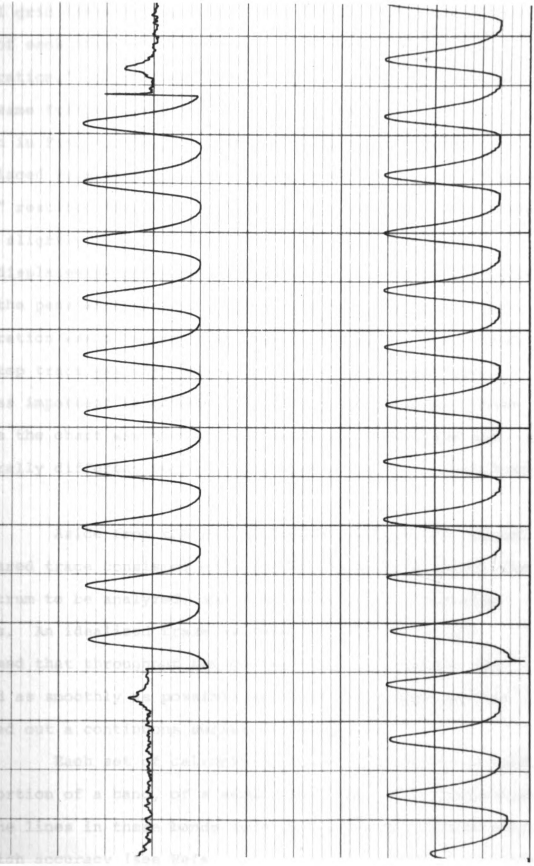

Fig. 4 Dynamic Pen Separations

tical grid lines on the chart paper. At the beginning and end of each chart it was necessary to run a "dynamic pen separation." This consisted of traces obtained by imposing the same fringe signal on both pens simultaneously. As shown in Fig. 4, this gave two identical traces slightly displaced from each other. The displacement or "pen separation" resulted from the necessity of displacing the recorder pens slightly to allow them to cross without colliding. The displacement was a few millimeters, but could depend on how the pens were adjusted for a particular run. The pen separation was obtained by measuring the distance by which the top trace was displaced relative to the lower trace. It was important to obtain a dynamic pen separation (taken while the chart was moving) since the pen separation was generally different for a moving chart than for a stationary one.

Aside from the pen separation sections, a typical infrared trace consisted of a set of calibration lines, the spectrum to be analyzed, and a second set of calibration lines. An idealized trace is shown in Fig. 5. It is assumed that throughout the entire chart the grating has moved as smoothly as possible and that the fringe pen has traced out a continuous series of fringes.

Each set of calibration lines consisted of a band, or portion of a band, of a simple molecule. The frequencies of the lines in these bands have been measured independently to high accuracy [see Refs. (18, 19, 20)]. These established

Fig. 5 Idealized Spectrum

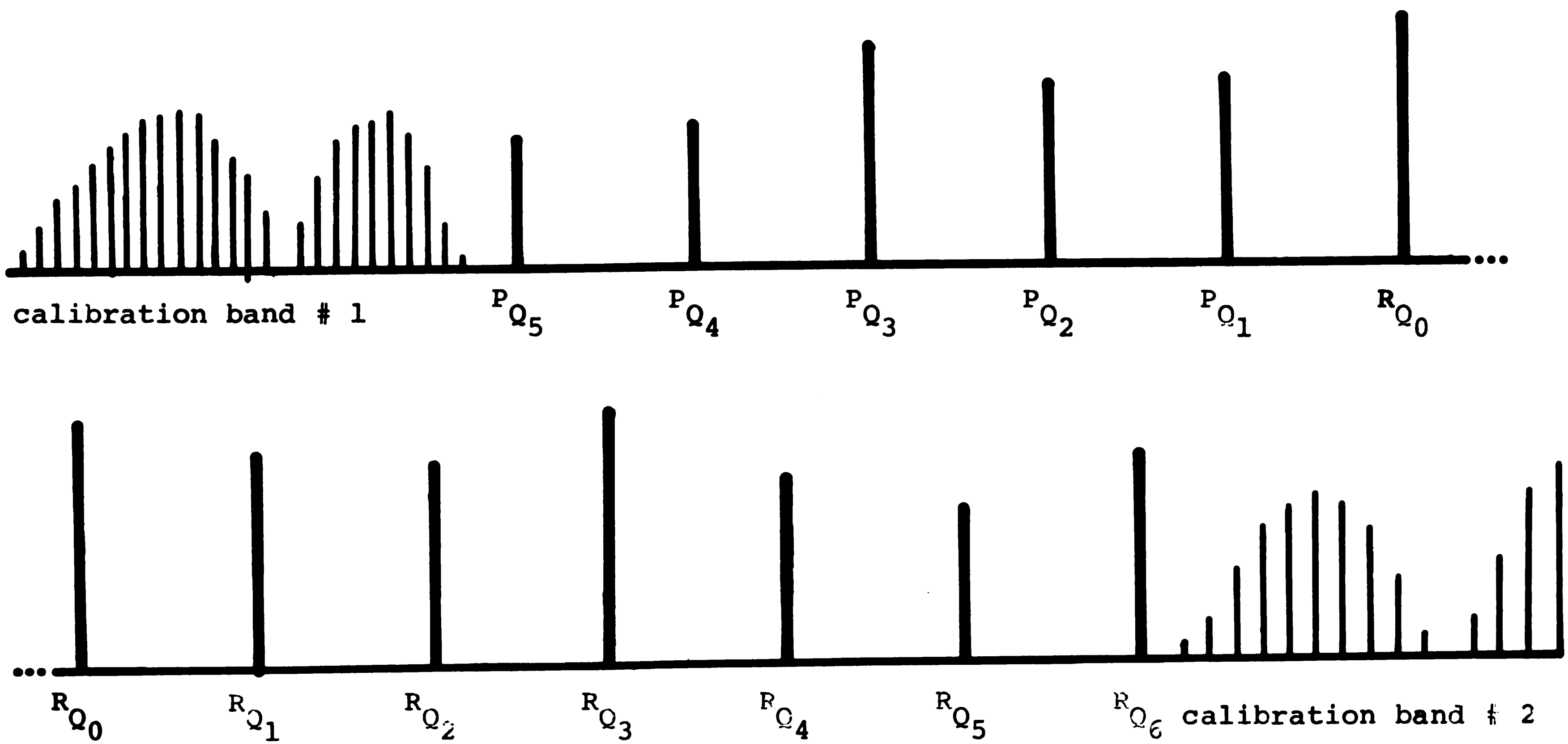

a set of known frequencies at each end of the chart.

The charts on which the high-resolution spectra were recorded could be as long as 40 yards. This encompassed a few hundred cm^{-1}. The relative scale was generally 2 - 4 inches/cm^{-1} along the chart. The spectra were photographed in 15 inch sections using a Nikkon F camera with special minimum distortion copying lens. The camera was mounted very rigidly on a specially constructed copying stand. The paper was carefully aligned parallel to the plane of the film.

The developed film was measured on a Hydel semi-automatic digitized film reader connected to an IBM 526 printing summary card punch. A schematic diagram of the Hydel optical system is shown in Fig. 6. An image of the film, held flat by vacuum on the projection stage, was projected onto a large (24"×24") ground-glass viewing screen. A fixed image of a reticle was simultaneously projected onto the center of the viewing screen. The image of the film was moved about relative to the reticle image by means of horizontal and vertical traverse controls. These traverse controls were connected to the projection stage with precisely machined and calibrated screws. The operator aligned the reticle image with a desired point on the film image and punched a readout button. This caused the (x, y) coordinates of that point, relative to an internal coordinate system, to be punched out on a computer card.

The Hydel measurement of a spectrum proceeded as

Fig. 6 Hydel Optics

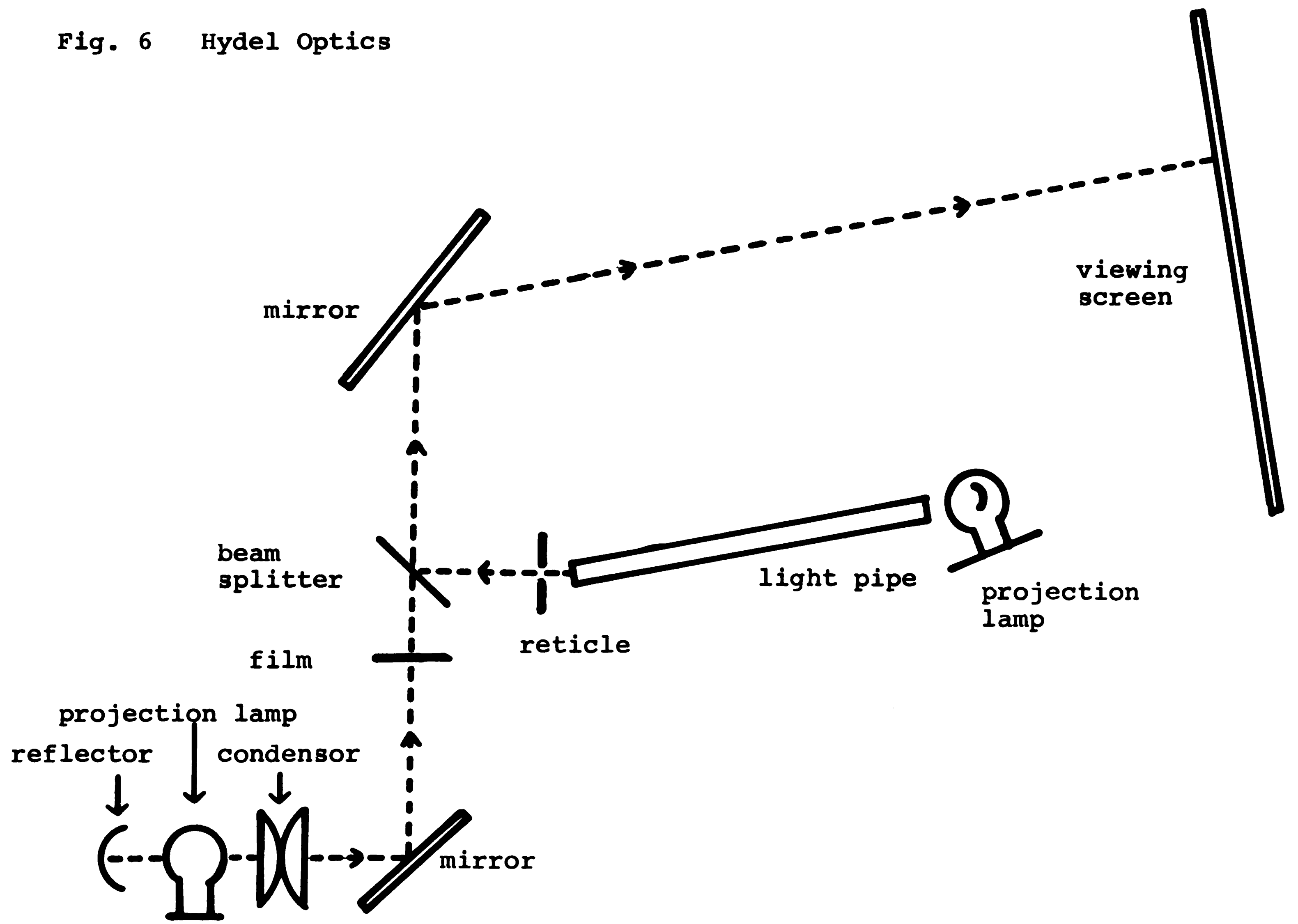

follows: Each frame on the film covered about 15" of chart. The film was measured one frame at a time. For each frame, two cards were always present. The first was a "parameter card" which contained the frame number, the fringe number of the leftmost fringe in the frame (or the fringe which was to be the first one measured), and a number identifying the operator. The second card in each frame was a "rotation card." This consisted of six measurements along the image of a vertical grid line on the chart. This was used to correct for any rotation of the chart image relative to the Hydel axis system. Normally the first and last frames on each film strip were of the dynamic pen separations. For these frames, in addition to the parameter card and rotation card, measurements were made of the fringe traces, alternating between the upper and lower traces (see Fig. 4). These were called "pen separation cards." All the other frames contained portions of the infrared spectrum and fringe traces. For these frames, in addition to the parameter and rotation cards, the fringes were first measured in sequence, starting with the fringe specified on the parameter card. As many cards as necessary were used for these. Next the infrared lines in the frame were measured, with no requirements on which ones were measured or in what order they were measured. Again, as many cards as necessary were used.

The raw data was converted into useable form by means of the computer program SCAN, listed in Appendix III. A typical, though short, data deck is included. The numbers at the far right are the codes: 1 - parameter card, 2 - rotation card, 3 - pen separation card, 4 - calibration card (explained later), 5 - fringe card, and 6 - infrared card. The data deck, as fed into the first run of SCAN, consisted of the heading or identification cards, two pen separation sections (codes 1, 2, 3, 3, 3, ..., 1, 2, 3, 3, 3, ...), and as many spectrum sections (codes 1, 2, 5, 5, 5, ..., 6, 6, 6, ..., 1, 2, 5, 5, 5, ..., 6, 6, 6, ...) as there were frames containing sections of spectra.

The SCAN program first corrected each of the first two pen separation frames for rotation and obtained the pen separations by subtracting the corrected x-coordinates of the lower fringes from the corresponding ones of the upper trace. These were averaged for each frame, and finally a grand average pen separation was obtained for the chart.

Then, for each successive frame the program corrected for rotation, counted the fringes starting from the one specified in the parameter card, corrected each infrared line for pen separation, and obtained the "fringe number" of each infrared line. The fringe number represented the number of the nearest fringe on the left plus the fractional distance from that fringe to the next fringe. These fringe numbers of the infrared lines constituted the main output of the first SCAN run.

With the fringe numbers and frequencies known for the calibration lines, the chart could be calibrated. This was done by making a linear least squares fit of the calibration lines to the formula $\nu = A + Bf$, where ν represents the frequency and f the fringe number. A modification of FALSTAF known as FITTUM was used to make the fit. This yielded values for the coefficients A and B. Since the fringes were equally spaced in frequency, the frequencies of all the infrared lines in the spectrum could be easily calculated.

The values of A and B were punched onto a "calibration card" (code 4). This card was included in the data deck in a second SCAN run. In this case, both the fringe numbers and the frequencies of the lines in the spectrum were output.

CHAPTER VII

ANALYSIS OF CH_3Br

Spectra of ν_4 of CH_3Br, with band origin near 3050 cm^{-1} and with useable region extending from about 2970 cm^{-1} to 3170 cm^{-1}, were run on the 300 line/mm grating with the spectrometer in single-pass configuration. Two charts of ν_4, 1065-Br and 1165-Br, were analyzed. They were calibrated with HCl (1-0) (<u>18</u>) on the low-frequency side and HCN (0,0,1) (<u>19</u>) on the high-frequency side. The standard deviations of the calibration fits were both 0.004 cm^{-1}. The details of the experimental conditions under which the spectra were run are given in Table X.

Spectra of the $2\nu_4$ band were run on the 600 line/mm grating with the spectrometer in both single and double-pass configurations. The parallel component of $2\nu_4$ has its band origin near 6045 cm^{-1} and extends from about 6020 cm^{-1} to 6070 cm^{-1}. The perpendicular component has band origin near 6095 cm^{-1}. Its useable portion extends from 6080 cm^{-1} to 6220 cm^{-1}. On the low frequency side of $^PQ_2(J)$ it is overlapped by the much stronger lines of the parallel component. Three charts of $2\nu_4$, 0565-Br, 0665-Br, and 1465-Br, were analyzed. The calibration bands for all of these were N_2O (3,0,1) (<u>20</u>) on the low-frequency side and HCN (0,0,2) (<u>19</u>) on the high-frequency side. In addition, a number of lines of the HCl (2-0) band (<u>18</u>) were run on the low-frequency side of the 1465-Br chart. The standard deviations of the calibration fits for all the charts were about 0.005

Table X Experimental Conditions (CH_3Br)

band	chart	calibration bands	grating lines/mm	s.p. or d.p.	source	detector	press. CH_3Br	path length
ν_4	1065-Br	HCl(1-0) HCN(0,0,1)	300	s.p.	Zr arc box	PbS-P	6 mm	6.4 m
ν_4	1165-Br	HCl(1-0) HCN(0,0,1)	300	s.p.	Zr arc box	PbS-P	6 mm	6.4 m
$2\nu_4$	0565-Br	N_2O(3,0,1) HCN(0,0,2)	600	d.p.	300 w Zr arc	PbS-N	10 mm	9.6 m
$2\nu_4$	0665-Br	N_2O(3,0,1) HCN(0,0,2)	600	d.p.	300 w Zr arc	PbS-N	10 mm	9.6 m
$2\nu_4$	1465-Br	HCl(2-0) N_2O(3,0,1) HCN(0,0,2)	600	s.p.	Zr arc box	PbS-N	20 mm	6.4 m

cm^{-1}. Details of the experimental conditions under which the spectra were run are given in Table X.

In the CH_3Br spectra it was a relatively simple matter to assign a large number of transitions, i. e., identify the set of selection rules and quantum numbers (ΔK, ΔJ, K, and J) which characterize each transition. The "missing lines" in the subband series, complemented by the subband intensity alternation, made the initial assignment of many lines unambiguous. These two effects are discussed below.

One very striking feature of the methyl bromide spectra, and of the spectra of any methyl halide-type molecule, is the fact that every third Q-branch is noticably more intense than its neighbors. Theoretically the ratio is 2:1. The ${}^{R}R_{K}(J)$, etc. lines of these subbands are also twice as intense as the corresponding lines of the neighboring subbands. This intensity alternation is due to the C_{3v} symmetry of the molecule [see King, p. 301 (21)] and makes the subbands for which K = 0, 3, 6, 9, ... twice as intense as their neighbors. The intensity alternation is quite clear in the methyl bromide rapid scan spectra, Fig. 7. In practice, the ${}^{R}Q_{0}(J)$ Q-branch is not necessarily the most intense, so that making assignments on this basis could lead to a misassignment by 3 in K. Such a mistake might easily be made in the case of ν_4 in Fig. 7.

The initial assignments of many lines were made with certainty on the basis of the "missing lines" in the

Fig. 7 CH_3Br Survey Spectra - ν_4 and $2\nu_4$

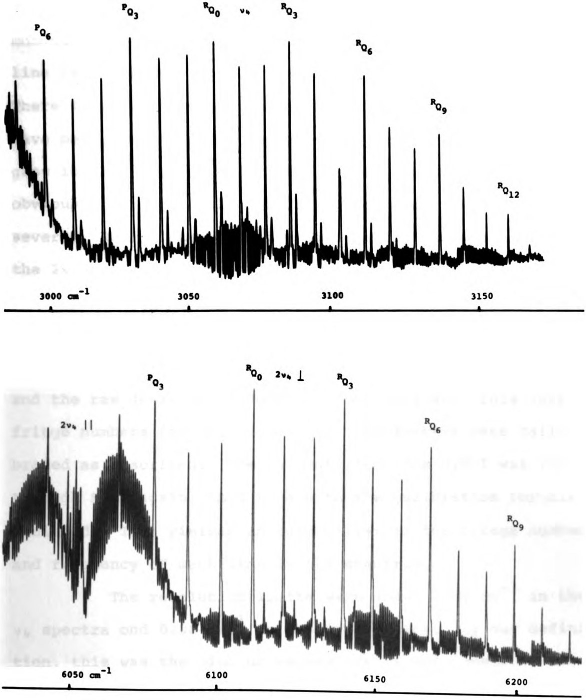

subband series. These are due to the requirement that K be less than or equal to J, in other words, the z-component of the angular momentum cannot be greater than the total angular momentum. For example, in the KΔK = +3 subband the ${}^{R}R_3(3)$ line is the first line of the ${}^{R}R_3(J)$ series which exists. There is a distinct gap where the lines ${}^{R}R_3(0 - 2)$ would have been. Even in the rapid scan spectra in Fig. 7 the gaps in the ${}^{R}R_3(J)$, ${}^{R}R_6(J)$, and ${}^{R}R_9(J)$ subbands are quite obvious. In Fig. 8 the ${}^{R}Q_3(J)$ Q-branch and the first several ${}^{R}R_3(J)$ lines from the high-resolution spectrum of the $2\nu_4$ band are shown.

The frequencies of all the spectral lines were obtained in the manner described in Chapter VI. The spectra were photographed, measured on the Hydel film reader, and the raw data run through the SCAN program. This gave fringe numbers for all the lines. The spectra were calibrated as described. The raw data from the Hydel was run through SCAN again, this time with the calibration formula included. This yielded an output listing the fringe number and frequency of each line in the spectrum.

The resolution limits were about 0.04 cm^{-1} in the ν_4 spectra ond 0.06 cm^{-1} in the $2\nu_4$ spectra. By our definition, this was the minimum separation of two "useable" lines. It generally ran slightly less than the true Rayleigh criterion distance. Lines which had neighbors so close were strongly downweighted in the fits.

After a considerable number of lines had been

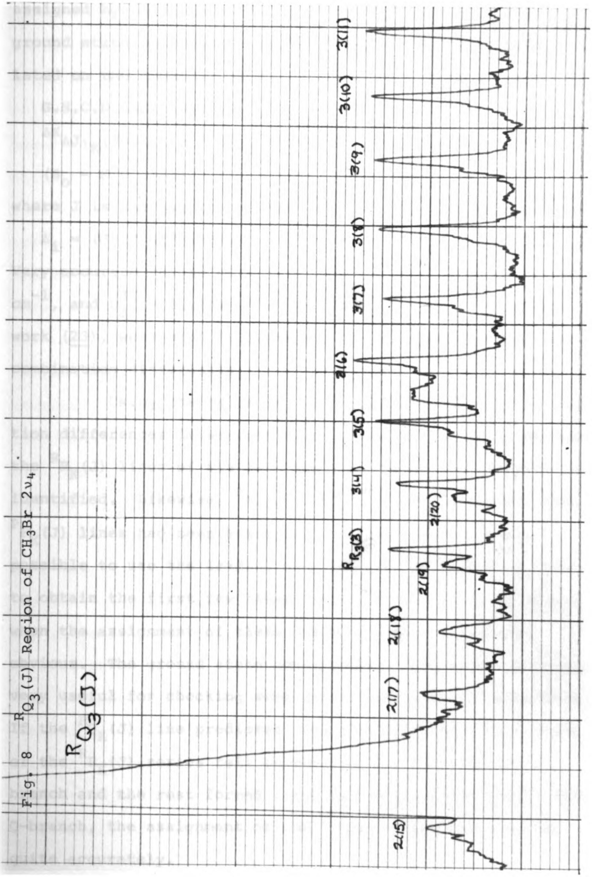

Fig. 8 $^RQ_3(J)$ Region of CH_3Br $2\nu_4$

assigned by inspection, further assignments were made using ground state combination differences. These were calculated on the computer using the formula (7, 22)

$$\text{G.S.C.D.}(\Delta J_1, \Delta J_2, K, J) =$$
$$^{\Delta K}\Delta J_{1_K}(J-\Delta J_1) - {}^{\Delta K}\Delta J_{2_K}(J-\Delta J_2) =$$
$$(B_o - K^2 D_o^{JK})(\Delta_2 - \Delta_1) + (-D_o^{J})(\Delta_2^{2} - \Delta_1^{2}),$$

where J is the quantum number of the common upper state and

$$\Delta_i = (J-\Delta J_i)(J+1-\Delta J_i), \quad i = 1 \text{ or } 2.$$

Very accurate values of $B_o = 0.3185537\ cm^{-1}$, $D_o^{J} = 3.33\times10^{-7}\ cm^{-1}$, and $D_o^{JK} = 4.27\times10^{-6}\ cm^{-1}$, available from microwave work (23), were used to calculate a table of ground state combination differences.

Using the table of calculated ground state combination differences it was possible to assign $^{R}P_K(J)$ lines when the $^{R}R_K(J)$ lines of the same subband series had already been identified. Likewise, $^{P}R_K(J)$ lines could be obtained when $^{P}P_K(J)$ lines had been assigned. In some cases it was possible to use the leading edge of the Q-branches in order to obtain the first few lines in an $^{R}R_K(J)$ or $^{P}P_K(J)$ series when the assignment of these lines was not immediately obvious. The ground state combination differences were also very useful for checking some series assigned by inspection. If the $^{R}Q_K(J)$ line predicted from the observed first member of the $^{R}R_K(J)$ series fell on the leading edge of the Q-branch and the rest formed a smooth progression through the Q-branch, the assignment of the $^{R}R_K(J)$ lines was checked quite accurately.

An interesting but annoying feature of the CH_3Br spectra was a small rotational isotope effect. This arose from the presence of two isotopic species of methyl bromide, $CH_3{}^{79}Br$ and $CH_3{}^{81}Br$, present in almost equal abundance. The observed isotope effect manifested itself as a gradual broadening and eventual splitting of the lines in each subband as J increased. The lines in a subband started out initially sharp, became appreciably broadened around J = 12, and were actually split into two components around J = 25. This splitting is due to the difference in the values of B_o for the two isotopic species. There was no noticeable difference of vibrational band origins for the two species, due apparently to the fact that the halogen atom participates very little in the ν_4 vibrational mode. This could be anticipated since the band origins of CH_3I, CH_3Br, and CH_3Cl are not much different.

The annoying feature of this isotope effect was that only the low-J lines of any subband were really sharp. The most useful lines, those of J ≈ 12 - 25, were broadened and therefore much more difficult to measure accurately. At high enough J that the two components of each doublet were resolved, the intensities had fallen so low that the individual lines were quite poor. Since there was no possibility of analyzing the spectra of the individual isotopic species, the analysis was made for $CH_3{}^{(av)}Br$. The frequencies of the centers of the broadened lines and the average frequencies of the resolved doublets were used.

Also the microwave values of B_o, D_o^J, and D_o^{JK} for each species were averaged to obtain the values for the average molecule $CH_3^{(av)}Br$ (values given previously).

Since all the lines in the spectra were not equally good, weights had to be assigned to each transition frequency. The weighting system used was based on our estimate of how well each line could be measured relative to the best lines in the spectrum. The very best lines were considered uncertain by an amount equal to the standard deviation of the calibration fit, at a minimum. Other less perfect lines were in error by this amount plus any uncertainty in determining the exact center of the line. If a line happened to be broad, or irregular, or blended with another line, there was considerable difficulty in measuring its exact center.

Because of the manner in which the weights enter the least squares fit, e. g., $\sum_i w_i x_i z_i$, the weights were assigned according to the scheme

$$w_i \propto (\Delta\nu_i)^2,$$

where $\Delta\nu_i$ represents the total uncertainty in the measured frequency of the line. The best lines were assigned weight 1.00. These were considered to have an inherent uncertainty equal to the standard deviation of the calibration fit. A line with estimated uncertainty twice that value received a weight of 0.25.

As mentioned before, two charts of the ν_4 band and three charts of the $2\nu_4$ band were measured. In many cases the weights assigned to the same line from different charts were different. The weighted average frequency was obtained from the formula

$$\nu_{av} = [\textstyle\sum_{i=1}^{n} w_i \nu_i]/[\sum_{i=1}^{n} w_i].$$

The average weight of the average frequency was

$$w_{av} = [\textstyle\sum_{i=1}^{n} w_i]/n.$$

As a rule, the course of procedure in analyzing the spectra of ν_4 and $2\nu_4$ was to first analyze the individual bands as well as possible, and then combine the data of both bands into a simultaneous fit. This step was bypassed in the case of methyl bromide. The data of both bands were good enough that an excellent simultaneous fit was obtained immediately. The data of both bands were fit to the frequency expression of Table VII. On the basis of the coefficients determined from this fit, predicted spectra were calculated for ν_4 and $2\nu_4$. From these, new lines could be found and perturbed series could be identified. The only badly perturbed subband was $K\Delta K = +7$ of $2\nu_4$. The frequencies of the lines in this subband were simply left out of the fit. Small, localized perturbations occured in a few subbands. These were handled acceptably by simply leaving out several lines on either side of the perturbed region.

The process of fitting, predicting new lines, and refitting with those lines included in the fit was continued until no more lines could be identified in the spectra. Then a final fit was made to a frequency expression involving only those terms whose coefficients were "significant" in the next to last fit. Significance was defined as the value of the coefficient being larger than its 95% simultaneous confidence interval.

The results of the final simultaneous analysis of ν_4 and $2\nu_4$ of $CH_3^{(av)}Br$ are given in Table XI. The estimators of the coefficients obtained from the least squares fit are listed, along with their 95% simultaneous confidence intervals. Microwave values of B_o, D_o^J, and D_o^{JK} were input as known quantities. The terms corresponding to these quantities were subtracted from each transition frequency before it was entered into the fit. The available data were apparently not sufficient to allow the program to determine values for the last five quantities listed in Table VII, hence, these were taken to be zero. In any case, they were expected to be extremely small. Values of the coefficients β_4^J, β_4^{JK}, η_4^J, H_o^J, H_o^{JK}, H_o^{KJ} were obtained in the next to last fit, but were not significant according to the above criterion. The terms corresponding to these coefficients were left out of the final fit, hence, these coefficients were also assumed to be zero. The standard deviation of the final simultaneous fit was 0.006 cm^{-1}. A list of the final assignments, observed and calculated frequencies, deviations, and assigned weights for CH_3Br is given in Appendix IV.

The two bands were also fit individually in order to compare the results with those from the simultaneous fit. The results of the single-band fits for ν_4 and $2\nu_4$ are shown in Tables XII and XIII respectively. These fits were made

Table XI Coefficients of Simultaneous Fit of CH_3Br ν_4 and $2\nu_4$.

Coefficient	Value (cm^{-1})	95% s. c. i.
$\nu_o(\nu_4)$	3056.35254097	0.00400511
$\nu_o(2\nu_4 \perp)$	6095.37929332	0.00876727
$\nu_o(2\nu_4 \parallel)$	6046.12775517	0.00755994
A_o	5.12908907	0.00097086
$A_e\zeta_4^z - 1/2\ \eta_4$	0.30493035	0.00070940
D_o^K	0.00003663	0.00003277
α_4^A	0.02849233	0.00038622
η_4^K	-0.00008277	0.00003732
α_4^B	-0.00018444	0.00000621
β_4^K	-0.00001623	0.00000931
H_o^K	0.00000011	0.00000009

All other coefficients were insignificant and were set = 0.

B_o *	0.3185537
D_o^J *	0.000000333
D_o^{JK} *	0.00000427

* Microwave values of $^{12}CH_3{}^{(av)}Br$ taken from Ref. (23).

Standard deviation of fit = 0.006 cm^{-1}.

Table XII Coefficients of Single-Band Fit of CH_3Br ν_4.

Coefficient	Value (cm^{-1})	95% s. c. i.
ν_o	3056.04303491	0.00305341
$A_o - A_e\zeta_4{}^z + 1/2\eta_4 + \eta_{44} - 1/2\eta_4{}^K$	4.82460782	0.00039907
$\alpha_4{}^A - 3/2\eta_4{}^K$	0.02846680	0.00028663
$D_o{}^K - 1/4\eta_4{}^K$	0.00009631	0.00001946
$\alpha_4{}^B$	-0.00021128	0.00001523

All other coefficients were insignificant and were set = 0.

B_o *	0.3185537	
$D_o{}^J$ *	0.000000333	
D_o^{JK} *	0.00000427	

* Microwave values of $^{12}CH_3{}^{(av)}Br$ taken from Ref. (23).

Standard deviation of fit = 0.004 cm^{-1}.

Table XIII Coefficients of Single-Band Fit of CH_3Br $2\nu_4$.

Coefficient	Value (cm^{-1})	95% s. c. i.
ν_o	6095.98964858	0.01222403
$A_o + 2A_e\zeta_4^z - \eta_4 - 3\eta_{44} + \eta_4^K$	5.74130602	0.01015969
$2\alpha_4^A + 3\eta_4^K$	0.05817770	0.00638908
α_4^B	-0.00017740	0.00003036
All other coefficients were insignificant and were set = 0.		
B_o *	0.3185537	
D_o^J *	0.000000333	
D_o^{JK} *	0.00000427	

* Microwave values of $^{12}CH^{(av)}Br$ taken from Ref. (23).

Standard deviation of fit = 0.006 cm^{-1}.

to the expression in Table VI with the appropriate value of k included.

A value of $A_o = 5.1291 \pm 0.0009$ cm^{-1} was obtained from the simultaneous analysis of ν_4 and $2\nu_4$ of $CH_3{}^{(av)}Br$. For comparison, the combined results of the two single-band fits yielded $A_o = 5.131 \pm 0.010$ cm^{-1}. The simultaneous confidence intervals indicate that this result is less accurate than that obtained from the simultaneous fit by a factor of more than ten.

Previous values of A_o for methyl bromide, obtained by application of the zeta-sum rule (Appendix Ia) to analyses using only the unresolved Q-branches of ν_4, ν_5, and ν_6, are given by Herzberg (1) as 5.08 cm^{-1} and Burke (24) as 5.126 cm^{-1}. No estimates of accuracy are listed.

The value of the Coriolis term coefficient, obtained from the simultaneous analysis, was $[A_e\zeta_4{}^z - 1/2\eta_4] = 0.3409 \pm 0.0007$ cm^{-1}. Under the approximations $\eta_4 \approx 0$ and $A_e \approx A_o$, then $\zeta_4{}^z \approx 0.0594$.

The band origins are represented by the pure vibrational terms

$$\nu_o(\nu_4) = (\omega_4+\Delta\omega_4) + 1/2x_{14} + 1/2x_{24} + 1/2x_{34} + 3x_{44} + x_{45} + x_{46} + x_{\ell_4\ell_4} + \text{y-terms},$$

$$\nu_o(2\nu_4 \perp) = 2(\omega_4+\Delta\omega_4) + x_{14} + x_{24} + x_{34} + 8x_{44} + 2x_{45} + 2x_{46} + 4x_{\ell_4\ell_4} + \text{y-terms},$$

$$\nu_o(2\nu_4 \parallel) = 2(\omega_4+\Delta\omega_4) + x_{14} + x_{24} + x_{34} + 8x_{44} + 2x_{45} + 2x_{46} + \text{y-terms}.$$

Numerical values of these band origin constants were obtained from the simultaneous least squares fit. When the second-anharmonic y-terms were neglected, values of two of the anharmonic terms could be extracted: $x_{44} \approx -20.977$ cm^{-1} and $x_{\ell_4\ell_4} \approx 12.313$ cm^{-1}.

The results of the methyl bromide analysis demonstrate very clearly the usefulness of the method of simultaneous analysis in determining A_o. It was very fortunate that methyl bromide was the first molecule to be analyzed in this manner. Subsequent work showed that either ν_4 or $2\nu_4$, or both, were badly perturbed for all of the other methyl halides. This made the analyses much more difficult and the results much less trustworthy. None of the simultaneous analyses attempted for the other methyl halides was nearly as satisfactory as that for methyl bromide.

CHAPTER VIII

ANALYSIS OF CH_3I

Spectra of ν_4 of CH_3I, with band origin near 3060 cm^{-1} and with useable region extending from about 3000 cm^{-1} to 3180 cm^{-1}, were run on the 300 line/mm grating with the spectrometer in single-pass configuration. Two charts of ν_4, 0365-I and 0465-I, were analyzed. They were calibrated with HCl (1-0) (18) on the low-frequency side and HCN (0,0,1) (19) on the high-frequency side. The standard deviations of the calibration fits for both charts were 0.004 cm^{-1}. The details of the experimental conditions under which the spectra were run are given in Table XIV.

Spectra of the $2\nu_4$ band were run on the 600 line/mm grating with the spectrometer in both single and double-pass configurations. The parallel component of $2\nu_4$ has its band origin near 6052 cm^{-1} and extends from about 6030 cm^{-1} to 6080 cm^{-1}. The perpendicular component has its band origin near 6102 cm^{-1}. Its useable region extends from about 6080 cm^{-1} to 6220 cm^{-1}. On the low frequency side, from about ${}^{P}Q_2(J)$ and lower, it is overlapped by the much stronger lines of the parallel component. Four charts of $2\nu_4$, 0165-I, 0265-I, 0166-I, and 0266-I, were analyzed. The calibration bands for all of these were N_2O (3,0,1) (20) on the low-frequency side and HCN (0,0,2) (19) on the high-frequency side. The standard deviations of the calibration fits of all four bands were about 0.006 cm^{-1}. Details of the experimental conditions under which the spectra were

Table XIV Experimental Conditions (CH_3I)

band	chart	calibration bands	grating lines/mm	s.p. or d.p.	source	detector	press. CH_3I	path length
ν_4	0365-I	HCl(1-0) HCN(0,0,1)	300	s.p.	Zr arc box	PbS-P	6 mm	6.4 m
ν_4	0465-I	HCl(1-0) HCN(0,0,1)	300	s.p.	Zr arc box	PbS-P	6 mm	6.4 m
$2\nu_4$	0165-I	N_2O(3,0,1) HCN(0,0,2)	600	s.p.	300 w Zr arc	PbS-N	10 mm	9.6 m
$2\nu_4$	0265-I	N_2O(3,0,1) HCN(0,0,2)	600	d.p.	300 w Zr arc	PbS-N	10 mm	9.6 m
$2\nu_4$	0166-I	N_2O(3,0,1) HCN(0,0,2)	600	s.p.	Zr arc box	PbS-N	30 mm	8 m
$2\nu_4$	0266-I	N_2O(3,0,1) HCN(0,0,2)	600	s.p.	Zr arc box	PbS-N	30 mm	8 m

run are given in Table XIV.

Survey spectra of the ν_4 and $2\nu_4$ bands of CH_3I are shown in Fig. 9. Even in these greatly compressed spectra the resolved rotational fine structure is evident. Perturbations are obvious in both bands. Note the anomalous intensity of the ${}^{R}Q_6(J)$ Q-branch of ν_4, and the split ${}^{R}Q_5(J)$ Q-branch in both bands. Such obvious perturbations serve as a warning to proceed with caution in analyzing the bands.

In the high-resolution spectra of CH_3I a great many lines could be assigned by inspection. The presence of perturbations made assignments in some subbands uncertain, however. The ${}^{R}Q_1(J)$ through ${}^{R}Q_7(J)$ Q-branches of $2\nu_4$ were obviously split. When the ${}^{R}R_K(J)$ series could be identified for these subbands, sharp discontinuities were found corresponding to the split in the Q-branch.

The frequencies of all the lines in each of the six charts were obtained as described in Chapter VI. The line frequencies were weighted according to how well the frequencies seemed to be determined. The frequencies from all the charts of each band were combined into a weighted average. The resolution limits were about 0.04 cm^{-1} in the ν_4 band and 0.06 cm^{-1} in the $2\nu_4$ band.

Since both bands showed considerable evidence of being perturbed, the most productive course of action seemed to be to first analyze the bands individually. They were then combined only after the best possible individual fits had indicated which lines were the least perturbed.

Fig. 9 CH_3I Survey Spectra - ν_4 and $2\nu_4$

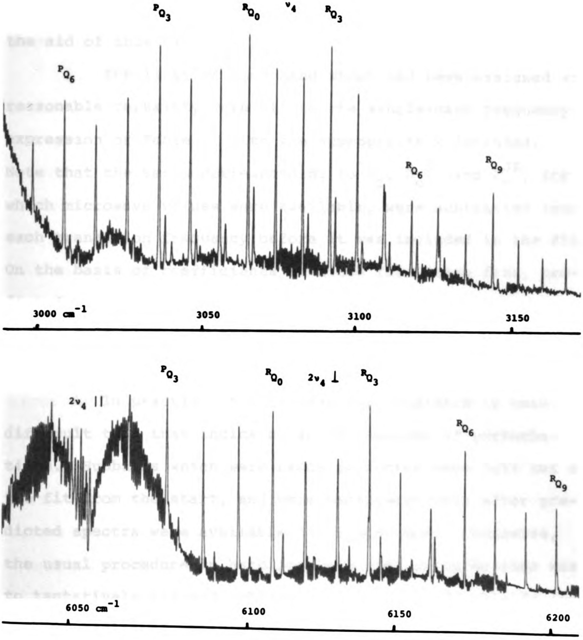

Microwave values of $B_o = 0.2502167\ cm^{-1}$, $D_o^J = 2.09\times10^{-7}\ cm^{-1}$, and $D_o^{JK} = 3.29\times10^{-6}\ cm^{-1}$ (23) were used to calculate a set of ground state combination differences, as described in Chapter VII. Many new lines were assigned with the aid of this table.

The lines of each band which had been assigned with reasonable certainty were fit to the single-band frequency expression of Table VI with the appropriate k included. Note that the terms corresponding to B_o, D_o^J, and D_o^{JK}, for which microwave values were available, were subtracted from each transition frequency before it was included in the fit. On the basis of coefficients obtained from these fits, predicted spectra were calculated. From these new lines were assigned, included in the data for new fits, and the whole process repeated until no further lines were found.

In practice, the process was considerably more difficult than that indicated above, because of perturbations. Subbands which were badly perturbed were left out of the fit from the start, and were considered only after predicted spectra were available for comparison. Otherwise, the usual procedure in handling localized perturbations was to tentatively discard subbands or portions of subbands (not individual lines) which did not seem to fit with the majority of the other lines. Of course, there must be a predominant population of unperturbed lines which fit well.

This procedure worked well for ν_4 of CH_3I. Although the $K\Delta K = -6, -5, +6, +7$, and $+8$ subbands all seemed to be somewhat perturbed and were left out of the final fit, there remained 364 apparently unperturbed lines of the other subbands. These were fit to the expression in Table VI. The results are shown in Table XV. The standard deviation of the fit was 0.005 cm^{-1}.

The perpendicular component of $2\nu_4$ proved to be impossible to treat in this manner. The entire P-side of the band, ${}^{P}Q_2(J)$ and lower, was overlapped by the parallel component. No perpendicular band transitions could be assigned with any degree of certainty in this region. A few of the ${}^{P}P_9(J)$ series should have been available, but none could be identified since $\nu_1 + \nu_4$ also ran through this region. In addition to the loss of nearly half of the band, the subbands $K\Delta K$ = +1 through +7 were all perturbed to varying degrees. ${}^{R}Q_5(J)$ was very badly split and no ${}^{R}R_5(J)$ lines could be identified. In the subbands on either side of ${}^{R}Q_5(J)$ the splitting could be observed to be moving through the Q-branches. In those in which the ${}^{R}R_K(J)$ series could be traced over a considerable distance, sharp discontinuities appeared in the line separations. Fig. 10 shows the ${}^{R}Q_3(J)$ region of $2\nu_4$ in which the split Q-branch and the corresponding shift in the ${}^{R}R_3(J)$ lines is clearly shown.

A discussion of the perturbation in the $2\nu_4$ band is given by Mme. Joffrin-Graffouillere and M. Nguyen Van Thanh (25). They interpret the perturbation as a Fermi resonance between the CH_3I $2\nu_4$ perpendicular component and

Table XV Coefficients of Single-Band Fit of CH_3I ν_4.

Coefficient	Value	95% s. c. i.
ν_o	3069.75141674	0.00469999
$A_o - A_e\zeta_4^z + 1/2\eta_4$ $+ \eta_{44} - 1/2\eta_4^K$	4.83319667	0.00137344
$\alpha_4^A - 3/2\eta_4^K$	0.03056726	0.00117964
$D_o^K - 1/4\eta_4^K$	0.00008539	0.00008007
α_4^B	-0.00012605	0.00001117
β_4^K	0.00012004	0.00008937
H_o^K	-0.00000247	0.00000134

All other coefficients were insignificant andwere set = 0.

B_o *	0.2502167	
D_o^J *	0.00000021	
D_o^{JK} *	0.0000033	

* Microwave values for $^{12}CH_3I$ taken from Ref. (23).

Standard deviation of fit = 0.010 cm^{-1}.

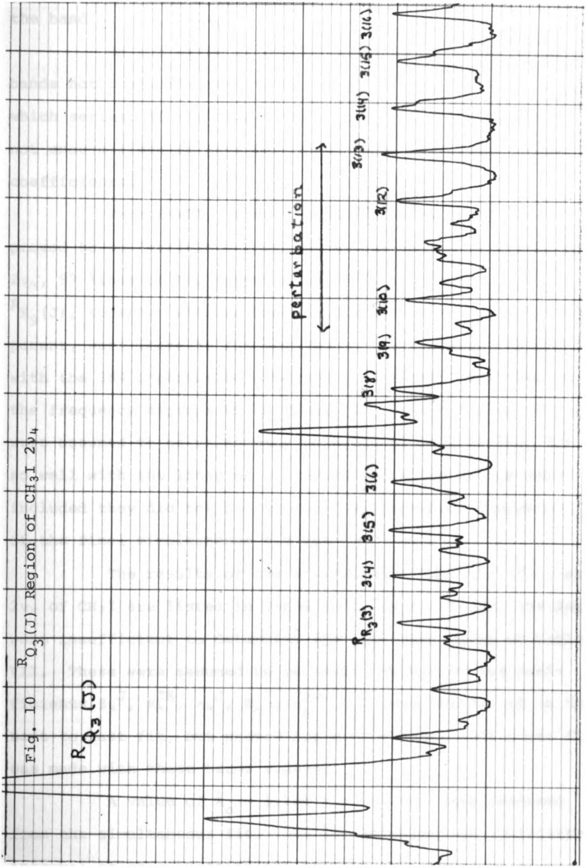

Fig. 10 $^{R}Q_3(J)$ Region of CH_3I $2\nu_4$

the band $\nu_2 + \nu_4 + 2\nu_6$.

On the basis of single-band fits to lines of sub-bands not obviously perturbed, it was not possible to decide which series, if any, were really unperturbed. There were not enough lines to give any sort of useful values of the coefficients.

Fortunately, a simultaneous fit of ν_4 and $2\nu_4$ proved to be feasible. From the perpendicular component of $2\nu_4$, 97 lines of the types ${}^{R}P_{0}(J)$, ${}^{R}R_{0}(J)$, ${}^{R}R_{8}(J)$, and ${}^{R}R_{9}(J)$, together with 56 low-J lines of the $2\nu_4$ parallel component, were found to fit very well in a simultaneous fit with the 364 unperturbed lines of ν_4. The fit was made to the frequency expression in Table VII. These series of $2\nu_4$ were assumed to be relatively unperturbed because they fit so well with the lines of ν_4. When the other series were included they did not fit at all. The standard deviation of the final simultaneous fit was 0.007 cm^{-1}.

The results of the simultaneous analysis of ν_4 and $2\nu_4$ of CH_3I are listed in Table XVI. As for CH_3Br, the data were insufficient to determine the last five terms of Table VII. These were assumed to be zero. Values of the coefficients β_4^{J}, β_4^{JK}, η_4^{J}, H_o^{J}, H_o^{JK}, H_o^{KJ} were determined in the next to last fit, but proved not significant. The final fit was made with these terms removed.

A value of $A_o = 5.134 \pm 0.003$ cm^{-1} was obtained from the simultaneous fit. The 95% simultaneous confidence interval on this quantity has been listed. Because of the

Table XVI Coefficients of Simultaneous Fit of CH_3I ν_4 and $2\nu_4$.

Coefficient	Value	95% s. c. i.
$\nu_o(\nu_4)$	3060.05691147	0.00493212
$\nu_o(2\nu_4 \perp)$	6101.88830686	0.01778452
$\nu_o(2\nu_4 \parallel)$	6052.03783417	0.01064939
A_o	5.13425925	0.00332773
$A_e\zeta_4{}^z - 1/2\ \eta_4$	0.30151603	0.00340549
$D_o{}^K$	0.00008500	0.00008000
$\alpha_4{}^A$	0.03108683	0.00088588
$\eta_4{}^K$	0.00028459	0.00011305
$\alpha_4{}^B$	-0.00012219	0.00000328
$\beta_4{}^K$	0.00008169	0.00003738
$H_o{}^K$	-0.00000215	0.00000083

All other coefficients were insignificant and were set = 0.

B_o *	0.2502167	
$D_o{}^J$ *	0.00000021	
$D_o{}^{JK}$ *	0.0000033	

* Microwave values for $^{12}CH_3I$ taken from Ref. (23).

Standard deviation of fit = 0.007 cm^{-1}.

lack of good data for $2\nu_4$, this value of A_o is statistically less accurate than that obtained for methyl bromide. It may also be less trustworthy. Not only are there fewer lines and fewer subbands of $2\nu_4$ represented in the fit, but there are probably also some slightly perturbed lines included in the fit.

Previous values of A_o for CH_3I, obtained by application of the zeta-sum rule to Q-branch analyses of the three degenerate fundamentals, are given by Herzberg (1) as 5.077 cm^{-1}, by Burke (24) as 5.104 cm^{-1}, and by Jones and Thompson (26) as 5.119 cm^{-1}. Maki and Hexter (8) obtained a value of 5.158 ± 0.02 cm^{-1} from a study of the Coriolis resonance between $\nu_3 + \nu_6$ and ν_5.

Under the approximations $\eta_4 \approx 0$ and $A_e \approx A_o$, one obtains from our results $\zeta_4{}^z \approx 0.059$. Jones and Thompson (26) obtained exactly this same value.

In the same manner as described for CH_3Br, one finds values for the two first-anharmonic consrants $x_{44} \approx -26.57$ cm^{-1} and $x_{\ell_4 \ell_4} \approx 12.46$ cm^{-1}.

CHAPTER IX

ANALYSIS OF CH_3F

For methyl fluoride, A_o was obtained from a simultaneous fit of $\nu_3 + \nu_4$ and $2\nu_4$ after ν_4 proved to be too badly perturbed. Details of how ν_4 and $2\nu_4$ were recorded and analyzed are given below. Details of the analysis of $\nu_3 + \nu_4$ are given in a thesis by W. E. Blass (7) and subsequent paper by Blass and Edwards (22).

Spectra of CH_3F ν_4, with band origin near 3006 cm^{-1} and extending from about 2940 cm^{-1} to 3150 cm^{-1}, were run on the 300 line/mm grating with the spectrometer in single-pass configuration. Two charts of ν_4, 0465-F and 0565-F, were measured and analyzed. They were calibrated with HCl (1-0) (18) and HCN (0,0,1) (19). The standard deviations of the calibration fits were 0.004 cm^{-1}. Details of the experimental conditions under which the spectra were run are given in Table XVII.

Spectra of the $2\nu_4$ band were run on the 600 line/mm grating with the spectrometer in both single and double-pass configurations. The perpendicular component had band origin near 6000 cm^{-1}. Its useable region extended from about 5940 cm^{-1} to 6130 cm^{-1}. No parallel component could be identified. Two charts of $2\nu_4$, 0365-F and 0166-F, were measured and analyzed. These were calibrated with HCl (2-0) (18) and HCN (0,0,2) (19). The standard deviations of the calibration fits were both 0.005 cm^{-1}. Details of the experimental conditions under which the spectra were run

Table XVII Experimental Conditions (CH_3F)

band	chart	calibration bands	grating lines/mm	s.p. or d.p.	source	detector	press. CH_3F	path length
ν_4	0465-F	HCl(1-0) HCN(0,0,1)	300	s.p.	Zr arc box	PbS-P	2 mm	6.4 m
ν_4	0565-F	HCl(1-0) HCN(0,0,1)	300	s.p.	Zr arc box	PbS-P	1.5 mm	6.4 m
$2\nu_4$	0365-F	HCl(2-0) HCN(0,0,2)	600	d.p.	300 w Zr arc	PbS-N	12 mm	9.6 m
$2\nu_4$	0166-F	HCl(2-0) HCN(0,0,2)	600	s.p.	Zr arc box	PbS-N	25 mm	8 m

are given in Table XVII.

The $\nu_3 + \nu_4$ band of CH_3F was analyzed by W. E. Blass as part of a thesis at Michigan State University. A detailed description of this band, ground state combination differences, single-band analyses, perturbations, etc. are given in his thesis, along with a listing of the line assignments and frequencies in this band. Many of these points are also included in the subsequent paper by Blass and Edwards (22).

Survey spectra of ν_4, $2\nu_4$, and $\nu_3 + \nu_4$ are shown in Fig. 11. Even in these compressed spectra the resolved rotational fine structure is evident. Figure 12 shows the $^RQ_6(J)$ region of the $2\nu_4$ band of CH_3F. This is a splendid example of a highly-resolved Q-branch. The individual transitions which make up the Q-branch are resolved and easily measurable. This region is typical of our high-resolution records. The resolution limits were ≈ 0.04 cm^{-1} for ν_4 and ≈ 0.06 cm^{-1} for $2\nu_4$.

The frequencies of the lines in the ν_4 and $2\nu_4$ bands were obtained as described in Chapter VI. The line frequencies were weighted on the basis of how well the frequencies seemed to be determined. The frequencies from both charts of each band were combined into a weighted average frequency.

It was our expectation that ν_4 and $2\nu_4$ of CH_3F would be fit simultaneously to obtain A_o and the other molecular parameters. The bands were fit individually to

Fig. 11 CH_3F Survey Spectra - ν_4, $2\nu_4$, $\nu_3+\nu_4$

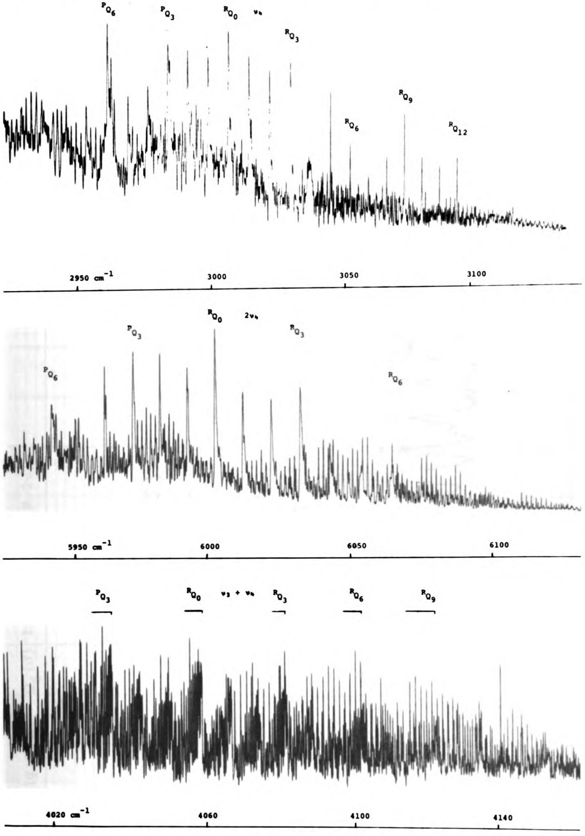

Fig. 12 $^{R}Q_6(J)$ Region of CH_3F $2\nu_4$

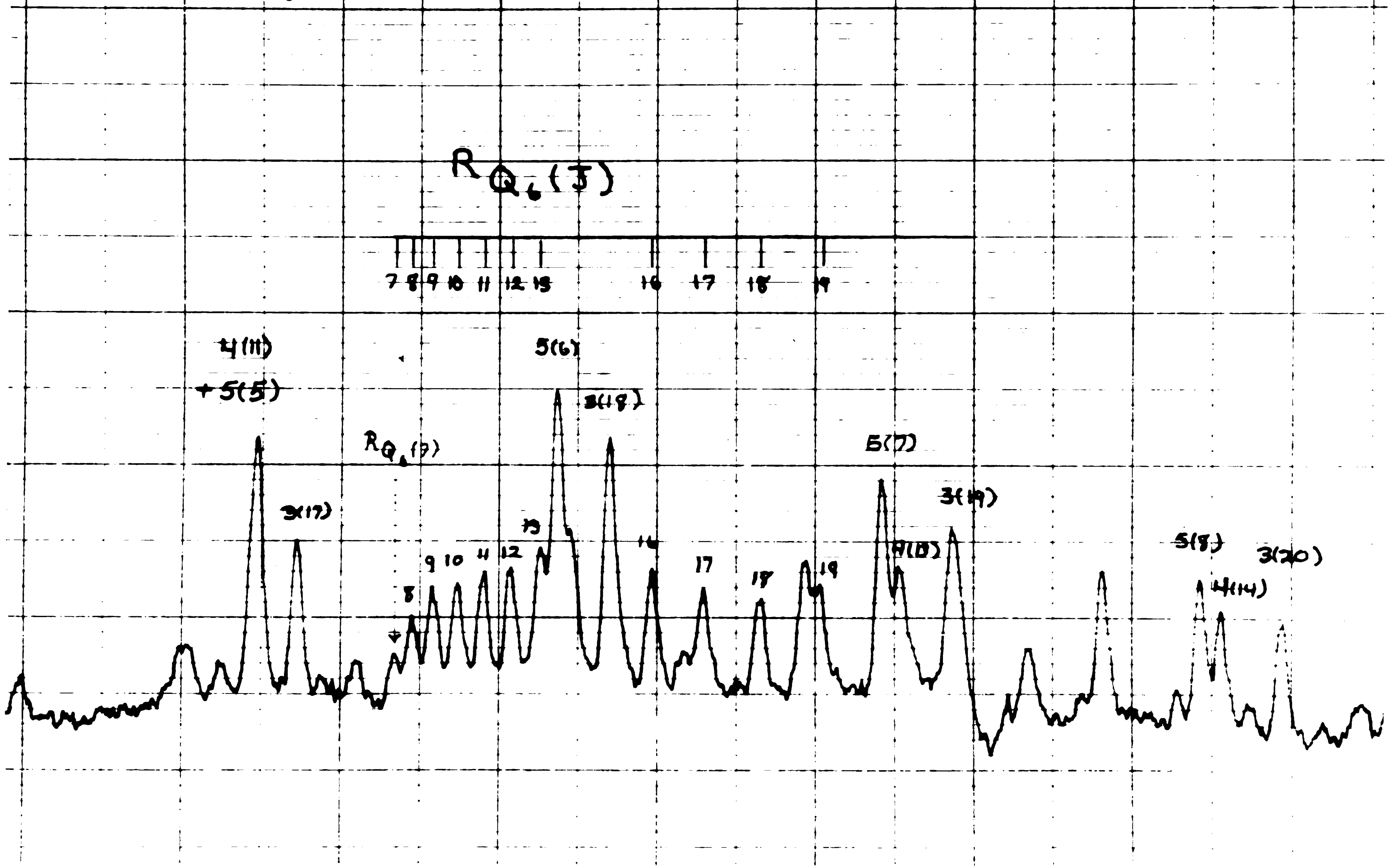

the expression listed in Table VI (with the appropriate value of k included). As usual, in these and subsequent fits, the terms involving $B_o = 0.8517935\ cm^{-1}$, $D_o{}^J = 2.015 \times 10^{-6}\ cm^{-1}$, and $D_o^{JK} = 1.4652 \times 10^{-5}\ cm^{-1}$ (27) were subtracted from each line frequency before it was entered into the fit.

In the high-resolution spectra of $2\nu_4$, two series, $K\Delta K = -4$ and -5 were obviously perturbed, having badly split Q-branches. Single-band fits of $2\nu_4$ soon indicated, in addition, that the $K\Delta K = +6$ through $+9$ series did not fit well with the rest of the band. Eventually 162 lines of the $2\nu_4$ perpendicular component were established as being apparently the least perturbed, although several obvious biases still existed. A fairly good single-band fit (standard deviation $0.013\ cm^{-1}$) was obtained for these lines. The results are given in Table XVIII.

The ν_4 band was obviously badly perturbed. The strong perturbation on the R-side, which Pickworth and Thompson (28) remarked upon in 1954, was quite obvious in our high-resolution spectra. While the normal Q-branches were wide and partly resolved, tailing off to the high frequency side, the $K\Delta K = +4$ Q-branch was spread out over a considerable distance and the $K\Delta K = +5$ and higher Q-branches appeared abnormally narrow. Lines from these subbands did not fit at all with the rest of the band. Even with these series eliminated, the rest of the band fit very poorly. It was difficult to decide which lines, if any could be reasonably called "unperturbed." However,

Table XVIII Coefficients of Single-Band Fit of CH_3F $2\nu_4$.

Coefficient	Value (cm^{-1})	95% s. c. i.
ν_o	6001.37242480	0.01230728
$A_o + 2A_e\zeta_4^z - \eta_4$ $- 3\eta_{44} - \eta_4^K$	5.97016254	0.00304190
$2\alpha_4^A - 3\eta_4^K$	-0.02275383	0.00188018
$D_o^K + 1/2\eta_4^K$	-0.00079118	0.00006587
α_4^B	-0.00112620	0.00004187
β_4^K	0.00003197	0.00002629

All other coefficients were insignificant and were set = 0.

B_o *	0.8517935
D_o^J *	0.000002015
D_o^{JK} *	0.000014652

* Microwave values for $^{12}CH_3F$ taken from Ref. (27).

Standard deviation of fit = 0.013 cm^{-1}.

it was finally found that 92 lines of this band gave a fairly good fit to the theoretical formula (standard deviation 0.020 cm^{-1}) and apparently a fairly well determined set of coefficients. The results are listed in Table XIX.

In spite of the fact that the ν_4 and $2\nu_4$ bands fit fairly well individually, a simultaneous fit of the "unperturbed" lines of both bands gave such a poorly determined set of coefficients and reproduced the data so poorly as to be nearly worthless. No reasonable estimate of A_o and $A_e\zeta_4{}^z$ could be obtained from this fit.

The situation was considerably improved by making use of the "unperturbed" lines of the $\nu_3 + \nu_4$ band, originally analyzed by Blass. The frequency expression to which the data were fit is given in Table VIII.

The results of the simultaneous fit of 196 lines of $\nu_3 + \nu_4$ and 162 lines of $2\nu_4$ are given in Table XX. In view of the perturbed nature of both bands, the fit seemed fairly good (standard deviation 0.015 cm^{-1}). A value of $A_o = 5.104 \pm 0.002$ cm^{-1} was obtained. For comparison, previous values of A_o for CH_3F, obtained from applications of the zeta-sum rule to Q-branch analyses of the three degenerate fundamentals, are listed by Herzberg (1) as 5.100 cm^{-1}, Pickworth and Thompson (28) as 5.11 cm^{-1}, and Andersen, Bak, and Brodersen (29) as 5.095 cm^{-1}. Smith and Mills (30) used 5.081 cm^{-1} obtained through private communication with Andersen, in their calculations.

Under the approximations $\eta_4 \approx 0$ and $A_e \approx A_o$ one

Table XIX Coefficients of Single-Band Fit of CH_3F ν_4.

Coefficient	Value (cm^{-1})	95% s. c. i.
ν_o	3005.28088945	0.01638834
$A_o - A_e\zeta_4^z + 1/2\eta_4$		
$+ \eta_{44} - 1/2\eta_4^K$	4.64091916	0.00327381
$\alpha_4^A - 3/2\eta_4^K$	0.01009577	0.00452974
α_4^B	-0.00144265	0.00012461
β_4^K	0.00023992	0.00023220
All other coefficients were insignificant and were set = 0.		
B_o *	0.8517935	
D_o^J *	0.000002015	
D_o^{JK} *	0.000014652	

* Microwave values for $^{12}CH_3F$ taken from Ref. (27).

Standard deviation of fit = 0.017 cm^{-1}.

Table XX Coefficients of Simultaneous Fit of CH_3F $\nu_3 + \nu_4$ and $2\nu_4$.

Coefficient	Value (cm^{-1})	95% s. c. i.
$\nu_o(\nu_3+\nu_4)$	4057.65311000	0.01446841
$\nu_o(2\nu_4 \perp)$	6000.50578000	0.01522262
A_o	5.10427102	0.00201388
$A_e\zeta_4^z - 1/2\eta_4$	0.43346464	0.00145493
D_o^K	-0.00012201	0.00007953
η_4^K	0.00135226	0.00018699
$\alpha_3^A+\alpha_4^A$	0.02386673	0.00150811
α_4^A	-0.00942605	0.00111255
(α_3^A)	(0.033)	
$\alpha_3^B+\alpha_4^B$	0.01083222	0.00012198
α_4^B	-0.00112829	0.00005408
(α_3^B)	(0.0119)	
$\beta_3^K+\beta_4^K$	0.00002868	0.00002956
β_4^K	0.00002992	0.00003391
(β_3^K)	(-0.000001)	
$\beta_3^J+\beta_4^J$	-0.00000014	0.00000026
β_4^J	0.00000073	0.00000009
(β_3^J)	(-0.0000008)	
$\beta_3^{JK}+\beta_4^{JK}$	-0.00000393	0.00000218
β_4^{JK}	0.00004555	0.00000209
(β_3^{JK})	(-0.00005)	

All other coefficients were insignificant and were set = 0.

Standard deviation of fit = 0.015 cm^{-1}.

obtains $\zeta_4^z \approx 0.085$ from our results. Andersen, Bak, and Brodersen (29) obtained $\zeta_4^z \approx 0.093$.

Our analyses must, however, be considered as, at best, a qualified success. There exists one glaring discrepancy. Our value of $\alpha_4^A = -0.009$ cm^{-1}, obtained essentially from the data of $2\nu_4$ alone, does not correspond to the value $\alpha_4^A = +0,008$ cm^{-1} listed by Andersen, Bak, and Brodersen, and also by Pickworth and Thompson. Their results were obtained from the ν_4 band, and, in fact, are just the result which was obtained when we fit the ν_4 band alone. This value of $\alpha_4^A = +0.008$ cm^{-1} appears to be correct, and that obtained from $2\nu_4$ wrong, for the reasons outlined below.

From $\nu_3 + \nu_4$ we obtained $\alpha_3^A + \alpha_4^A = +0.024$ cm^{-1}. Our value of α_4^A yielded $\alpha_3^A = +0.033$ cm^{-1}. Smith and Mills (30) obtained $\alpha_3^A = +0.011$ cm^{-1} from an analysis of ν_3, and also $2\nu_3$. This seems to be correct, since the appearance of the ν_3 band permits no other conclusion than $\alpha_3^A \approx \alpha_3^B$. There seems to be no difficulty with α_3^B and α_4^B; our results were in good agreement with previous results (28, 29, 30). Furthermore, when $\alpha_4^A = +0.008$ cm^{-1} was used, the result $\alpha_3^A = +0.012$ cm^{-1} was obtained from our results, in excellent agreement with Smith and Mills.

Hence, none of our values of the coefficients are to be trusted implicitly. There does exist some corroborating evidence, however, for at least the values of A_o and $A_e\zeta_4^z$. Single-band fits of the $\nu_3 + \nu_4$ and $2\nu_4$ bands yielded the values of the coefficients $(A_o - A_e\zeta_4^z + \ldots) =$

4.6717 ± 0.0015 cm^{-1} and ($A_o + 2A_e\zeta_4^z + \ldots$) = 5.970 ± 0.003 cm^{-1} respectively. When the above quantities were calculated using the values of A_o and $A_e\zeta_4^z$ from the simultaneous fit of these two bands, the numerical results were identical with those above within the confidence intervals. Since the individual A_o and $A_e\zeta_4^z$ values were obtained from the data of both bands simultaneously, this is strong evidence that the values of these two parameters, at least, are reasonably correct.

CHAPTER X

ANALYSIS OF CH_3CN

Methyl cyanide, CH_3CN, is not one of the methyl halides, but is a C_{3v} axially symmetric molecule. The CN radical takes the place of the halogen atom, lying along the symmetry axis above the apex of the CH_3 radical. The fact that CH_3CN has six atoms rather than five means that there is one more non-degenerate mode and one more degenerate mode of vibration. Because of relabeling, the ν_5 mode of CH_3CN is the one in which the atomic motions are essentially the same as in ν_4 of the methyl halides. Indeed, this band occurs at nearly the same frequency as the ν_4 methyl halide bands.

Only one spectrum of ν_5 of CH_3CN was analyzed, 0266-CN. It was run on the 300 line/mm grating with the spectrometer in single-pass configuration. The band origin was near 3009 cm^{-1}. The spectrum was calibrated with HCl (1-0) (18) and HCN (0,0,1) (19). The standard deviation of the calibration fit was 0.004 cm^{-1}. The experimental conditions under which the spectra were run are given in Table XXI.

Like ν_5, only one spectrum of $2\nu_5$ was run. The reason for this was the extremely poor quality of the $2\nu_5$ spectrum. For some reason, $2\nu_5$ was extremely weak, much weaker relative to ν_5 than any of the methyl halide $2\nu_4$ bands relative to their ν_4 fundamentals. In order to obtain sufficient absorption it was necessary to increase the pressure

Table XXI Experimental Conditions (CH_3CN)

band	chart	calibration bands	grating lines/mm	s.p. or d.p.	source	detector	press. CH_3CN	path length
ν_5	0266-CN	HCl(1-0) HCN(0,0,1)	300	s.p.	Zr arc box	PbS-P	3 mm	6 m
$2\nu_5$	0166-CN	N_2O(3,0,1) HCN(0,0,2)	600	s.p.	Zr arc box	PbS-N	50 mm	6 m

so much that the spectrum was nearly ruined by pressure broadening. The single $2\nu_5$ chart, 0166-CN. was run on the 600 line/mm grating with the spectrometer in single-pass configuration. The band was calibrated with N_2O (3,0,1) (20) and HCN (0,0,2) (19). The standard deviation of the calibration fit was 0.006 cm^{-1}. Details of the experimental conditions under which the spectra were run are given in Table XXI.

Survey spectra of the ν_5 and $2\nu_5$ bands of CH_3CN are shown in Fig. 13. Under high resolution the ν_5 band was quite good, with the resolution limit about 0.04 cm^{-1}. Because of the extreme pressure broadening of lines in $2\nu_5$ the effective resolution in this spectrum is probably no better than ≈ 0.2 cm^{-1}.

Assignment of lines in the two bands presented no difficulty, although there were few identifiable lines in the $2\nu_5$ spectrum. Apparently both bands were nearly unperturbed. The P-side of ν_5 was badly overlapped, so that most of the lines in this band were ${}^{R}R_{K}(J)$ types. All of the $2\nu_5$ lines were ${}^{R}R_{K}(J)$ types.

The ν_5 band was first analyzed alone. The 125 lines assigned in ν_5 gave a quite good fit (standard deviation 0.009 cm^{-1}). The results are given in Table XXII. Microwave values of $B_o = 0.30684219$ cm^{-1}, $D_o^J = 1.27\times10^{-8}$ cm^{-1}, and $D_o^{JK} = 5.901\times10^{-6}$ cm^{-1} (27) were input and held constant. Of course, the few lines of the $2\nu_5$ band could not be meaningfully fit alone.

Fig. 13 CH_3CN Survey Spectra - ν_5 and $2\nu_5$

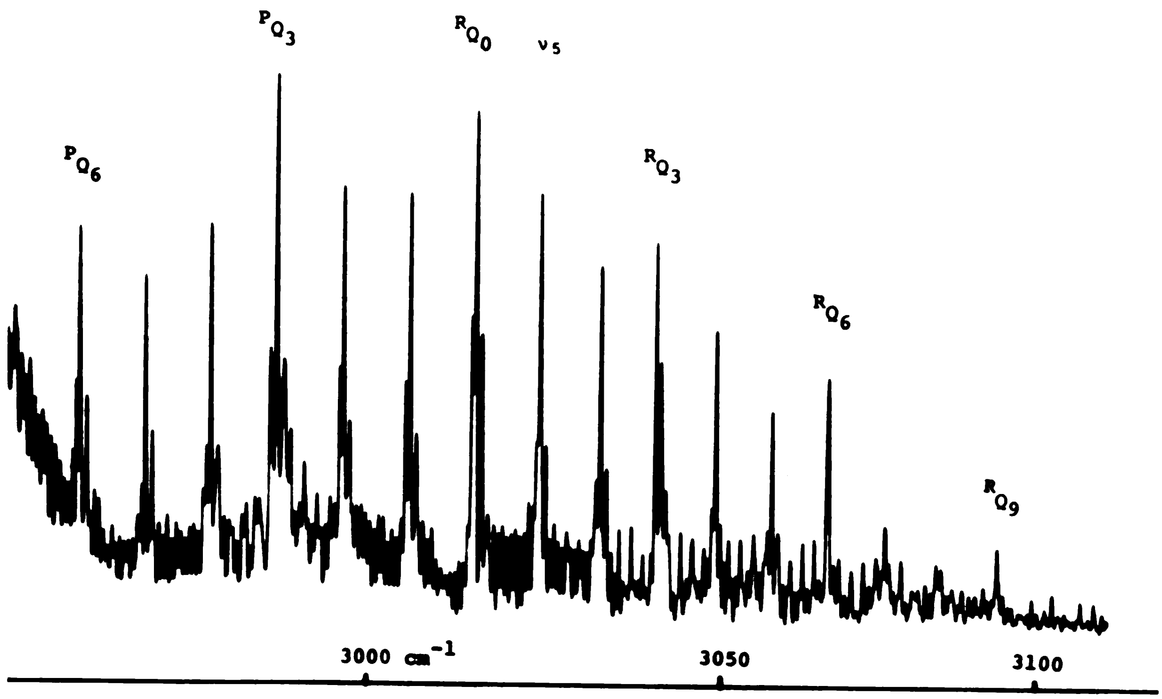

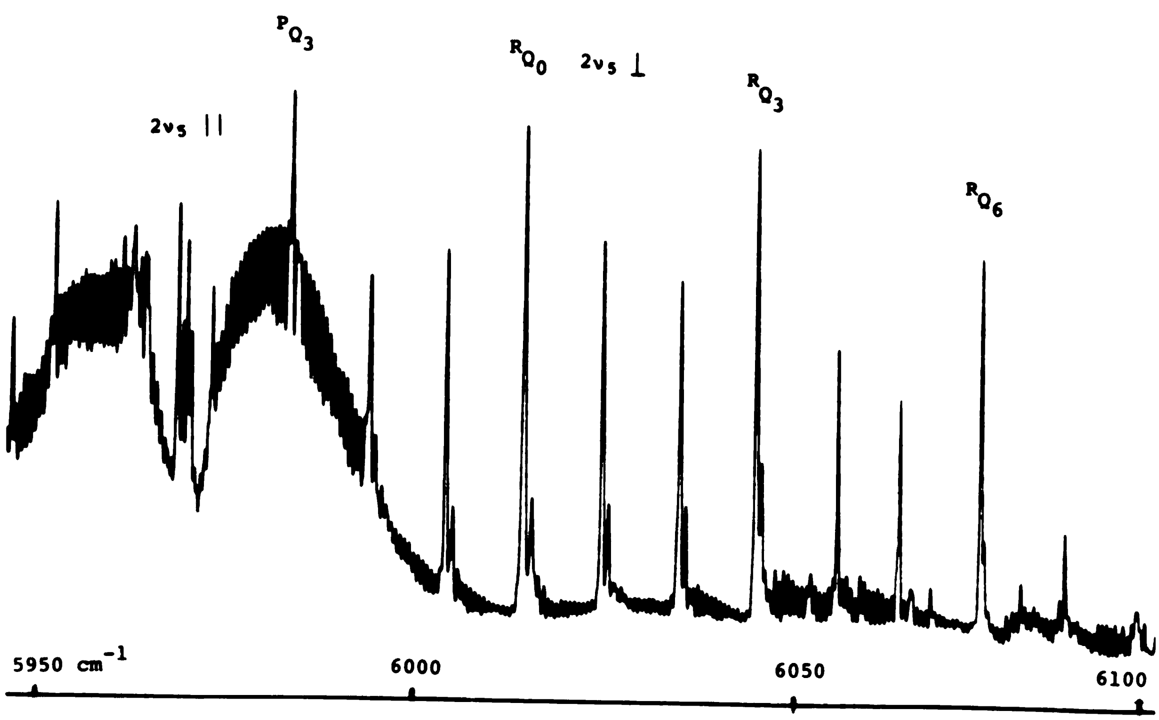

Table XXII Coefficients of Single-Band Fit of CH_3CN ν_5.

Coefficient	Value (cm^{-1})	95% s. c. i.
ν_o	3008.69693446	0.01493334
$A_o - A_e\zeta_5{}^z + 1/2\eta_5$ $+ \eta_{55} - 1/2\eta_5{}^K$	4.96070950	0.00667738
$\alpha_5{}^A - 3/2\eta_5{}^K$	0.03225829	0.00217414
$\alpha_5{}^B$	0.00005397	0.00003211
$\beta_5{}^K$	-0.00002691	0.00001136
All other coefficients were insignificant and were set = 0.		
B_o *	0.30684219	
D_o^J *	0.0000000127	
D_o^{JK} *	0.000005901	

* Microwave values for $^{12}CH_3CN$ taken from Ref. (27).

Standard deviation of fit = 0.009 cm^{-1}.

The results of the simultaneous fit of 125 lines of ν_5 and 20 lines of $2\nu_5$ are given in Table XXIII. They are quite poor, as would be expected under the circumstances, although the standard deviation of the fit was 0.008 cm^{-1}. There was simply not enough data from $2\nu_5$ to permit an accurate calculation of A_o. The value of A_o obtained from the simultaneous fit was 5.03 ± 0.06 cm^{-1}.

Table XXIII Coefficients of Simultaneous Fit of CH_3CN ν_5 and $2\nu_5$.

Coefficient	Value (cm^{-1})	95% s. c. i.
$\nu_o(\nu_5)$	3009.11122113	0.01541944
$\nu_o(2\nu_5\ \perp)$	6005.95747459	0.23498695
A_o	5.02644866	0.06439253
$A_e\zeta_5{}^z + 1/2\ \eta_5$	0.32828684	0.02075757
$D_o{}^K$	0.02382226	0.00162153
$\alpha_5{}^A$	-0.14282842	0.02742596
$\eta_5{}^K$	0.02476328	0.00146676
$\alpha_5{}^B$	0.00007866	0.00001360
$\beta_5{}^K$	0.00655623	0.00027944
$H_o{}^K$	-0.00004544	0.00000185

All other coefficients were insignificant and were set = 0.

B_o *	0.30684219	
$D_o{}^J$ *	0.0000000127	
D_o^{JK}	0.000005901	

* Microwave values for $^{12}CH_3CN$ taken from Ref. (27).

Standard deviation of fit = 0.008 cm^{-1}.

CHAPTER XI

ANALYSIS OF CH_3Cl

Spectra of ν_4 of CH_3Cl, with band center near 3044 cm^{-1} were run on the 300 line/mm grating with the spectrometer in single-pass configuration. Two charts of ν_4, 0465-Cl and 0565-Cl, were measured and analyzed. They were calibrated with HCl (1-0) (18) and HCN (0,0,1) (19). The standard deviations of both calibration fits were 0.004 cm^{-1}. The experimental conditions under which the spectra were run are given in Table XXIV.

Spectra of the $2\nu_4$ band were run on the 600 line/mm grating with the spectrometer in both single and double-pass configurations. The parallel component had its band origin near 6015 cm^{-1}; the perpendicular component had its band origin near 6065 cm^{-1}. Like the corresponding bands of CH_3Br and CH_3I, its P-side was lost due to overlap of the parallel component. Two charts were measured, 0365-Cl and 0166-Cl. They were calibrated with N_2O (3,0,1) (20) and HCN (0,0,2) (19). The standard deviations of the calibration fits were 0.006 cm^{-1}. Details of the experimental conditions under which the spectra were run are given in Table XXIV.

Survey spectra of the ν_4 and $2\nu_4$ bands of CH_3Cl are shown in Fig. 14. The resolved rotational fine structure is evident even in these rapid scan spectra.

Also evident, however, in even these highly compressed spectra is the very pronounced perturbation in the $2\nu_4$ band. Under high-resolution the effects of the per-

Table XXIV Experimental Conditions (CH_3Cl)

band	chart	calibration bands	grating lines/mm	s.p. or d.p.	source	detector	press. CH_3Cl	path length
ν_4	0465-Cl	HCl(1-0) HCN(0,0,1)	300	s.p.	Zr arc box	PbS-P	6 mm	6.4 m
ν_4	0565-Cl	HCl(1-0) HCN(0,0,1)	300	s.p.	Zr arc box	PbS-P	3 mm	6.4 m
$2\nu_4$	0365-Cl	N_2O(3,0,1) HCN(0,0,2)	600	d.p.	300 w Zr arc	PbS-N	10 mm	9.6 m
$2\nu_4$	0166-Cl	N_2O(3,0,1) HCN(0,0,2)	600	s.p.	Zr arc box	PbS-N	30 mm	8 m

Fig. 14 CH_3Cl Survey Spectra - ν_4 and $2\nu_4$

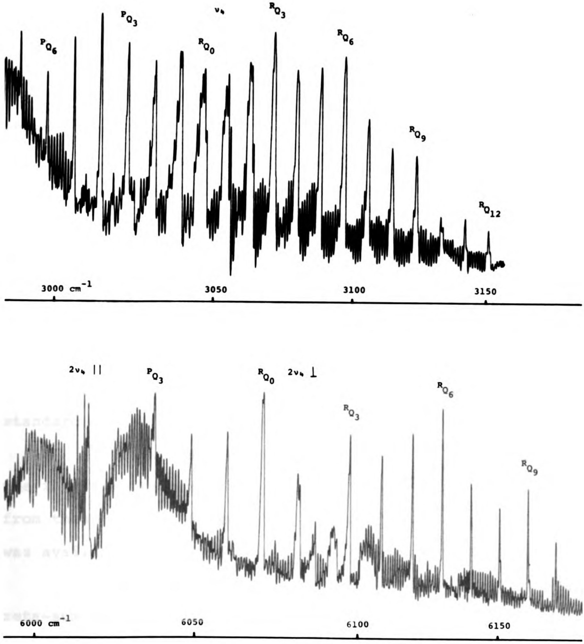

turbation are even more pronounced. The ${}^{R}Q_{2}(J)$ Q-branch is split and spread over a wide region. The neighboring Q-branches are also badly split and pushed about. It was quite impossible to obtain any sort of reasonable unperturbed fit of this band, either alone or in a simultaneous fit with ν_4. Alamichel, Bersellini, and Joffrin-Graffouillere (31) have interpreted the perturbation as a Fermi resonance between $2\nu_4$ and $\nu_4 + \nu_5 + \nu_6 + \nu_3$.

The ν_4 band of CH_3Cl was considerably better, though by no means perfect. Most of the center of the band appeared to be somewhat perturbed, but a quite good single-band fit was obtained from the ${}^{P}P_{3}(J)$ series and the ${}^{R}R_{4}(J)$ through ${}^{R}R_{12}(J)$ series. Microwave values of $B_o = 0.443402$ cm^{-1}, $D_o^{J} = 6.04\times10^{-7}$ cm^{-1}, and $D_o^{JK} = 6.60\times10^{-6}$ cm^{-1} (23) for $CH_3{}^{(av)}Cl$ were taken as known quantities. The results of the single-band fit of ν_4 are given in Table XXV. The standard deviation of the fit was 0.010 cm^{-1}.

The $2\nu_4$ band was simply too badly perturbed to use in a simultaneous fit, hence A_o could not be determined from these bands. No substitute band of the type $\nu_n + 2\nu_4$ was available, nor is one likely to soon become available.

Previous values of A_o, determined by means of the zeta-sum rule method, are given by Herzberg (1) as 5.097 cm^{-1} and Burke (24) as 5.069 cm^{-1}. This represents one case where the zeta-sum rule is still the only method for determining A_o because of perturbations in the $2\nu_4$ spectrum.

Table XXV Coefficients of Single-Band Fit of CH_3Cl ν_4.

Coefficient	Value (cm^{-1})	95% s. c. i.
ν_o	3043.34494889	0.06030692
$A_o - A_e\zeta_4{}^z + 1/2\eta_4 + \eta_{44} - 1/2\eta_4{}^K$	4.37359326	0.00566803
$\alpha_4{}^A - 3/2\eta_4{}^K$	-0.07489814	0.00595875
$D_o{}^K - 1/4\eta_4{}^K$	0.00140707	0.00016057
$\alpha_4{}^B$	0.00101681	0.00009425
$H_o{}^K$	0.00000150	0.00000025

All other coefficients were insignificant and were set = 0.

B_o *	0.443402	
$D_o{}^J$ *	0.000000604	
D_o^{JK} *	0.00000660	

* Microwave values for $^{12}CH_3Cl$ taken from Ref. (23).

Standard deviation of fit = 0.011 cm^{-1}.

CHAPTER XII

ANALYSIS OF CH_3D

This section on CH_3D is included only for the sake of completeness, since both the ν_4 and $2\nu_4$ bands were too badly perturbed to treat in the usual manner.

Two charts of CH_3D ν_4, 0465-D and 0565-D, and two charts of $2\nu_4$, 0365-D and 0166-D, were measured. The calibration bands were the same as those for CH_3F (Chapter IX) and the standard deviations of the calibration fits were the same. The experimental conditions under which the spectra of CH_3D were run are given in Table XXVI. Survey spectra of ν_4 and $2\nu_4$ are shown in Fig. 15.

The spectrum of $2\nu_4$ of CH_3D under high resolution was quite beautiful. All the individual lines, even in the perpendicular band Q-branches, are resolved. Unfortunatly, the appearence of this band belies its true nature. The assignments of most of the lines were quite obvious and unambiguous. They simply did not fit the theoretical formula, however. In the end, no satisfactory fit was obtained for this band. The results of such fits have not even been included here. For future reference, the values of B_o = 3.88047 cm^{-1}, D_o^J = 5.277×10^{-5} cm^{-1}, and D_o^{JK} = 1.238×10^{-4} cm^{-1} were given us by Bruce D. Olson (32). These seemed to be quite good, since a table of ground state combination differences calculated from these constants permitted accurate identification of a large number of lines in the $2\nu_4$ spectrum.

Table XXVI Experimental Conditions (CH_3D)

band	chart	calibration bands	grating lines/mm	s.p. or d.p.	source	detector	press. CH_3D	path length
ν_4	0465-D	HCl(1-0) HCN(0,0,1)	300	s.p.	Zr arc box	PbS-P	2 mm	6.4 m
ν_4	0565-D	HCl(1-0) HCN(0,0,1)	300	s.p.	Zr arc box	PbS-P	2 mm	6.4 m
$2\nu_4$	0365-D	HCl(2-0) HCN(0,0,2)	600	d.p.	300 w Zr arc	PbS-N	12 mm	9.6 m
$2\nu_4$	0166-D	HCl(2-0) HCN(0,0,2)	600	s.p.	Zr arc box	PbS-N	25 mm	8 m

Fig. 15 CH_3D Survey Spectra - ν_4 and $2\nu_4$

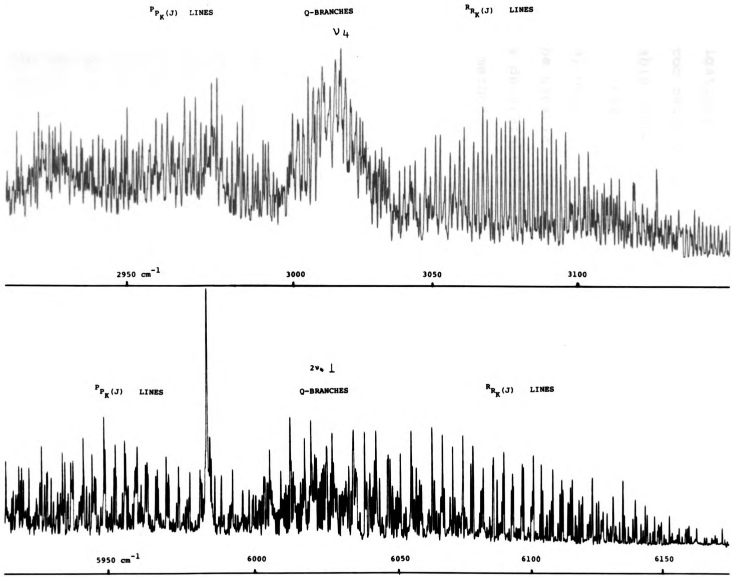

The ν_4 band was not even attempted. The perturbations in this band have been the subject of intensive investigations by Olson and co-workers (33). The band seems to be too badly perturbed to have any hope of making a reasonable "unperturbed" fit.

Olson (32) has suggested to us that, in his opinion, only $\nu_3 + \nu_4$ of the possible alternative bands might be useable. The lack of a good fit to $2\nu_4$, however, makes a determination of A_o for this molecule unfeasible by our method.

CHAPTER XIII

STRUCTURAL CONSIDERATIONS

Once A_o had been determined for methyl bromide, it seemed that the calculation of the structure of this molecule would be a simple and productive project. This quickly proved to be a much more difficult undertaking than it appeared at first glance.

The structure of methyl bromide is specified by three structural parameters (see Fig. 16) - r_{CBr}, r_{CH}, and β or α. The two moment of inertia equations, corresponding to A_o and B_o, for a single isotopic molecular species are not sufficient to completely determine these three unknown parameters. Thus, measurements of A_o and B_o for a second isotopic species, for example Br or C substituted, are needed. For the non-deuterated species, A_o can be assumed to be the same, since substitution of Br or C should make little difference in the positions of the hydrogen atoms. Very accurate values of B_o are available from microwave work for the various isotopic species.

Let us consider the problem of determining a "ground state" or "r_o" structure directly from measured values of A_o and B_o for two isotopic species of CH_3Br. Assume that the values of A_o and B_o are available for the isotopic species $^{12}CH_3{}^{79}Br$ and $^{12}CH_3{}^{81}Br$ (A_o can be assumed to be the same for both species). Thus the structural parameters r_{CBr}, r_{CH}, and β are to be determined from the moment of inertia equations corresponding to I_o^B (for $^{12}CH_3{}^{79}Br$),

$I_o^{B'}$ (for $^{12}CH_3{}^{81}Br$), and I_o^A(for both) - three equations in three unknowns. A major assumption implicit here is that the ground state structure is identical for both species.

The principal axes system is chosen as shown in Fig. 16, with the origin at the center of mass, the z-axis along the symmetry axis, and the x-axis chosen (arbitrarily) such that one of the hydrogen atoms lies in the x-z plane. For convenience, "s" represents the distance from the bromine atom to the center of mass of the particular molecular species under consideration. The equations will be written in terms of r_{CBr}, r_{CH}, and β. The set of equations can be made simpler in appearence if they are left written in terms of the above three parameters plus s and s' for the two species, and the s and s' quantities are related to the structural parameters through the two center of mass equations. The moment of inertia and center of mass equations which are solved for the r_o-structure are given below, with I_o^B, M_{Br}, and s being unique to $^{12}CH_3{}^{79}Br$ and $I_o^{B'}$, M_{Br}', and s' being unique to $^{12}CH_3{}^{81}Br$:

1. $I_o^A = 3M_H[r_{CH}\sin(\pi/2 - \beta)]^2$

2. $I_o^B = M_{Br}s^2 + M_C(r_{CBr} - s)^2 + M_H[(r_{CBr} - s)$
   $+ r_{CH}\cos(\pi/2 - \beta)]^2 + 2M_H\{[(r_{CBr} - s) + r_{CH}\cos(\pi/2 - \beta)]^2$
   $+ [r_{CH}\sin(\pi/2 - \beta)\cos30°]^2\}$

3. $M_{Br}s - M_C(r_{CBr} - s) - 3M_H[(r_{CBr} - s) + r_{CH}\cos(\pi/2 - \beta)]$

4. $I_o^{B'} = M_{Br}'s'^2 + M_C(r_{CBr} - s')^2 + M_H[(r_{CBr} - s')$

Fig. 16 CH_3Br Structural Parameters

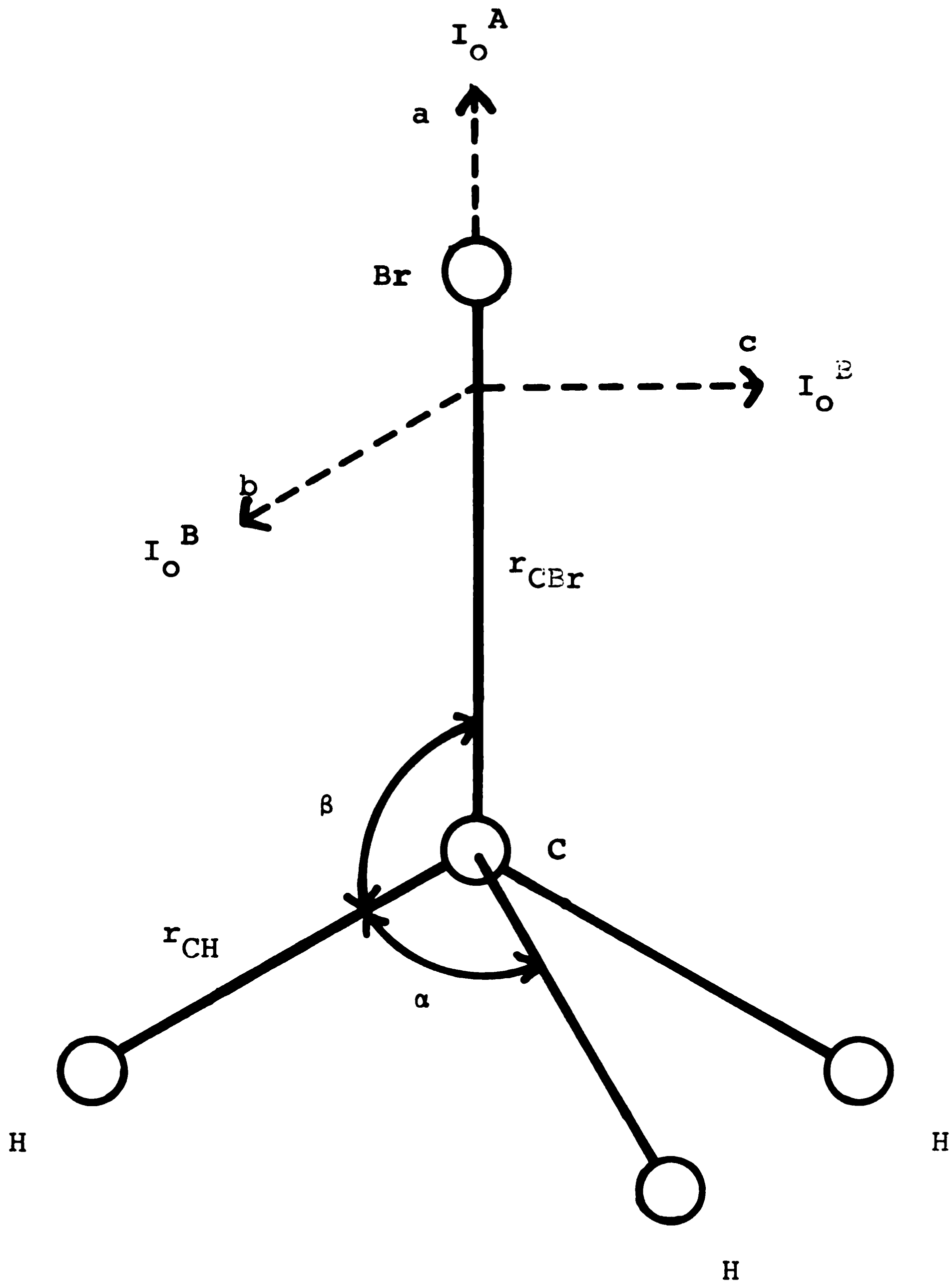

$+ r_{CH}\cos(\pi/2 - \beta)]^2 + 2M_H\{[(r_{CBr} - s') + r_{CH}\cos(\pi/2 - \beta)]^2$

$+ [r_{CH}\sin(\pi/2 - \beta)\cos 30°]^2\}$

5. $M_{Br}'s' - M_C(r_{CBr} - s') - 3M_H[(r_{CBr} - s') + r_{CH}\cos(\pi/2 - \beta)]$

The reduction of these equations to formulas for r_{CBr}, r_{CH}, and β is quite complicated but straightforeward. The final values were calculated on the computer using a program which substituted the known quantities into the above equations and performed the complicated calculations quickly and accurately.

Calculations of the r_o-structure were carried out for the four pairs of isotopic species ($^{12}CH_3{}^{79}Br$ and $^{12}CH_3{}^{81}Br$), ($^{13}CH_3{}^{79}Br$ and $^{13}CH_3{}^{81}Br$), ($^{12}CH_3{}^{79}Br$ and $^{13}CH_3{}^{79}Br$), and ($^{12}CH_3{}^{81}Br$ and $^{13}CH_3{}^{81}Br$). The results are shown in Table XXVII.

The results are obviously very inconsistant. Costain (34) discusses this problem. He points out that the molecular parameter B_o (and similarly A_o) is proportional to the average over the zero-point vibrations of the reciprocal of the "true" moment of inertia, viz.,

$$B_o = \frac{h}{8\pi^2 c}\left\langle \frac{1}{\sum_i m_i r_i^2} \right\rangle ,$$

where the r_i are the "true" instantaneous distances of the atoms from the b-axis. The effective ground state moment of inertia, I_o^B, is defined through

$$B_o = \frac{h}{8\pi^2 c}\frac{1}{I_o^B} ,$$

Table XXVII r_o Structural Parameters

Isotropic species from which structure is derived	r_{CBr}	r_{CH}	β(Br-C-H)	α(H-C-H)
$^{12}CH_3{}^{79}Br$, $^{12}CH_3{}^{81}Br$	1.9295 A	1.111 A	110° 11'	108° 46'
$^{13}CH_3{}^{79}Br$, $^{13}CH_3{}^{81}Br$	1.9314	1.109	109° 54'	109° 02'
$^{12}CH_3{}^{79}Br$, $^{13}CH_3{}^{79}Br$	1.9391	1.098	108° 12'	110° 43'
$^{12}CH_3{}^{81}Br$, $^{13}CH_3{}^{81}Br$	1.9391	1.098	108° 12'	110° 43'

hence I_o^B is actually given by

$$I_o^B = \left\langle \frac{1}{\sum_i m_i r_i^2} \right\rangle^{-1}.$$

In setting up the moment of inertia equations in the manner described above, one implicitly defines the effective atomic distances, $(r_o)_i$, such that

$$I_o^B = \sum_i m_i (r_o)_i^2 = \left\langle \frac{1}{\sum_i m_i r_i^2} \right\rangle^{-1}.$$

When isotopic substitutions are made, the zero-point vibrations change, hence the averages over the zero-point vibrations also change. This makes the r_o distances slightly different for each species.

In order to solve the moment of inertia equations one must assume that the r_o quantities are not changed by isotopic substitution, since, otherwise, new unknown parameters enter into the problem. The r_o-structures for different isotopic species obtained in this manner are usually inconsistant. Our results have borne out this conclusion.

Costain points out that these large variations arise essentially from the attempt to force the r_o parameters to exactly reproduce the I_o values from which they were obtained. There is no reason why an artificial structure of this sort, which is known to be not consistant among different isotopic species, should exactly reproduce the effective moments of inertia. The criterion that correctness is defined by the closeness with which the calculated parameters reproduce the original data should be reconsidered in this case.

The problem of determining a meaningful structure from the ground state constants is discussed by Kraitchman (35) and Costain (34). Both stress the point that the assumption of identical structures for different isotopic species is, at best, valid only for the equilibrium structure.

The equilibrium structure is generally the ideal of structural investigations. In the first place, the equilibrium structure is theoretically the same for all the isotopic species of a molecule. Also, it should be directly and simply comparable among different molecules of the same type. Secondly, although the equilibrium structure is not a true physical structure (the molecule is never more than instantaneously in the equilibrium state), all sorts of other structures, ground state, upper state, average, etc. can be determined from the equilibrium structure. Also, structures directly comparable to electron diffraction, etc. structures can be calculated from the equilibrium structure.

The equilibrium structure would be calculated by means of the moment of inertia and center of mass equations listed previously, with the difference that now I_e^A, I_e^B, and $I_e^{B'}$ would be used. This means that theoretically the equations are exactly true then - the quantities $r_{CBr}|_e$, $r_{CH}|_e$, and $\beta|_e$ are actually the same for both species. Unfortunately, the equilibrium constants A_e and B_e are related to the ground state constants A_o and B_o through the α_s^A and

α_s^B constants which must be determined experimentally for each of the six vibrational modes of the molecule. The relations are

$$A_e = A_o + \sum_{s=1}^{6} \alpha_s^A (g_s/2),$$

$$B_e = B_o + \sum_{s=1}^{6} \alpha_s^B (g_s/2).$$

Until the six values of α_s^A and α_s^B, or at least the value of the above sums, have been determined spectroscopically, the quantities A_e and B_e cannot be determined.

Kraitchman (35) and Costain (34) discuss the calculation of a much more consistant structure known as the "substitution structure." Kraitchman develops the formulas for determining the distance of a substituted atom in an isotopic molecule from the center of mass of the original "normal" molecule. These are developed as an aid to obtaining equilibrium structures when the equilibrium moments of inertia are known. In this context, the basic assumption, that the structure is identical for both species, is entirely valid.

For axially symmetric molecules two cases have to be considered. If the substituted atom lies on the symmetry axis (e. g., substitution of ^{81}Br for ^{79}Br in CH_3Br) then the distance from the substituted atom to the center of mass of the original molecule ($CH_3{}^{79}Br$) is given by

$$|z| = [\mu^{-1}(I^{B'} - I^{B})]^{1/2},$$

where I^B and $I^{B'}$ represent the moments of inertia about a principal axis perpendicular to the symmetry axis for the "normal" and isotopically substituted molecule respectively, and $\mu = M\Delta m/(M + \Delta m)$, M being the mass of the "normal" molecule and $(M + \Delta m)$ being the mass of the isotopically substituted molecule.

For the substitution of an off-axis atom (e. g., substitution of D for one H in CH_3Br) Kraitchman derives expressions for the distance of that atom from the center of mass of the original molecule. Since deuterium substitutions were never used in our calculations, these expressions are not reproduced here.

Costain suggests that these same expressions, while exact only for the equilibrium structure, are nevertheless very useful in calculating a "substitution" structure. Although this substitution structure is still quite artificial, it should be a great deal more consistant than the r_o-structures.

Briefly, a complete substitution structure requires measurement of the moments of inertia for enough isotopically substituted species that each independent atom in the molecule has been substituted once. For example, to obtain a complete substitution structure for CH_3Br one should measure A_o and B_o for $^{12}CH_3{}^{79}Br$, $^{12}CH_3{}^{81}Br$, $^{13}CH_3{}^{79}Br$, and $^{13}CH_3{}^{81}Br$, and A_o, B_o, and C_o for at least one of the singly-deuterated species, and preferably all of them.

One point must be considered, however, before proceeding with the calculation of a substitution structure of CH_3Br. The basic assumption underlying all of this is, again, that all of the isotopic species have identical substitution or r_s-structures. Since we are now dealing with ground state effective moments of inertia this assumption does not necessarily hold. Most certainly it does not hold in the case of substitution of deuterium for hydrogen. The bond lengths are known to generally shrink appreciably when deuterium is substituted for hydrogen (36). Thus, determination of the positions of the H atoms using D substitution seemed unlikely to yield satisfactory results.

The final procedure which we settled upon was as follows. Fortunately for us, Schwendeman and Kelley (37) had already determined the $r_{CBr}|_s$ substitution bond lengths from microwave measurements of the B_o values for the four non-deuterated species of CH_3Br. Using each isotopic molecule in turn as the basis molecule, they calculated $r_{CBr}|_s$ for each species as follows: Referring to Fig. 17, assume that $^{12}CH_3{}^{79}Br$ is taken as the basis molecule. A substitution of ^{81}Br for ^{79}Br permits a calculation of distance z (the distance from the substituted atom to the center of mass of the original molecule),

$$|z| = [\mu^{-1}(I_o^{B'} - I_o^{B})]^{1/2},$$

where I_o^B and $I_o^{B'}$ refer to $^{12}CH_3{}^{79}Br$ and $^{12}CH_3{}^{81}Br$ respectively, and $\mu = M\Delta m/(M + \Delta m)$, where M represents the mass of the former species and $(M + \Delta m)$ the mass of the latter. Again, with $^{12}CH_3{}^{79}Br$ as the basis molecule, a substitution of ^{13}C for ^{12}C will give distance z',

$$|z'| = [\mu'^{-1}(I_o^{B''} - I_o^{B})]^{1/2},$$

where I_o^B refers to $^{12}CH_3{}^{79}Br$ and $I_o^{B''}$ refers to $^{13}CH_3{}^{79}Br$;

Fig. 17 CH_3Br Substitution Parameters

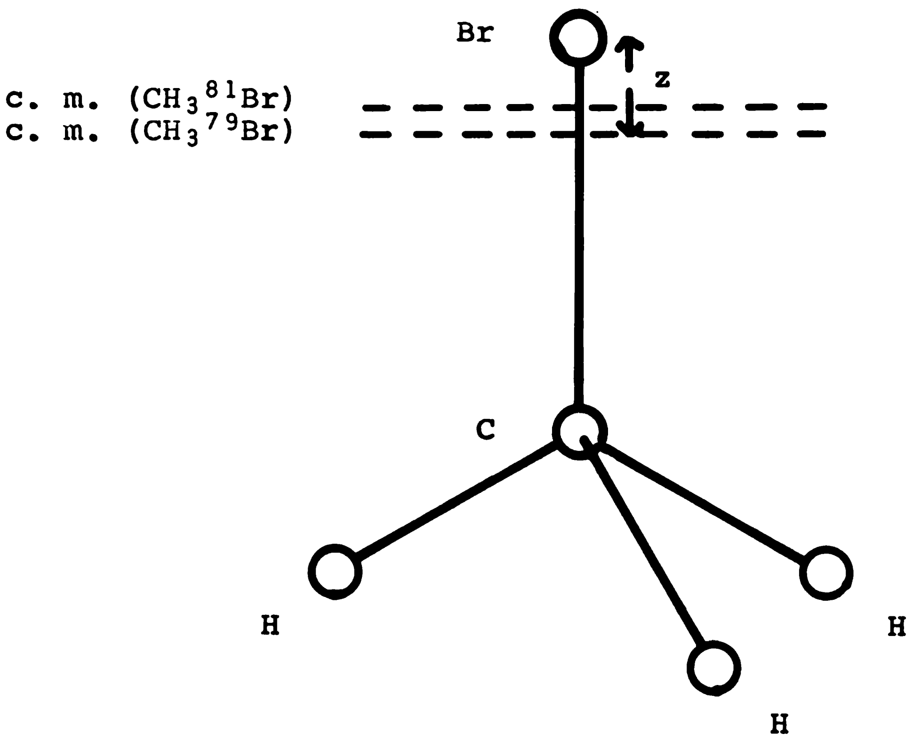

Assume $CH_3{}^{79}Br$ is the basis molecule and $CH_3{}^{81}Br$ is the substituted molecule. Then

$$z^2 = \frac{M + \Delta M}{M\Delta M} \Delta I_o^B$$

where

ΔM = $M' - M$,

M = total mass of $CH_3{}^{79}Br$ molecule,

M' = total mass of $CH_3{}^{81}Br$ molecule,

ΔI_o^B = $I_o^{B'} - I_o^B$.

μ' is the appropriate redefinition of μ above. The sum of the two distances gives $r_{CBr}|_s$ for $^{12}CH_3{}^{79}Br$.

We used Schwendeman and Kelley's values of $r_{CBr}|_s$ as known quantities, and from our value of A_o and the microwave values of B_o for each species as given by Schwendeman and Kelley (37), calculated the r_{CH} and β parameters for each isotopic species. This did not yield a true substitution structure (as defined by Costain), but gave some sort of effective values for r_{CH} and β. For want of a better name, however, they will be referred to here as substitution values. Our results of these calculations are listed in Table XXVIII, along with Schwendeman and Kelley's values of $r_{CBr}|_s$. It is clear that these results are much better than the r_o-structural parameters, but there is still considerable inconsistancy.

Table XXIX shows results obtained in just the same manner except that the appropriate center of mass equation was used instead of the I_o^B equation. These results are remarkably consistant among all the species. For this reason we feel that these constitute our best results for the structure of methyl bromide.

Table XXX gives the single set of values which we consider to be the best average structure of methyl bromide. This consists of an average of Schwendeman and Kelley's values of $r_{CBr}|_s$ and an average of our values of r_{CH} and β. For comparison, results obtained by Miller, Aamodt, Dousmanis, Townes, and Kraitchman (38) who combined values of

Table XXVIII r_s Structural Parameters Derived from $r_{CBr}|_s$, I_o^A, and I_o^B

Isotopic species from which structure is derived	r_{CBr}*	r_{CH}	β(Br-C-H)	α(H-C-H)
$^{12}CH_3{}^{79}Br$	1.9388 A	1.108 A	109° 46'	109° 11'
$^{12}CH_3{}^{81}Br$	1.9389	1.108	109° 45'	109° 12'
$^{13}CH_3{}^{79}Br$	1.9389	1.106	109° 33'	109° 24'
$^{13}CH_3{}^{81}Br$	1.9389	1.107	109° 34'	109° 22'

* $r_{CBr}|_s$ values from Schwendeman and Kelley (37).

Table XXIX r_s Structural Parameters Derived from $r_{CBr}|_s$, I_o^A, and Center of Mass Equation

Isotopic species from which structure is derived	r_{CBr}*	r_{CH}	β(Br–C–H)	α(H–C–H)
$^{12}CH_3{}^{79}Br$	1.9388	1.096	107° 55'	110° 59'
$^{12}CH_3{}^{81}Br$	1.9389	1.096	107° 55'	110° 59'
$^{13}CH_3{}^{79}Br$	1.9389	1.096	107° 57'	110° 56'
$^{13}CH_3{}^{81}Br$	1.9389	1.096	107° 57'	110° 56'

* $r_{CBr}|_s$ values from Schwendeman and Kelley (<u>37</u>).

Table XXX r_s Structural Parameters - Best Average

Source of r_s structure	r_{CBr}	r_{CH}	β(Br-C-H)	α(H-C-H)
This work, best average	1.9389 A*	1.096 A†	107° 56'†	110° 58'†
Miller, et al. (38)	1.9393 A	1.100 A	107° 53'	111° 00'

* $r_{CBr}|_s$ values from Schwendeman and Kelley (37).

† Average of structural parameters from Table XXIX.

B_o for the four non-deuterated isotopic species of CH_3Br with values of $B_o - C_o$ for two doubly-deuterated species. The agreement between their result and ours is excellent.

Our conclusion is that, while one can calculate various sorts of artificial structures which are more or less consistant among themselves, determination of a really satisfying and meaningful structure must probably wait until equilibrium molecular constants are available.

CHAPTER XIV

CONCLUSION

A method has been developed here for determining accurate values of A_o for axially symmetric molecules. It consists essentially of simultaneously analyzing a degenerate fundamental band, ν_t, and its first overtone, $2\nu_t$. In such an analysis the A_o and Coriolis terms in the frequency expression representing those bands are linearly independent of each other. A least squares fit of the data of both bands to a frequency expression general enough to represent both simultaneously yielded individual values of these parameters. The frequency expression used in the analyses was the appropriate specialization of the Amat-Nielsen generalized frequency expression.

The data which was fit to this expression consisted of frequencies of the individual transitions in the resolved rotational fine structure - lines of the types $^PP_K(J)$, $^PR_K(J)$, $^RP_K(J)$, $^RR_K(J)$, and in cases where the Q-branches were resolved, $^PQ_K(J)$ and $^RQ_K(J)$. In some cases, lines of the overtone parallel component were also included. The least squares fits were performed on a large computer capable of inverting the large normal equation matrices.

Excellent values of A_o, $A_e\zeta_4{}^z + \ldots$, and the other molecular constants were obtained for CH_3Br. None of the other methyl halides or methyl halide-types yielded comparable results, due to perturbations in one or more of the bands.

Descriptions of our method of obtaining A_o and its application to CH_3Br and CH_3I have been recently published in the Journal of Molecular Spectroscopy (39, 40, 41).

Accurate values of A_o for the methyl halides are essential for the calculation of molecular structures. As noted in Chapter XIII, our value of A_o for CH_3Br could be combined with microwave values of B_o for four isotopic species of CH_3Br to obtain a consistant, though artificial, "substitution structure."

Calculation of the equilibrium structures of these molecules is our main goal. It will be a difficult goal to realize. Accurate values of A_e and B_e are needed, and these can be obtained only after values of $\alpha_s{}^A$ and $\alpha_s{}^B$ for each of the six normal modes of the molecules have been measured experimentally.

The equilibrium structure is a very worthwhile goal, however. There are many advantages to having such a structure. The equilibrium structures should be directly comparable among isotopic species of a molecule and among different molecules of the same type. Also, many of the other interesting structures (ground state, upper state, average, r. m. s., etc.) can be calculated from the equilibrium structure.

Accurate equilibrium structures for the methyl halides should also provide a firm base for determining accurate and consistant sets of force constants and potential functions for these molecules. In this way it should be possible to eventually arrive at a detailed understanding of the interactions involved in one of the few many-body problems in nature in which a theory is available of an accuracy equalling that of the experimental data.

LIST OF REFERENCES

1. G. Herzberg, "Infrared and Raman Spectra of Polyatomic Molecules," Van Nostrand, Princeton, New Jersey, 1945.

2. M. Goldsmith, G. Amat, and H. H. Nielsen, J. Chem. Phys. 24, 1178 (1956);

   G. Amat, M. Goldsmith, and H. H. Nielsen, J. Chem. Phys. 27, 838 (1957);

   G. Amat and H. H. Nielsen, J. Chem. Phys. 27, 845 (1957);

   G. Amat and H. H. Nielsen, J. Chem. Phys. 29, 665 (1958);

   G. Amat and H. H. Nielsen, J. Chem. Phys. 36. 1859 (1962);

   M. Grenier-Besson, G. Amat, and H. H. Nielsen, J. Chem. Phys. 36, 3454 (1962);

   S. Maes, J. Mol. Spectry. 9, 204 (1962);

   Stewart K. Kurtz, thesis, Ohio State University, 1960.

3. B. T. Darling and D. M. Dennison, Phys. Rev. 57, 128 (1940).

4. G. Amat, Compt. rend. 250, 1439 (1960).

5. H. Allen and P. Cross, "Molecular Vib-Rotors," Wiley, New York, 1963.

6. I. M. Mills, Mol. Phys. 8, 363 (1964).

7. W. E. Blass, thesis, Michigan State University, 1962.

8. A. G. Maki and R. Hexter, to be published.

9. R. G. Brown and T. H. Edwards, J. Chem. Phys. 28, 384 (1958).

10. F. B. Hildebrand, "Introduction to Numerical Analysis," McGraw-Hill, New York, 1956.

11. M. A. Efroymsen, "Mathematical Methods for Digital Computers," Ralston and Wilf (Eds.), p 191, New York, 1960.

12. Henry Scheffe, "The Analysis of Variance," p. 78 ff, Wiley, New York, 1959.

13. J. W. Boyd, thesis, Michigan State University, 1962.

14. J. L. Aubel, thesis, Michigan State University, 1964.

15. D. B. Keck, J. L. Aubel, T. H. Edwards, and C. D. Hause, 1966 Symposium on Molecular Spectroscopy and Molecular Structure, Columbus, Ohio.

16. D. B. Keck, forthcoming thesis, Michigan State University, 1967.

17. K. N. Rao, C. J. Humphreys, and D. H. Rank, "Wavelength Standards in the Infrared," Academic Press, New York, 1966.

18. D. H. Rank, D. P. Eastman, B. S. Rao, and T. A. Wiggins, J. Opt. Soc. Am. 52, 1 (1962).

19. D. H. Rank, G. Skorinko, D. P. Eastman, and T. A. Wiggins, J. Mol. Spectry. 4, 518 (1960).

20. D. H. Rank, D. P. Eastman, B. S. Rao, and T. A. Wiggins, J. Opt. Soc. Am. 51, 929 (1961).

21. Gerald W. King, "Spectroscopy and Molecular Structure," Holt, Reinhart, and Winston, New York, 1964.

22. W. E. Blass and T. H. Edwards, to be published.

23. W. O. J. Thomas, J. T. Cox, and W. Gordy, J. Chem. Phys. 22, 1718 (1954).

24. Richard J. Burke, thesis, University of Maryland, 1954.

25. C. Joffrin-Grafouillere and Nguyen Van Thanh, to be published.

26. E. W. Jones and H. W. Thompson, Proc. Roy. Soc., London 288A, 50 (1965).

27. D. A. Steiner and W. Gordy, J. Mol. Spectry. 21, 291 (1966).

28. J. Pickworth and H. W. Thompson, Proc. Roy. Soc., London A222, 443 (1954).

29. F. A. Andersen, Børge Bak, and S. Brodersen, J. Chem. Phys. 24, 989 (1956).

30. W. L. Smith and I. M. Mills, J. Mol. Spectry. 11, 11 (1963).

31. C. Alamichel, A. Bersellini, and C. Joffrin-Grafouillere, to be published.

32. B. W. Olson, private communication.

33. B. W. Olson, 1966 Symposium on Molecular Spectroscopy and Structure, Columbus, Ohio.

34. C. C. Costain, J. Chem. Phys. 29, 864 (1958).

35. J. Kraitchman, Am. J. Phys. 21, 17 (1958).

36. C. H. Townes and A. L. Schawlow, "Microwave Spectroscopy," p. 54, McGraw-Hill, New York, 1955.

37. R. H. Schwendeman and J. D. Kelley, J. Chem. Phys. 42, 1132 (1965).

38. S. L. Miller, L. C. Aamodt, G. Dousmanis, C. H. Townes, and J. Kraitchman, J. Chem. Phys. 20, 1112 (1952).

39. T. L. Barnett and T. H. Edwards, J. Mol. Spectry. 20, 347 (1966).

40. T. L. Barnett and T. H. Edwards, J. Mol. Spectry. 20, 352 (1966).

41. T. L. Barnett and T. H. Edwards, to be published.

42. D. R. J. Boyd and H. C. Longuet-Higgins, Proc. Roy. Soc. A213, 55 (1952).

43. E. H. Richardson, S. Brodersen, L. Krause, and H. L. Welch, J. Mol. Spectry. 8, 406 (1962).

APPENDIX I

ALTERNATE METHODS OF OBTAINING A_o

a. Use of the Zeta-Sum Rule

Almost all previous determinations of A_o for the methyl halides have been based on the zeta-sum rule. The theory of the zeta-sum rule has been developed by D. R. J. Boyd and H. C. Longuet-Higgins (42). For a C_{3v} type molecule one has

$$\sum_t \zeta_t^z = (\#\text{ atoms on symmetry axis}) - 2 + B/2A,$$

which becomes for a CH_3X type molecule

$$\sum_t \zeta_t^z = B/2A.$$

The application of the zeta-sum rule in the determination of A_o proceeds as follows: From single-band analyses of ν_4, ν_5, and ν_6 (Q-branch analyses are sufficient at a minimum) one determines the numerical values, represented by C_4, C_5, and C_6, of the coefficients

$$[A_o - A_e\zeta_4^z + \ldots] = C_4$$

$$[A_o - A_e\zeta_5^z + \ldots] = C_5$$

$$[A_o - A_e\zeta_6^z + \ldots] = C_6.$$

Then

$$3A_o - A_e(\zeta_4^z + \zeta_5^z + \zeta_6^z) + \ldots = C_4 + C_5 + C_6,$$

or

$$3A_o - A_e(B_o/2A_o) + \ldots = C_4 + C_5 + C_6.$$

Then, to the approximations $A_e \approx A_o$ and the η-terms (represented + ...) being negligible, one finds

$$A_o \approx (1/3)(C_4 + C_5 + C_6) + B_o/6.$$

The zeta-sum rule is exactly true only to the approximation of purely harmonic vibrations. This arises from the ζ_t^{z} constants being defined in terms of purely harmonic quantities, the $\ell_{is\sigma}^{\alpha}$ (2),

$$\zeta_{s\sigma s'\sigma'}^{\alpha} = \sum_i (\ell_{is\sigma}^{\beta}\ell_{is'\sigma'}^{\gamma} - \ell_{is'\sigma'}^{\beta}\ell_{is\sigma}^{\gamma}).$$

The $\ell_{is\sigma}^{\alpha}$ are coefficients involved in the small-vibration expansion of the potential energy of the molecule. As such, they are inherently harmonic, since all usual small-vibration expansions assume harmonic vibrations.

b. Analysis of Raman Spectra

A_0 can be determined for the methyl halides directly from a fully resolved Raman spectrum of the molecule in the gas phase. Let us consider the Raman spectrum of the ν_4 band. If available, the infrared ν_4 band might be fit along with the Raman spectrum for statistically better determination of the coefficients.

As in the case of the simultaneous analysis of ν_4 and $2\nu_4$, the vital factor in the determination of A_0 from Raman spectra is the selection rule on $\Delta\ell_4$. The selection rules on $\Delta\ell_4$ for Raman spectra are given by Mills (6) or may be derived from Amat's Rule (4) for the ν_4 Raman band:

$$\Delta K - \Delta\ell_4 = \pm 3p, \quad p = 0,1,2,\ldots$$

$$|\Delta\ell_4| = 1, 3, \ldots$$

Then, for $\Delta K = \pm 1$,

$$\pm 1 - \Delta\ell_4 = 0, \quad p = 0$$

$$\Delta\ell_4 = \pm 1 \text{ or}$$

$$\Delta\ell_4 = \Delta K;$$

and for $\Delta K = \pm 2$,

$$\pm 2 - \Delta \ell_4 = \pm 3, \quad p = 1$$

$$-\Delta \ell_4 = \pm 1 \text{ or}$$

$$\Delta \ell_4 = -1/2 \Delta K.$$

If lines of both the $\Delta K = \pm 1$ and $\Delta K = \pm 2$ types are available from the Raman spectrum, the A_o and Coriolis terms are linearly independent and the two coefficients can be determined individually, just as in the case of the simultaneous fit of ν_4 and $2\nu_4$. Such an analysis has already been carried out by Richardson, Brodersen, Krause, and Welch (43) for CH_3D.

APPENDIX II

LISTING OF FALSTAF PROGRAM

FALSTAF was the least squares computer program which was used to analyze the spectra considered in this thesis. Using this program the observed individual transition frequencies were fit to the appropriate specializations of the Amat-Nielsen generalized frequency expression. The program listed here is that used for the final simultaneous analysis of ν_4 and $2\nu_4$ of methyl bromide.

LISTING OF FALSTAF PROGRAM FOR LEAST SQUARES SIMULTANEOUS ANALYSIS OF CH3BR NU4 AND 2NU4.

```
      PROGRAM FALSTAF
      DIMENSION DATA(20),VECTOR(21,21),AVE(20),SIGMA(20),COEN(20),
     1SIGMCO(20),INDEX(20),FVAL(15,5,4),CONFINT(20),IHEAD(20),KDEL(1000),
     2,JDEL(1000),KAY(1000),JAY(1000),FREQOBS(1000),WHT(1000),DEV(1000),
     3INCRVIB(1000),WGT(1000)
      COMMON NOIN, INDEX, COEN, BZRO, DZROJK, DZROJ
      TYPE DOUBLE VECTOR,SIGMA,SIGY,SIGMCO,COEN,AVE
C     IFWT = 1,THEN ALL WHTS = 1.0                                      MPR2
C     IFSTEP = 1, DO NOT PRINT EACH STEP                                MPR2
C     IFRAW  = 1   DO NOT PRINT RAW SUMS AND SQUARES                    MPR2
C     IFAVE  = 1   DO NOT PRINT AVERAGES                                MPR2
C     IFRESD = 1   DO NOT PRINT RESIDUAL SUMS SQUARES                   MPR2
C     IFCOEN = 1   DO NOT PRINT PARTIAL COEFFICIENTS                    MPR2
C     IFPRED = 1   DO NOT CALC PREDICTED VALUES                         MPR2
C     IFCNST = 1   DO NOT HAVE CONST TERM IN EQUATION                   MPR2
C     HEADING AND INPUT
      CALL FAULT(0)
  100 TOL = .00000001 $ EFIN = .00000001 $ EFOUT = .00000001 $ NOPROB=0
      IFSTEP=0 $ IFRAW=0 $ IFAVE=0 $ IFRESD=0 $ IFCOEN=0 $ IFPRED=0
      IFCNST=1 $ NOTIMES=0 $ VAR=0.0 $ K=0 $ FLEVEL=0.0 $ NOENT=0
      NOMIN=0 $ NOMAX=0
      PRINT 107
  107 FORMAT (1H1)
      NZILCH = 0
      NOIN = 0
  102 REWIND 50
      DO 103 NUM = 1, 100
      READ 101, (IHEAD(M), M=1,12)
  101 FORMAT (12A6)
      IF (IHEAD(2) - 6HENDHED) 103,104,103
  103 PRINT 101, (IHEAD(M), M=1,12)
  104 CONTINUE
      READ 105, NOVAR
  105 FORMAT (I2)
      NVP1 = NOVAR + 1
      DO 120 I = 1,NVP1
      DO 120 J = 1,NVP1
  120 VECTOR (I,J) = 0.0
      SUMWT = 0.0
      DO 125 IPROB = 1,4,2
C     IPROB = 1, 2, 3, 4 IMPLIES CONFIDENCE LEVELS OF 95, 97.5, 99, 99.5
      DO 124 IDEGF = 1, 5
C     IDEGF = 1, 2, 3, 4, 5 IMPLIES DEGREES OF FREEDOM (N - P) = 30,
C     40, 60, 120, INFINITE
      READ 123, (FVAL(INOV,IDEGF,IPROB),INOV=1,13)
C     INOV = 1, 2, ..., 10, 11, 12, 13 IMPLIES NUMBER OF VARIABLES (P) =
C     1, 2, ..., 10, 12, 15, 20
  123 FORMAT (13F4.2)
  124 CONTINUE
  125 CONTINUE
```

```
      READ 140, BZRO, DZROJK, DZROJ
  140 FORMAT (F15.8)
      READ 141, NORFTS
  141 FORMAT (I2)
      DO 160 L = 1, 500
      L1 = 3*L - 2  $  L2 = 3*L
      READ 145, (KDEL(N),JDEL(N),KAY(N),JAY(N),FREQOBS(N),WHT(N),
     1INCRVIB(N), N = L1, L2)
  145 FORMAT (3(A1,A1,I2,1X,I2,1X,F8.3,1X,F4.2,1X,I1,2X))
      DO 159 N = L1, L2
      IF (WHT(N)) 109, 110,109
  110 NZILCH = NZILCH + 1
  109 CONTINUE
      IF (KDEL(N) - 1HF) 146,161,146
  146 SUMWT = SUMWT + WHT(N)
      NODATA = N
  159 CONTINUE
  160 CONTINUE
  161 AVEWT = SUMWT/NODATA
      DO 510 N = 1, NODATA
      WHT(N) = WHT(N) / AVEWT
      IF (KDEL(N) - 1HQ) 162,163,164
  162 KDEL(N) = -1  $  GO TO 165
  163 KDEL(N) = 0  $  GO TO 165
  164 KDEL(N) = +1  $  GO TO 165
  165 IF (JDEL(N) - 1HQ) 166,167,168
  166 JDEL(N) = -1  $  GO TO 169
  167 JDEL(N) = 0  $  GO TO 169
  168 JDEL(N) = +1  $  GO TO 169
  169 CONTINUE
      DELTA1 = KAY(N) + KDEL(N)
      DELTA2 = KAY(N)
      DELTA3 = JAY(N) + 1 + JDEL(N)
      DELTA4 = JAY(N) + JDEL(N)
      DELTA5 = JAY(N) + 1
      DELTA6 = JAY(N)
      IF (INCRVIB(N) - 1) 210, 190,200
C      FORMS DATA(L) FOR NU-4
  190 DATA(1) = 1.0  $  DATA(2) = 0.0  $  DATA(3) = 0.0
      LDEL = KDEL(N)
      GO TO 210
  200 IF (KDEL(N)) 201,202,201
C      FORMS DATA(L) FOR 2NU-4 PERPENDICULAR
  201 DATA(2) = 1.0  $  DATA(1) = 0.0  $  DATA(3) = 0.0
      GO TO 203
C      FORMS DATA(L) FOR 2NU-4 PARALLEL
  202 DATA(3) = 1.0  $  DATA(1) = 0.0  $  DATA(2) = 0.0
  203 LDEL = -2*KDEL(N)
  210 AA = INCRVIB(N)*(DELTA4*DELTA3 - DELTA1**2)
      AB = INCRVIB(N)*DELTA1**4
      AC = LDEL*DELTA1*DELTA4*DELTA3
      AD = INCRVIB(N)*DELTA4**2*DELTA3**2
      AE = INCRVIB(N)*DELTA1**2*DELTA4*DELTA3
      AF = DELTA4*DELTA3-DELTA6*DELTA5 - DELTA1**2+DELTA2**2
```

```
      AG = DELTA1**2*DELTA4*DELTA3 - DELTA2**2*DELTA6*DELTA5
      AH = DELTA4**2*DELTA3**2 - DELTA6**2*DELTA5**2
      AI = INCRVIB(N)*DELTA1**2
      AJ = LDEL*DELTA1**3
      AK = DELTA1**4 - DELTA2**4
      AL = DELTA3**3*DELTA4**3 - DELTA5**3*DELTA6**3
      AM = DELTA3**2*DELTA4**2*DELTA1**2 - DELTA5**2*DELTA6**2*DELTA2**2
      AN = DELTA3*DELTA4*DELTA1**4 - DELTA5*DELTA6*DELTA2**4
      AO = DELTA1**6 - DELTA2**6
      AP = (INCRVIB(N) + 1)*LDEL*DELTA1
      AQ = (INCRVIB(N)**2 + 2*INCRVIB(N))*DELTA1**2
      AR = LDEL**2*DELTA1**2
      AS = (INCRVIB(N)**2 + 2*INCRVIB(N))*(DELTA4*DELTA3 - DELTA1**2)
      AT = LDEL**2*(DELTA4*DELTA3 - DELTA1**2)
      DATA(4) = DELTA1**2 - DELTA2**2
      DATA(5) = -2.*LDEL*DELTA1
      DATA(6) = AK
      DATA(7) = AI
      DATA(8) = AJ
      DATA(9) = AA
      DATA(10) = AB
      DATA(11) = AO
      SUBTOFF = BZRO*AF - DZROJK*AG - DZROJ*AH
      DATA(NOVAR) = FREQOBS(N) - SUBTOFF
      RUN = N
      WRITE TAPE 50, RUN,(DATA(L), L=1,NOVAR),SUBTOFF,IDBAND
C     MAIN PROGRAM
  530 DO 540 I = 1, NOVAR
  550 VECTOR(I,NOVAR+1) = VECTOR(I,NOVAR+1) + DATA(I)*WHT(N)
  560 DO 540 J = I, NOVAR                                               MPR
  540 VECTOR(I,J) = VECTOR(I,J) + DATA(I)*DATA(J)*WHT(N)
  510 VECTOR(NVP1,NVP1) = VECTOR(NVP1,NVP1) + WHT(N)
      REWIND 50
      NOSTAT = NODATA - NZILCH
  565 NOVMI = NOVAR - 1                                                 MPR
  566 NOVPL = NOVAR + 1                                                 MPR
      DMAXM = 0.0
  567 PRINT 90, NOPROB,NODATA,NOVAR,VECTOR(NOVPL,NOVPL)
  570 IF (IFRAW) 900, 580, 650                                          MPR
  580 PRINT 15
  590 PRINT 20, (I,VECTOR(I,NOVPL),I=1,NOVMI)
  600 PRINT 25, VECTOR(NOVAR,NOVPL)
  610 PRINT 30
  620 PRINT 35, ((I,J,VECTOR(I,J),J=1,NOVMI),I=1,NOVMI)
  630 PRINT 40, (I,VECTOR(I,NOVAR),I=1,NOVMI)
  640 PRINT 45, VECTOR(NOVAR,NOVAR)
  645 GO TO 650                                                         MPR
C     CALCULATION OF RESIDUAL SUMS OF SQUARES AND CROSS PRODUCTS        MPR
  650 IF(IFCNST) 900,651,735                                            MPR
  651 IF(VECTOR(NOVPL,NOVPL)) 652,652,655                               MPR
  652 PRINT 654
  653 GO TO 910
  655 DO 660 I = 1, NOVAR
  670 DO 660 J = I, NOVAR
```

```
660 VECTOR (I,J) = VECTOR (I,J) - (VECTOR(I,NOVPL) * VECTOR (J,NOVPL) MPR2
   - / VECTOR (NOVPL, NOVPL))
680 DO 690  I = 1, NOVAR
690 AVE(I)  = VECTOR(I,NOVPL) / VECTOR(NOVPL,NOVPL)                  MPR2
700 IF (IFAVE)   900, 710, 735                                       MPR2
710 PRINT 50
720 PRINT 20, (I,AVE(I),I=1,NOVMI)
730 PRINT 25, AVE(NOVAR)
735 IF (IFRESD)  900, 740, 780                                       MPR2
740 PRINT 55
750 PRINT 35, ((I,J,VECTOR(I,J),J=1,NOVMI),I=1,NOVMI)
760 PRINT 40, (I,VECTOR(I,NOVAR),I=1,NOVMI)
770 PRINT 45, VECTOR(NOVAR,NOVAR)
780 NOSTEP = -1                                                      MPR2
781 ASSIGN  1320  TO NUMBER                                          MPR2
782 DEFR   = VECTOR(NOVPL,NOVPL) - 1.0                               MPR2
790 DO 800  I = 1,NOVAR                                              MPR2
791 IF(VECTOR(I,I)) 792,794,810                                      MPR2
792 PRINT  793, I                                                    MPR2
798 GO TO 910                                                        MPR2
793 FORMAT (31H ERROR RESIDUAL SQUARE VARIABLE I4,31H IS NEGATIVE,PROBMPR2
   1LEM TERMINATED )                                                 MPR2
794 PRINT 795, I
796 SIGMA(I) =     1.0                                               MPR2
797 GO TO 800                                                        MPR2
795 FORMAT (1H010H VARIABLE I5,13H IS CONSTANT )                     MPR2
810 SIGMA(I) = DSQRT(VECTOR(I,I))
800 VECTOR(I,I) = 1.0                                                MPR2
820 DO 830  I = 1,NOVMI                                              MPR2
840 IP1 = I + 1                                                      MPR2
841 DO 830 J = IP1, NOVAR                                            MPR2
850 VECTOR(I,J) = VECTOR(I,J) /( SIGMA(I)* SIGMA(J))                 MPR2
830 VECTOR(J,I) = VECTOR(I,J)                                        MPR2
860 IF (IFCOEN)  900, 870, 1000                                      MPR2
870 PRINT 60
874 NOVM2  = NOVMI  - 1                                              MPR2
875 DO 885  I = 1, NOVM2                                             MPR2
880 IP1 =  I + 1                                                     MPR2
885 PRINT 35, (I,J,VECTOR(I,J),J=IP1,NOVMI)
890 PRINT 40, (I,VECTOR(I,NOVAR),I=1,NOVMI)
900 CONTINUE
1000 NOSTEP = NOSTEP + 1                                             MPR2
1001 IF (VECTOR( NOVAR,NOVAR)) 1002,1002,1010                        MPR2
1002 NSTPM1 = NOSTEP - 1                                             MPR2
1003 PRINT 1004, NSTPM1
1005 GO TO 1381
1010 SIGY = SIGMA(NOVAR) * DSQRT(VECTOR(NOVAR,NOVAR)/ DEFR)
1015 DEFR =DEFR-1.0                                                  MPR2
1016 IF (DEFR )  1017,1017, 1020                                     MPR2
1017 PRINT  1019 ,NOSTEP                                             MPR2
1021 GO TO 1381
1020 VMIN = 0.0                                                      MPR2
1030 VMAX = 0.0                                                      MPR2
1035 NOIN = 0                                                        MPR2
```

```
1040 DO 1050  I = 1,NOVMI                                              MPR2
1041 IF (VECTOR (I,I)) 1042,1050,1060                                  MPR2
1042 PRINT 1044, I, NOSTEP                                             MPR2
1045 GO TO 1381                                                        MPR2
1060 IF(VECTOR(I,I) - TOL)   1050,1080,1080                            MPR2
1080 VAR = VECTOR(I,NOVAR) * VECTOR(NOVAR,I) / VECTOR(I,I)             MPR2
1090 IF(VAR)1100,1050,1110                                             MPR2
1100 NOIN = NOIN + 1                                                   MPR2
1120 INDEX(NOIN) = I                                                   MPR2
1130 COEN(NOIN)  = VECTOR(I,NOVAR) * SIGMA(NOVAR) / SIGMA (I)          MPR2
1140 SIGMCO(NOIN) = (SIGY / SIGMA(I)) * DSQRT(VECTOR(I,I))
1150 IF (VMIN) 1160,1170,904                                           MPR2
 904 PRINT 906
1155 GO TO 910                                                         MPR2
1170 VMIN = VAR                                                        MPR2
1180 NOMIN = I                                                         MPR2
1190 GO TO 1050                                                        MPR2
1160 IF(VAR - VMIN)1050,1050,1170                                      MPR2
1110 IF (VAR - VMAX)1050,1050,1210                                     MPR2
1210 VMAX = VAR                                                        MPR2
1220 NOMAX = I                                                         MPR2
1050 CONTINUE                                                          MPR2
1230 IF (NOIN) 903,1240,1245                                           MPR2
 903 PRINT 907
1235 GO TO  910
1240 PRINT 65, SIGY
1260 GO TO 1350                                                        MPR2
1245 CNST = 0.0
1305 IF (IFSTEP) 900,1310,1320
1310 IF (NOENT) 1311,1311,1313                                         MPR2
1311 PRINT 91, NOSTEP,K
1312 GO TO 1314                                                        MPR2
1313 PRINT 92, NOSTEP,K
1314 PRINT70, FLEVEL,SIGY,(INDEX(J),COEN(J),SIGMCO(J),J=1,NOIN)
1315 GO TO NUMBER, (1320,1580)                                         MPR2
1320 FLEVEL = VMIN * DEFR / VECTOR (NOVAR,NOVAR)                       MPR2
1330 IF(EFOUT + FLEVEL) 1350, 1350, 1340                               MPR2
1340 K =  NOMIN                                                        MPR2
1345 NOENT = 0                                                         MPR2
1346 GO  TO  1391                                                      MPR2
1350 FLEVEL = VMAX * DEFR / (VECTOR(NOVAR,NOVAR)-  VMAX)               MPR2
1360 IF (EFIN - FLEVEL) 1370,1361,1380                                 MPR2
1361 IF (EFIN) 1380,1380,1370                                          MPR2
1370 K = NOMAX
1390 NOENT = K
1391 IF(K) 1392,1392,1400                                              MPR2
1392 PRINT 1395, NOSTEP
1394 GO TO 910                                                         MPR2
1400 DO 1410   I = 1,NOVAR                                             MPR2
1420 IF (I-K) 1430,1410,1430                                           MPR2
1430 DO 1440   J = 1, NOVAR                                            MPR2
1450 IF (J-K) 1460,1440,1460                                           MPR2
1460 VECTOR(I,J) = VECTOR(I,J) - (VECTOR(I,K) * VECTOR (K,J) / VECTOR  MPR2
    *(K,K))                                                            MPR2
```

```
 1440 CONTINUE                                                     MPR2
 1410 CONTINUE                                                     MPR2
 1470 DO 1480  I = 1, NOVAR                                        MPR2
 1490 IF (I-K) 1500,1480,1500                                      MPR2
 1500 VECTOR (I,K)  =  -  VECTOR (I,K) / VECTOR (K,K)              MPR2
 1480 CONTINUE                                                     MPR2
 1510 DO 1520 J = 1, NOVAR                                         MPR2
 1530 IF (J-K) 1540,1520,1540                                      MPR2
 1540 VECTOR(K,J) =   VECTOR (K,J) / VECTOR (K,K)                  MPR2
 1520 CONTINUE                                                     MPR2
 1550 VECTOR(K,K) =  1.0 / VECTOR(K,K)                             MPR2
 1560 GO TO 1000                                                   MPR2
 1380 PRINT 75, NOSTEP                                             MPR2
 1381 IF (IFSTEP) 900, 1580,1570                                   MPR2
 1570 ASSIGN  1580  TO NUMBER                                      MPR2
 1571 GO TO  1310                                                  MPR2
 1580 PRINT 1586, (L, VECTOR(L,L),L=1,NOVMI)
 1581 IF( IFPRED)  900,1582,910                                    MPR2
 1582 CONTINUE
 1586 FORMAT (24H0      DIAGONAL  ELEMENTS //20H   VAR.NO.     VALUE//   MPR2
     1(1H  I 7, F16.6))                                            MPR2
C      OUTPUT SECTION
      PRINT 2085
 2085 FORMAT (* OBSERVED VS CALCULATED RESULTS* //)
      PRINT 2086
 2086 FORMAT (3X,3HRUN,16X,8HOBS FREQ,5X,9HCALC FREQ,4X,5HRESID,6X,
     X6HWEIGHT)
      DMAXM = 0.0  $  SRES2WT = 0.0
      DO 1750 N = 1, NODATA
      READ  TAPE 50, RUN,(DATA(L), L=1,NOVAR),SUBTOFF,IDBAND
      YPRED = CNST + SUBTOFF
      DO 1630 I = 1, NOIN
      K = INDEX(I)
 1630 YPRED = YPRED + COEN(I)*DATA(K)
      DEV(N) = DATA(NOVAR) -(YPRED - SUBTOFF)
      WGT(N) = WHT(N)
      ABDEV = DEV(N)**2*WGT(N)
      IF (ABDEV - DMAXM) 1660,1651,1651
 1651 DMAXM = ABDEV
 1660 SRES2WT = SRES2WT + DEV(N)**2*WHT(N)
      WHT(N) = WHT(N)*AVEWT
      IF (NOTIMES) 7999,1661,1725
 1661 IF (KDEL(N)) 1670,1680,1690
 1670 KDEL(N) = 1HP  $  GO TO 1695
 1680 KDEL(N) = 1HQ  $  GO TO 1695
 1690 KDEL(N) = 1HR  $  GO TO 1695
 1695 IF(JDEL(N)) 1700,1710,1720
 1700 JDEL(N) = 1HP  $  GO TO 1725
 1710 JDEL(N) = 1HQ  $  GO TO 1725
 1720 JDEL(N) = 1HR  $  GO TO 1725
 1725 PRINT 1745, RUN,KDEL(N),JDEL(N),KAY(N),JAY(N),FREQOBS(N),YPRED,
     1DEV(N),WHT(N),ABDEV
 1745 FORMAT (1X,F5.0,6X,A1,A1,I2,1H,,I2,3X,F9.4,5X,F9.4,5X,F7.4,4X,
     1F5.2,5X,10X,F15.8)
```

```
 1750 CONTINUE
      REWIND 50
      PRINT 1760, DMAXM
 1760 FORMAT(///9H DMAXM = , F15.8,///)
C     STANDARD DEVIATIONS FROM RESIDUALS
      S2 = (NOSTAT*SRES2WT)/((NOSTAT-NOVAR)*VECTOR(NOVPL,NOVPL))
 1770 PRINT 1775, S2
 1775 FORMAT (//24H SUM SQ. OF RESIDUALS = , F14.8)
 1780 STDDEV = SQRTF(S2)
 1785 PRINT 1790, STDDEV
 1790 FORMAT (39H STD. DEV. CALCULATED FROM RESIDUALS = , F10.8)
C     CONFIDENCE INTERVALS
C     HERE WE WISH A 95 PERCENT PROBABILITY
      IPROB = 1  $  CONFLEV = 95.
      DEGFR = NODATA - NOVAR
      IF (DEGFR - 35.) 2183,2183,2184
 2183 IDEGF = 1  $  GO TO 2192
 2184 IF (DEGFR - 50.) 2185,2185,2186
 2185 IDEGF = 2  $  GO TO 2192
 2186 IF (DEGFR - 90.) 2187,2187,2188
 2187 IDEGF = 3  $  GO TO 2192
 2188 IF (DEGFR - 120.) 2189, 2189, 2190
 2189 IDEGF = 4  $  GO TO 2192
 2190 IDEGF = 5
 2192 IF (NOVAR-10) 2001,2001,2002
 2001 INOV = NOVAR  $  GO TO 2007
 2002 IF (NOVAR - 13) 2003,2003,2004
 2003 INOV = 11  $  GO TO 2007
 2004 IF (NOVAR - 17) 2008,2008,2006
 2008 INOV = 12  $  GO TO 2007
 2006 INOV = 13
 2007 CIRATIO = SQRTF (NOVAR*FVAL(INOV,IDEGF,IPROB))
      DO 2010 I = 1, NOIN
 2010 CONFINT(I) = CIRATIO*SIGMCO(I)
      PRINT 2011, CONFLEV
 2011 FORMAT(1H4,*COEFF, STD ERRORS, CONF INT USING CORR STD DEV*, //
     120H CONFIDENCE LEVEL = F5.2//45H FINAL COEFFICIENTS WITH CONFIDENC
     2E INTERVALS  ,// 20X, 11HCOEFFICIENT, 14X,18HSTD ERROR OF COEFF,
     37X, 19HCONFIDENCE INTERVAL //)
      DO 2020 I = 1, NOIN
 2020 PRINT 2013, INDEX(I),COEN(I),SIGMCO(I),CONFINT(I)
 2013 FORMAT (12H COEFF OF X(I2,1H), 5X,E18.8,7X,F18.8,7X,E18.8)
C     REFIT SECTION
      REWIND 51
      NOTIMES = NOTIMES + 1  $  NODEL = 0
      SUMWT = 0.0
      IF (NOTIMES - NORFTS) 7001, 7001, 7900
 7001 DO 7021 N=1,NODATA
      READ TAPE 50, RUN,(DATA(L),L=1,NOVAR),SUBTOFF,IDBAND
      ABDEV = DEV(N)**2*WGT(N)
      IF (DMAXM - ABDEV) 7002,7010,7020
 7002 PRINT 7003, N
 7003 FORMAT (//*DIDNT FORM MAX OF RESIDUALS CORRECTLY, SET WHT(N) = 0 F
     1OR PT. NO.*, I3)
```

```
      WHT(N) = 0.0
      GO TO 7020
 7010 NODEL = NODEL + 1
      PRINT 7015, NOTIMES, N
 7015 FORMAT (1H1,21H REFIT OF DATA NUMBER  , I2/  18H DATA POINT NUMBER
     1 , I4, 26H HAS BEEN REMOVED FROM FIT)
      WHT(N) = 0.0
 7020 WRITE TAPE 51,KDEL(N),JDEL(N),KAY(N),JAY(N),FREQOBS(N),WHT(N),RUN,
     1(DATA(L),L=1,NOVAR),SUBTOFF,INCRVIB(N),IDBAND
      SUMWT = SUMWT + WHT(N)
 7021 CONTINUE
      REWIND 50  $  REWIND 51
      AVEWT = SUMWT/NODATA
      DO 7022 I = 1,NVP1
      DO 7022 J = 1,NVP1
 7022 VECTOR(I,J) = 0.0
      DO 7045 N = 1, NODATA
      READ  TAPE 51,KDEL(N),JDEL(N),KAY(N),JAY(N),FREQOBS(N),WHT(N),RUN,
     1(DATA(L),L=1,NOVAR),SUBTOFF,INCRVIB(N),IDBAND
      WHT(N) = WHT(N) / AVEWT
      WRITE TAPE 50, RUN,(DATA(L), L=1,NOVAR),SUBTOFF,IDBAND
      DO 7050 I = 1,NOVAR
      VECTOR (I, NOVAR+1) = VECTOR (I, NOVAR+1) + DATA(I)*WHT(N)
      DO 7050 J = 1, NOVAR
      VECTOR (I,J) = VECTOR(I,J) + DATA(I)*DATA(J)*WHT(N)
 7050 CONTINUE
      VECTOR(NVP1,NVP1) = VECTOR(NVP1,NVP1) + WHT(N)
 7045 CONTINUE
      REWIND 50  $  REWIND 51
      GO TO 565
 7900 CONTINUE
 7999 CONTINUE
   10 FORMAT (F14.8)
   15 FORMAT (1H 49H                                 SUM  OF  VARIABLES//)MPR2
   20 FORMAT (1H 11H     SUM X( I2,3H) = D15.8,8H  SUM X( I2,3H) =D15.8,
     18H  SUM X( I2,3H) =D15.8,8H  SUM X(I2,3H) =D15.8 )
   25 FORMAT (17H     SUM   Y   =D15.8 )
   30 FORMAT(1H0 70H                            RAW  SUM  OF  SQUARES  AMPR2
     1ND  CROSS PRODUCTS// )                                           MPR2
   35 FORMAT (1H 7H     X(I2,7H) VS X(I2,3H) = D15.8,
     1        6H    X(I2,7H) VS X(I2,3H) = D15.8,
     2        6H    X(I2,7H) VS X(I2,3H) = D15.8   )
   40 FORMAT (1H 7H      X(I2,12H) VS    Y   =D15.8,
     1        6H    X(I2,12H) VS    Y   =D15.8,
     2        6H    X(I2,12H) VS    Y   =D15.8   )
   45 FORMAT (1H 21H     Y      VS    Y   =D15.8)
   50 FORMAT (1H063H                                  AVERAGE  VALUE  OFMPR2
     -  VARIABLES// )                                                  MPR2
   55 FORMAT(1H077H                            RESIDUAL  SUMS  OF  SQUAMPR2
     -RES  AND  CROSS PRODUCTS//)                                      MPR2
   60 FORMAT(1H069H                                  PARTIAL  CORRELATIMPR2
     -ON  COEFFICIENTS//)                                              MPR2
   65 FORMAT (25H0  STANDARD ERROR OF Y = F14.8 )
   70 FORMAT (11H   F LEVEL  F14.8/25H   STANDARD ERROR OF Y = F14.8/
```

```
   $                         56H                 VARIABLE   COEFFICIENT   STD ERRMPR2
    2OR OF COEF //  (16H                       X-I3,F15.8,F15.8))                 MPR2
  75 FORMAT (10H COMPLETED I5,20H STEPS OF REGRESSION)                            MPR2
  90 FORMAT (22H4STEPWISE  REGRESSION //12H PROBLEM NO I10 //13H NO OF MPR2
    1DATA = I5 //18H NO OF VARIABLES = I10 //30H WEIGHTED DEGREES OF FRMPR2
    2EEDOM = F12.2 //)
  91 FORMAT (9H0STEP NO.I5 /19H   VARIABLE REMOVED I8)                            MPR2
  92 FORMAT (9H0STEP NO.I5 /20H   VARIABLE ENTERING I8)                           MPR2
  93 FORMAT (5H RUN  F6.0,3H   F10.5,3H   F10.5,3H   F10.5,3H   F10.5, MPR2
    13H   F10.5/(14H                 F10.5,3H   F10.5,3H   F10.5,3H   F10.MPR2
    25,3H   F10.5))                                                               MPR2
 654 FORMAT (31H  ZERO NUMBER OF DATA. SO LONG.)                                  MPR2
 905 FORMAT (42H ERROR IN CONTROL CARD, PROBLEM TERMINATED)                       MPR2
 906 FORMAT (25H ERROR, VMIN PLUS, SOLONG)                                        MPR2
 907 FORMAT (26H  ERROR,NOIN MINUS, SOLONG )                                      MPR2
1004 FORMAT (1H037HY SQUARE NON-POSITIVE,TERMINATE STEP  I 5)                     MPR2
1019 FORMAT (1H029H NO MORE DEGREES FREEDOM STEP I 5 )                            MPR2
1044 FORMAT (1H010H SQUARE X-I5,17H NEGATIVE, SOLONG I5,6H STEPS)                 MPR2
1395 FORMAT (12H  K=0. STEP I6, 7H SOLONG)                                        MPR2
 910 CONTINUE
     READ 9999, KONTIN
9999 FORMAT (A8)
     IF (KONTIN - 8HCONTINUE ) 3175, 100, 3175
3175 STOP
     END
     SIMULTANEOUS FIT OF CH3BR NU4 AND 2NU4.
     FIT IS IDENTICAL TO THAT REPORTED IN PAPERS(  OBJECT HERE IS TO
     OBTAIN A PUNCHED DECK OF RESULTS.
     COEFF OF DATA(1) = NUZRO FOR NU-4
     COEFF OF DATA(2) = NUZRO FOR 2NU-4 PERPENDICULAR
     COEFF OF DATA(3) = NUZRO FOR 2NU-4 PARALLEL
     COEFF OF DATA(4) = AZRO
     COEFF OF DATA(5) = AE*ZETA + GARBAGE
     COEFF OF AA = - ALPHAB4
     COEFF OF AB = BETAK4
     COEFF OF AC = ETAJ4
     COEFF OF AD = BETAJ4
     COEFF OF AE = BETAJK4
     COEFF OF AF = H7RO
     COEFF OF AG = - DZROJK
     COEFF OF AH = - DZROJ
     COEFF OF AI = - ALPHAA4
     COEFF OF AJ = ETAK4
     COEFF OF AK = - DZROK
     COEFF OF AL = H7ROJ
     COEFF OF AM = H7ROJK
     COEFF OF AN = H7ROKJ
     COEFF OF AO = H7ROK
     COEFF OF AP = ETA44
     COEFF OF AQ = GAMMA-A(44)
     COEFF OF AR = GAMMA-A(L4L4)
     COEFF OF AS = GAMMA-B(44)
     COEFF OF AT = GAMMA-B(L4L4)

     IN THIS PROGRAM
```

```
      DATA(6) = AK
      DATA(7) = AI
      DATA(8) = AJ
      DATA(9) = AA
      DATA(10) = AB
      DATA(11) = AO
      AND FROM THE MICROWAVE QUANTITIES WE FORMED
      SUBTOFF = BZRO*AF - DZROJK*AG - DZROJ*AH
      ENDHED
12                  NOVAR
4.173.322.922.692.532.422.332.272.212.162.092.011.93
4.083.322.842.612.452.342.252.182.122.082.001.921.84
4.003.152.762.552.372.252.172.102.041.991.921.841.75
3.923.072.682.452.292.172.092.021.961.911.831.751.66
3.843.002.602.372.212.102.011.941.881.831.751.671.57
7.565.394.514.023.703.473.303.173.072.982.842.702.55
7.315.184.313.833.513.293.122.992.892.802.662.522.37
7.084.984.133.653.343.122.952.822.722.632.502.352.20
6.854.793.953.483.172.962.792.662.562.472.342.192.03
6.634.613.783.323.022.802.642.512.412.322.182.041.88
0.3185537           = BZRO, CH3BR
0.00000427          = DZROJK, CH3BR
0.000000333         = DZROJ, CH3BR
 0                  = NORFTS
PP 4, 6 3020.451 0.07 1  PP 4, 7 3019.809 0.02 1  PP 4, 8 3019.179 0.12 1  H3
PP 4, 9 3018.540 0.14 1  PP 4,10 3017.913 0.07 1  PP 4,11 3017.288 0.05 1  H3
PP 4,12 3016.657 0.05 1  PP 4,13 3016.016 0.07 1  PP 4,15 3014.755 0.02 1  H3
PP 4,16 3014.129 0.07 1  PP 4,17 3013.497 0.05 1  PP 4,18 3012.866 0.02 1  H3
PP 4,19 3012.248 0.05 1  PP 4,20 3011.634 0.01 1  PP 4,21 3010.999 0.01 1  H3
PP 4,23 3009.777 0.00 1  PP 4,24 3009.087 0.00 1  PP 3, 3 3031.493 0.12 1  H3
PP 3, 4 3030.854 0.05 1  PP 3, 5 3030.217 0.14 1  PP 3, 6 3029.587 1.00 1  H3
PP 3, 7 3028.955 1.00 1  PP 3, 8 3028.322 0.40 1  PP 3, 9 3027.688 0.07 1  H3
PP 3,10 3027.054 0.14 1  PP 3,11 3026.428 0.14 1  PP 3,12 3025.791 1.00 1  H3
PP 3,13 3025.164 1.00 1  PP 3,15 3023.901 0.10 1  PP 3,16 3023.272 0.07 1  H3
PP 3,17 3022.644 0.07 1  PP 3,18 3022.017 0.07 1  PP 3,19 3021.390 0.02 1  H3



QP 3, 4 6043.077 0.07 2  QP 3, 6 6041.813 0.07 2  QP 3, 7 6041.184 0.17 2  H3
QP 3, 8 6040.566 0.07 2  QP 3, 9 6039.912 0.67 2  QP 3,10 6039.278 0.4  2  H3
QP 3,11 6038.641 0.67 2  QP 3,12 6038.022 0.03 2  QP 3,13 6037.380 0.67 2  H3
PP 1, 6 6086.745 0.00 2  PP 1, 7 6086.118 0.00 2  PP 1, 8 6085.473 0.00 2  CH
PP 1, 9 6084.845 0.01 2  PP 1,11 6083.588 0.00 2  PP 1,12 6082.965 0.01 2  CH
PP 1,13 6082.352 0.05 2  PP 1,14 6081.705 0.05 2  PP 1,15 6081.091 0.01 2  CH
PP 1,19 6078.573 0.00 2  PP 1,20 6077.973 0.10 2  PP 1,21 6077.353 0.10 2  CH
PP 1,25 6074.882 0.00 2  PP 1,26 6074.183 0.00 2  PP 1,27 6073.543 0.00 2  CH
RP 0, 1 6100.689 0.00 2  RP 0, 2 6100.059 0.00 2  RP 0, 3 6099.445 0.01 2  CH
```

APPENDIX III

LISTING OF SCAN PROGRAM

SCAN was used to translate the raw data from the Hydel film reader into fringe numbers and ultimately into frequencies for the transitions comprising the spectra. Included is a typical, though short, data deck.

LISTING OF SCAN PROGRAM

```
      PROGRAM SCAN
      DIMENSION XM(6), YM(6), DELX(6), XROT(6), FRNGX(50), PSEP(50),
     1NFGSEP(50), KHED1(3),KHED2(3),IPSEP(3),IHEAD(10)
      COMMON THETA, DELX
      READ 4, KHED1(1),KHED2(1),KHED1(2),KHED2(2)
    4 FORMAT (A8,A8,10X,A8,A8)
    1 READ 3, (IHEAD(I), I=1,10)
      PRINT 3, (IHEAD(I), I=1,10)
      IF (IHEAD(10) - 8HEND HEAD) 1,2,1
    2 IH = 1
      NCAL = 1
      IP = 0
      NFRM = 0
      PENSEP = 0.
  101 READ 100, (XM(I), YM(I), I = 1,6), ICODE, NFIN
      IF (ICODE - 0 ) 200,101,205
  205 IF (ICODE - 7) 210,210,200
  200 PRINT 206
  206 FORMAT(///* IMPROPER CODE NUMBER IN THIS FRAME - ENTIRE FRAME NO G
     1OOD *///)
      GO TO 101
  210 CONTINUE
      GO TO (1000,2000,3000,4000,5000,6000,102), ICODE
  102 IF (NFIN - 1HC) 103, 110, 103
  110 GO TO 1
  103 STOP
 1000 NIR = 1
      IFRAME = XM(1)
      IFRNG = YM(1)
      IOP = XM(2)
      NOFR = 0
      IF (NFRM - 2) 101,7000,101
 2000 FRNG = IFRNG
      NFRM = NFRM + 1
      CALL LSTAN(XM,YM)
      GO TO (2003,2004), IH
 2004 PRINT 9701
 2003 PRINT 9702
      PRINT 3, (IHEAD(I), I=1,9)
      PRINT 9200,IFRAME,KHED1(IH),KHED2(IH),IOP,IFRNG,THETA,(DELX(I),
     1I=1,6)
      GO TO 101
 3000 IH = 1
      DO 3007 J = 1,6,2
      IF (XM(J)) 101,101,3003
 3003 IF (XM(J+1)) 101,101,3002
 3002 IP = IP + 1
      PSEP(IP)=ROTATE(XM(J+1),YM(J+1),THETA) - ROTATE(XM(J),YM(J),THETA)
      JCNT = (J+1)/2
 3007 IPSEP(JCNT) = PSEP(IP)
```

```
      PRINT 9300, (IPSEP(I),I=1,3)
      GO TO 101
 4000 NCAL = 2
      A = YM(1) + XM(2)*0.00001
      B = YM(2) + XM(3)*0.00001 + YM(3)*0.0000000001
      PRINT 9400, A, B
      GO TO 101
 5000 DO 5001 J = 1,6
      IF (XM(J)) 5002,101,5002
 5002 NOFR = NOFR + 1
      FRNGX(NOFR) = ROTATE(XM(J),YM(J),THETA)
 5001 NFGSEP(NOFR) = FRNGX(NOFR) - FRNGX(NOFR-1)
      GO TO 101
 6000 GO TO (6100,6200), NIR
 6100 PRINT 9500, IFRAME,(NFGSEP(I),I=1,NOFR)
      PRINT 9702
      NIR = 2
      GO TO (6600,6650), NCAL
 6600 PRINT 9600, IFRAME
      GO TO 6200
 6650 PRINT 9650, IFRAME, A, B
 6200 DO 6001 J=1,6
      IF (XM(J)) 6002,101,6002
 6002 XIR = PENSEP + ROTATE(XM(J),YM(J),THETA)
      DO 6003 I=1,NOFR
      IF (XIR - FRNGX(I)) 6004,6005,6003
 6003 CONTINUE
      GO TO 6010
 6004 IF (I-1) 6015,6015,6006
 6006 FRACT = (XIR-FRNGX(I-1))/(FRNGX(I)-FRNGX(I-1))
      FRK = I - 2
      FRNO = FRNG + FRK + FRACT
      INTERP = 3H
 6011 GO TO (9000,9050), NCAL
 6020 CONTINUE
 6001 CONTINUE
      GO TO 101
 6015 FRACT = (XIR - FRNGX(1))/(FRNGX(2) - FRNGX(1))
      FRNO = FRNG + FRACT
      INTERP = 3HEXL
      GO TO 6011
 6010 FRACT = (XIR - FRNGX(NOFR))/(FRNGX(NOFR) - FRNGX(NOFR-1))
      FNOFR = NOFR
      FRNO = FRNG + FRACT + FNOFR - 1.
      INTERP = 3HEXR
      GO TO 6011
 6005 FRK = I - 1
      FRNO = FRNG + FRK
      GO TO 6011
 7000 IH = 2
      PSEPSUM = 0
      PIP = IP
      DO 7001 J = 1,IP
 7001 PSEPSUM = PSEPSUM + PSEP(J)
```

```
      PENSEP = PSEPSUM/PIP
      PRINT 9700, PENSEP
      GO TO 101
 9000 PRINT 9651, FRNO, INTERP
      GO TO 6020
 9050 FREQ = A + B*FRNO
      PRINT 9652, FRNO, FREQ, INTERP
      GO TO 6020
    3 FORMAT (10A8)
  100 FORMAT (6(2F5.0,1X),I1,A1)
 9200 FORMAT(10H FRAME NO.I5,5X2A8,10X7HOP. NO.I5,/5X19HFIRST FRINGE IS
     1NO.I5/5X17HROTATION ANGLE ISF9.6,8H RADIANS/9X17H(ROTATION FITS TO
     26(F5.1,1H,),9H MICRONS)/)
 9300 FORMAT (38H OBSERVED PEN SEPARATIONS (IN MICRONS),6(I5,1H,))
 9400 FORMAT(52H THE FOLLOWING CALIBRATION CONSTANTS HAVE BEEN INPUT/5X
     13HA =F10.4,5X3HB =F9.8//52H THE FRINGE POSITIONS AND FREQUENCIES W
     2ILL BE OUTPUT/1H1)
 9500 FORMAT(28H FRINGE SEPARATIONS IN FRAMEI5,10H (MICRONS)/(5X10I7))
 9600 FORMAT (48H0FRINGE POSITIONS OF LINES MEASURED IN FRAME NO., I5/)
 9650 FORMAT(55H FRINGE POSITIONS AND FREQUENCIES MEASURED IN FRAME NO.
     1I5/5X30HCALIBRATION CONSTANTS USED ARE/10X3HA =F10.4,5X3HB =F9.6//
     25X15HFRINGE POSITION10X18HOBSERVED FREQUENCY/)
 9651 FORMAT (F16.3, 5X, A3)
 9652 FORMAT (F16.3, F27.3, 5X, A3)
 9700 FORMAT (32H0PEN SEPARATION FOR THIS CHART =F5.1, 8H MICRONS)
 9701 FORMAT (1H1)
 9702 FORMAT (1H0)
      END
      FUNCTION ROTATE (ALPHA, BETA, GAMMA)
      ROTATE = (1. - GAMMA*GAMMA/2.)*ALPHA - GAMMA*BETA
      END
      SUBROUTINE LSTAN (X,Y)
      DIMENSION X(6), Y(6), XCALC(6), DELX(6)
      COMMON THETA, DELX
      SUMY = 0
      SUMX = 0
      SUMYY = 0
      SUMYX = 0
      DO 20 I = 1,6
      SUMY = SUMY + Y(I)
      SUMX = SUMX + X(I)
      SUMYY = SUMYY + Y(I)*Y(I)
   20 SUMYX = SUMYX + Y(I)*X(I)
      THETA = (SUMYX - SUMY*(SUMX/6.))/(SUMYY - SUMY*(SUMY/6.))
      DO 30 I = 1,6
   30 DELX(I) = (SUMX-THETA*SUMY)/6. + THETA*Y(I) - X(I)
      END
LINE POSITIONS             LINE FREQUENCIES
      FREQUENCIES FOR 0365-F                                             END
      5537.42404     0.5359293000                                      4  0365-F
    8  000      7                                                      1
1975621326 1976425947 1977630197 1977634538 1977637419 1978341477 2
1282131122 1302622877 1462231147 1482222831 1640631159 1661322867 3
1810131116 1830922932 1972131199 1994222961 2149431281 2170822915 3
```

```
2313131217 2335622880 2474631505 2497223024                       3
   51   000       7                                               1
1591821207 1590127155 1589431687 1588336190 1588537611 1587341437 2
1186630907 1210022931 1308931068 1332822845 1426730960 1449922936 3
1548831108 1572722889 1673330815 1697422795 1791431094 1816622817 3
1913131199 1938322981 2036131022 2059923000                       3
   17   515       7                                               1    0365-
1912320089 1913924962 1914629135 1915633405 1916737401 1917141681 2    0365-
1242923362 1403623362 1552923362 1699023362 1848723362 2008123362 5    0365-
2162823362 2324623362 2478823362 2638123362 2796223362 2947623362 5    0365-
3106423362 3261323362                                             5    0365-
1366627875 1408827950 1479027875 1542128014 1604728739 1676229233 6    0365-
1713628441 1752428201 1815330226 1840730527 1880130162 1914430055 6    0365-
1948630055 1987330103 2041130317 2063829999 2119129579 2246329446 6    0365-
2289129351 2322328283 2351128604 2436329844 2510728758 2567328680 6    0365-
2633928774 2685328355 2738329425 2845629137 2881129669 2926528498 6    0365-
2992129342 3009129061 3070129157 3123629668 3197329810 3240629792 6    0365-
   18   526       7                                               1    0365-
2120620060 2120624583 2120829112 2120932495 2121336324 2121441439 2    0365-
1242623204 1401323204 1555823204 1707323204 1858123204 2006623204 5    0365-
2167923204 2337123204 2497423204 2653123204 2802223204 2952423204 5    0365-
3105423204 3262623204 3416123204 3571623204 3735123204 3897623204 5    0365-
4048723204 4211623204 4367923204 4509623204                       5    0365-
1175329635 1220428565 1285829351 1300629070 1372929070 1417329638 6    0365-
1491129836 1534929836 1668629369 1761328859 1830529013 1888630294 6    0365-
1949929149 2064228049 2094928369 2155728371 2277628900 2305629037 6    0365-
2373230459 2371630459 2371630459 2422931363 2467630941 2520330056 6    0365-
2559931168 2635228297 2740329708 2767929571 2803129493 2865828404 6    0365-
2917628241 2953229137 3033629713 3075828403 3149129097 3221629298 6    0365-
3311129240 3392627673 3444330450 3544129529 3588628475 3828830231 6    0365-
3906931333 3962028742 3997828376 4028528701 4086433600 4174129211 6    0365-
4194129383 4221630089 4254129057 4304929057 4323529702 4373630749 6    0365-
4510629081 4563829385 4584130312                                  6    0365-
   19   545       7                                               1    0365-
2335120039 2335625254 2336330296 2336134004 2336638024 2336841497 2    0365-
1078823415 1234623415 1377123415 1531923415 1688123415 1845223415 5    0365-
2005923415 2167123415 2315123415 2467823415 2625823415 2779123169 5    0365-
2943623169 3109623169 3258623169 3402823169 3559323169 3717823169 5    0365-
3876123169 4031623169 4188323169 4351823169 4513123169            5    0365-
1088330128 1171529143 1191129659 1241730643 1377329002 1451630186 6    0365-
1481528548 1503728835 1588629259 1616328810 1675129807 1748028609 6    0365-
1809129060 1863127460 1952327884 2006127669 2033327579 2114529590 6    0365-
2188227698 2253327698 2331629095 2381628013 2454928295 2497629371 6    0365-
2609627476 2668628043 2680628134 2734228566 2787728304 2831828991 6    0365-
2858829401 2924628224 2969630219 3052628469 3145627668 3194829273 6    0365-
3213329152 3248328745 3288629047 3340629637 3427631145 3463729470 6    0365-
3495928845 3534827975 3583928276 3656129001 3667029336 3720629208 6    0365-
3918331619 3935630753 4020427943 4134328673 4165627737 4200327471 6    0365-
4242328649 4426130446 4542827647                                  6    0365-
```

APPENDIX IV

LISTING OF OUTPUT FROM SIMULTANEOUS FIT OF CH_3Br ν_4 AND $2\nu_4$

The data listed here were part of the output of the final simultaneous least squares computer fit of CH_3Br ν_4 and $2\nu_4$, and correspond to the values of the molecular constants listed in Table XI. Listed here are:

1. the assignment of each transition $[{}^{\Delta K}\Delta J_K(J)]$,
2. the observed frequency of each transition,
3. the calculated frequency for each transition, obtained from the values of the molecular constants listed in Table XI,
4. the deviations $(\nu_{obs} - \nu_{calc})$,
5. the weight assigned to each transition.

LISTING OF FINAL DATA FROM SIMULTANEOUS ANALYSIS OF CH3BR NU4 AND 2NU4 BY MEANS OF FALSTAF PROGRAM LISTED IN APPENDIX II.

ASSIGN.	OBS. FREQ.	CALC. FREQ.	RESID.	WHT.
PP 5, 5	3011.8740	3011.8717	0.0023	0.00
PP 5, 6	3011.2400	3011.2371	0.0029	0.00
PP 5, 7	3010.5910	3010.6031	-0.0121	0.00
PP 5, 8	3009.9950	3009.9695	0.0255	0.00
PP 5, 9	3009.3420	3009.3364	0.0056	0.00
PP 5,10	3008.7210	3008.7039	0.0171	0.00
PP 5,11	3008.0960	3008.0719	0.0241	0.01
PP 4, 4	3021.7130	3021.7120	0.0010	0.05
PP 4, 5	3021.0810	3021.0768	0.0042	0.30
PP 4, 6	3020.4510	3020.4421	0.0089	0.07
PP 4, 7	3019.8090	3019.8079	0.0011	0.02
PP 4, 8	3019.1790	3019.1741	0.0049	0.12
PP 4, 9	3018.5400	3018.5409	-0.0009	0.14
PP 4,10	3017.9130	3017.9081	0.0049	0.07
PP 4,11	3017.2880	3017.2758	0.0122	0.05
PP 4,12	3016.6570	3016.6441	0.0129	0.05
PP 4,13	3016.0160	3016.0128	0.0032	0.07
PP 4,15	3014.7550	3014.7520	0.0030	0.02
PP 4,16	3014.1290	3014.1223	0.0067	0.07
PP 4,17	3013.4970	3013.4933	0.0037	0.05
PP 4,18	3012.8660	3012.8648	0.0012	0.02
PP 4,19	3012.2480	3012.2368	0.0112	0.05
PP 4,20	3011.6340	3011.6095	0.0245	0.01
PP 4,21	3010.9990	3010.9827	0.0163	0.01
PP 4,23	3009.7770	3009.7310	0.0460	0.00
PP 4,24	3009.0870	3009.1060	-0.0190	0.00
PP 3, 3	3031.4930	3031.4979	-0.0049	0.12
PP 3, 4	3030.8540	3030.8622	-0.0082	0.05
PP 3, 5	3030.2170	3030.2268	-0.0098	0.14
PP 3, 6	3029.5870	3029.5920	-0.0050	1.00
PP 3, 7	3028.9550	3028.9576	-0.0026	1.00
PP 3, 8	3028.3220	3028.3236	-0.0016	0.40
PP 3, 9	3027.6880	3027.6902	-0.0022	0.07
PP 3,10	3027.0540	3027.0572	-0.0032	0.14
PP 3,11	3026.4280	3026.4247	0.0033	0.14
PP 3,12	3025.7910	3025.7927	-0.0017	1.00
PP 3,13	3025.1640	3025.1612	0.0028	1.00
PP 3,15	3023.9010	3023.8997	0.0013	0.10
PP 3,16	3023.2720	3023.2698	0.0022	0.07
PP 3,17	3022.6440	3022.6404	0.0036	0.07
PP 3,18	3022.0170	3022.0115	0.0055	0.07
PP 3,19	3021.3900	3021.3832	0.0068	0.02
PP 3,20	3020.7640	3020.7555	0.0085	0.05
PP 3,21	3020.1370	3020.1283	0.0087	0.05
PP 3,22	3019.5120	3019.5017	0.0103	0.05
PP 3,23	3018.8910	3018.8757	0.0153	0.01
PP 3,24	3018.2580	3018.2503	0.0077	0.01
PP 3,25	3017.6400	3017.6255	0.0145	0.01

ASSIGN.	OBS. FREQ.	CALC, FREQ,	RESID.	WHT.
PP 3,26	3017.0070	3017,0013	0,0057	0.02
PP 3,27	3016.3890	3016.3777	0,0113	0.01
PP 3,28	3015.7650	3015,7548	0,0102	0.01
PP 3,30	3014.5160	3014,5107	0,0053	0.02
PP 3,31	3013.9030	3013,8897	0,0133	0.00
PP 3,32	3013.2840	3013,2693	0,0147	0.01
PP 3,33	3012.6570	3012,6496	0,0074	0.00
PP 3,34	3012.0520	3012,0306	0,0214	0.02
PP 3,35	3011.4150	3011,4122	0,0028	0.04
PP 3,36	3010.8000	3010,7945	0,0055	0.02
PP 3,38	3009.5820	3009,5613	0,0207	0.00
PP 3,39	3008.9800	3008,9457	0,0343	0.00
PP 3,41	3007.7400	3007,7167	0,0233	0.00
PP 2, 2	3041.2230	3041,2292	-0,0062	0.05
PP 2, 3	3040.5930	3040,5929	0,0001	0.02
PP 2, 4	3039.9590	3039,9571	0,0019	0.05
PP 2, 5	3039.3190	3039,3217	-0,0027	0.05
PP 2, 6	3038.6860	3038,6867	-0,0007	0.02
PP 2, 7	3038.0480	3038,0521	-0,0041	0.07
PP 2, 8	3037.4130	3037,4180	-0,0050	0.12
PP 2, 9	3036.7840	3036,7844	-0,0004	0.02
PP 2,10	3036.1410	3036,1512	-0,0102	0.01
PP 2,11	3035.5130	3035,5185	-0,0055	0.05
PP 2,12	3034.8860	3034,8862	-0,0002	0.10
PP 2,13	3034.2550	3034,2545	0,0005	0.10
PP 2,15	3033.0000	3032,9925	0,0075	0.00
PP 2,16	3032.3560	3032,3623	-0,0063	0.00
PP 2,17	3031.7340	3031,7325	0,0015	0.00
PP 2,18	3031.1110	3031.1034	0,0076	0.01
PP 2,19	3030.4780	3030,4747	0,0033	0.00
PP 2,20	3029.8570	3029,8466	0,0104	0.01
PP 2,21	3029.2290	3029,2191	0,0099	0.00
PP 2,25	3026.7220	3026,7145	0,0075	0.01
PP 2,26	3026.0090	3026,0898	-0,0808	0.00
PP 2,27	3025,4810	3025,4658	0,0152	0.00
PP 2,28	3024.8460	3024,8423	0,0037	0.00
PP 2,30	3023.6130	3023,5972	0,0158	0.01
PP 2,31	3022.9870	3022,9756	0,0114	0.01
PP 2,32	3022.3640	3022,3547	0,0093	0.00
PP 1, 1	3050.9070	3050,9052	0,0018	0.01
PP 1, 2	3050.2570	3050,2685	-0,0115	0.01
PP 1, 3	3049.6420	3049,6321	0,0099	0.00
PP 1, 4	3048.9890	3048,9962	-0,0072	0.01
PP 1, 5	3048.3520	3048,3607	-0,0087	0.03
PP 1, 6	3047.7230	3047,7256	-0,0026	0.05
PP 1, 7	3047.0830	3047,0909	-0,0079	0.07
PP 1, 8	3046.4540	3046,4567	-0,0027	0.07
PP 1, 9	3045.8190	3045,8228	-0,0038	0.07
PP 1,10	3045.1860	3045,1895	-0,0035	0.10
PP 1,11	3044.5540	3044,5566	-0,0026	0.04
PP 1,12	3043.9280	3043,9241	0,0039	0.04
PP 1,13	3043.2910	3043,2922	-0,0012	0.12

ASSIGN.	OBS. FREQ.	CALC. FREQ.	RESID.	WHT.
PP 1,15	3042.0330	3042,0296	0,0034	0.05
PP 1,16	3041.4070	3041,3991	0,0079	0.02
PP 1,17	3040.7740	3040,7691	0,0049	0.01
PP 1,18	3040.1440	3040,1396	0,0044	0.01
PP 1,19	3039.5160	3039,5106	0,0054	0.01
PP 1,20	3038.8880	3038,8822	0,0058	0.01
PP 1,26	3035.1360	3035,1230	0,0130	0.01
PP 1,27	3034.5080	3034,4984	0,0096	0.01
PP 1,29	3033.2620	3033,2511	0,0109	0.01
PP 1,30	3032.6400	3032,6284	0,0116	0.01
PP 1,31	3032.0240	3032,0062	0,0178	0.00
PP 1,32	3031.4050	3031,3847	0,0203	0.00
RP 0, 6	3056.7050	3056,7076	-0,0026	0.02
RP 0, 7	3056.0690	3056,0728	-0,0038	0.07
RP 0, 8	3055.4340	3055,4385	-0,0045	0.30
RP 0, 9	3054.8030	3054,8045	-0,0015	0.30
RP 0,10	3054.1710	3054,1710	0,0000	0.30
RP 0,11	3053.5340	3053,5379	-0,0039	0.40
RP 0,12	3052.9070	3052,9053	0,0017	0.25
RP 0,13	3052.2760	3052,2731	0,0029	0.05
RP 0,15	3051.0160	3051,0101	0,0059	0.07
RP 0,16	3050.3820	3050,3793	0,0027	0.07
RP 0,17	3049.7490	3049,7490	-0,0000	0.01
RP 0,18	3049.1260	3049,1192	0,0068	0.04
RP 0,19	3048.5000	3048,4899	0,0101	0.04
RP 0,20	3047.8650	3047,8611	0,0039	0.02
RP 0,21	3047.2600	3047,2329	0,0271	0.00
RP 0,22	3046.6500	3046,6051	0,0449	0.00
RP 0,23	3045.9890	3045,9779	0,0111	0.00
RP 0,24	3045.3700	3045,3512	0,0188	0.00
RP 0,26	3044.1180	3044,0995	0,0185	0.00
RP 0,27	3043.4910	3043,4745	0,0165	0.00
RP 0,29	3042.2520	3042,2263	0,0257	0.00
RP 0,30	3041.6280	3041,6030	0,0250	0.00
RP 0,31	3041.0150	3040,9804	0,0346	0.00
RP 0,32	3040.3890	3040,3583	0,0307	0.00
RP 0,33	3039.7600	3039,7369	0,0231	0.00
RP 0,34	3039.1440	3039,1161	0,0279	0.00
RP 0,35	3038.5270	3038,4959	0,0311	0.00
RP 0,36	3037.9060	3037,8763	0,0297	0.00
RP 0,37	3037.2880	3037,2574	0,0306	0.00
RP 0,38	3036.6730	3036,6392	0,0338	0.00
RP 1,15	3059.8780	3059,9322	-0,0542	0.00
RP 1,16	3059.2290	3059,3012	-0,0722	0.00
RP 1,17	3058.5840	3058,6707	-0,0867	0.00
RP 1,18	3057.9350	3058,0406	-0,1056	0.00
RP 1,19	3057.3060	3057,4110	-0,1050	0.00
RP 1,20	3056.6440	3056,7819	-0,1379	0.00
RP 1,21	3055.9930	3056,1533	-0,1603	0.00
RP 1,22	3055.3390	3055,5252	-0,1862	0.00
RP 1,23	3054.6900	3054,8976	-0,2076	0.00
RP 1,24	3054.0260	3054,2705	-0,2445	0.00

ASSIGN.	OBS. FREQ.	CALC. FREQ.	RESID.	WHT.
RP 1,25	3053,3700	3053,6440	-0,2740	0,00
RP 1,26	3052,7320	3053,0180	-0,2860	0,00
RP 1,27	3052,0790	3052,3926	-0,3136	0,00
RP 1,28	3051,4420	3051,7677	-0,3257	0,00
RP 1,29	3050,7920	3051,1434	-0,3514	0,00
RP 1,30	3050,5510	3050,5197	0,0313	0,00
RR 2, 2	3080,2200	3080,2250	-0,0050	0,10
RR 2, 3	3080,8600	3080,8633	-0,0033	0,10
RR 2, 4	3081,4990	3081,5019	-0,0029	0,30
RR 2, 5	3082,1370	3082,1408	-0,0038	0,25
RR 2, 6	3082,7760	3082,7800	-0,0040	0,14
RR 2, 7	3083,4200	3083,4194	0,0006	0,30
RR 2, 8	3084,0560	3084,0591	-0,0031	0,14
RR 2, 9	3084,7010	3084,6991	0,0019	0,14
RR 2,10	3085,3430	3085,3393	0,0037	0,14
RR 2,11	3085,9890	3085,9797	0,0093	0,07
RR 2,12	3086,6260	3086,6203	0,0057	0,07
RR 2,14	3087,8970	3087,9023	-0,0053	0,02
RR 2,15	3088,5500	3088,5436	0,0064	0,02
RR 2,16	3089,2060	3089,1851	0,0209	0,01
RR 2,17	3089,8310	3089,8268	0,0042	0,05
RR 2,18	3090,4750	3090,4686	0,0064	0,01
RR 2,19	3091,1260	3091,1107	0,0153	0,01
RR 2,25	3094,9920	3094,9660	0,0260	0,00
RR 2,26	3095,6200	3095,6090	0,0110	0,00
RR 2,28	3096,9090	3096,8953	0,0137	0,01
RR 2,29	3097,5480	3097,5386	0,0094	0,01
RR 2,30	3098,1940	3098,1820	0,0120	0,01
RR 2,31	3098,8450	3098,8255	0,0195	0,02
RR 2,32	3099,4830	3099,4690	0,0140	0,01
RR 2,33	3100,1300	3100,1126	0,0174	0,01
RR 2,34	3100,7860	3100,7562	0,0298	0,00
RR 2,36	3102,0630	3102,0437	0,0193	0,01
RR 2,37	3102,7000	3102,6874	0,0126	0,00
RR 3, 3	3089,6570	3089,6638	-0,0068	0,25
RR 3, 4	3090,3020	3090,3023	-0,0003	1,00
RR 3, 5	3090,9420	3090,9410	0,0010	1,00
RR 3, 6	3091,5850	3091,5800	0,0050	1,00
RR 3, 7	3092,2210	3092,2193	0,0017	1,00
RR 3, 8	3092,8550	3092,8588	-0,0038	1,00
RR 3, 9	3093,4990	3093,4985	0,0005	1,00
RR 3,10	3094,1380	3094,1385	-0,0005	0,40
RR 3,11	3094,7820	3094,7787	0,0033	0,40
RR 3,12	3095,4220	3095,4191	0,0029	0,40
RR 3,14	3096,7020	3096,7005	0,0015	1,00
RR 3,15	3097,3420	3097,3414	0,0006	1,00
RR 3,16	3098,0020	3097,9826	0,0194	0,00
RR 3,17	3098,6250	3098,6239	0,0011	0,07
RR 3,18	3099,2690	3099,2654	0,0036	0,07
RR 3,19	3099,9130	3099,9070	0,0060	0,02
RR 3,20	3100,5590	3100,5488	0,0102	0,02
RR 3,21	3101,2000	3101,1908	0,0092	0,00

ASSIGN.	OBS. FREQ.	CALC. FREQ.	RESID.	WHT.
RR 3,22	3101.8420	3101.8328	0.0092	0.01
RR 3,23	3102.4830	3102.4750	0.0080	0.01
RR 3,24	3103.1280	3103.1173	0.0107	0.02
RR 3,25	3103.7730	3103.7597	0.0133	0.02
RR 3,27	3105.0590	3105.0448	0.0142	0.01
RR 3,28	3105.7050	3105.6875	0.0175	0.01
RR 3,29	3106.3490	3106.3302	0.0188	0.02
RR 3,30	3106.9910	3106.9730	0.0180	0.02
RR 3,31	3107.6340	3107.6159	0.0181	0.02
RP 3, 5	3083.9430	3083.9308	0.0122	0.00
RP 3, 6	3083.2880	3083.2954	-0.0074	0.00
RP 3, 7	3082.6430	3082.6604	-0.0174	0.01
RP 3, 8	3082.0250	3082.0257	-0.0007	0.05
RP 3, 9	3081.3980	3081.3914	0.0066	0.01
RP 3,11	3080.1260	3080.1240	0.0020	0.00
RP 3,12	3079.4850	3079.4909	-0.0059	0.00
RR 4, 4	3099.0380	3099.0376	0.0004	0.14
RR 4, 5	3099.6740	3099.6762	-0.0022	0.10
RR 4, 6	3100.3160	3100.3151	0.0009	0.07
RR 4, 7	3100.9540	3100.9541	-0.0001	0.30
RR 4, 8	3101.5960	3101.5934	0.0026	0.07
RR 4, 9	3102.2350	3102.2329	0.0021	0.14
RR 4,10	3102.8750	3102.8726	0.0024	0.12
RR 4,11	3103.5150	3103.5125	0.0025	0.07
RR 4,12	3104.1560	3104.1526	0.0034	0.12
RR 4,14	3105.4410	3105.4334	0.0076	0.05
RR 4,15	3106.0850	3106.0741	0.0109	0.02
RR 4,17	3107.3570	3107.3558	0.0012	0.02
RR 4,18	3108.0030	3107.9969	0.0061	0.02
RR 4,19	3108.6500	3108.6382	0.0118	0.05
RR 4,20	3109.2930	3109.2795	0.0135	0.01
RR 4,21	3109.9320	3109.9210	0.0110	0.01
RR 4,22	3110.5670	3110.5626	0.0044	0.00
RR 4,23	3111.2270	3111.2044	0.0226	0.00
RR 4,24	3111.8580	3111.8462	0.0118	0.01
RR 4,25	3112.5030	3112.4881	0.0149	0.01
RR 4,27	3113.7910	3113.7721	0.0189	0.02
RR 4,28	3114.4330	3114.4142	0.0188	0.01
RR 4,29	3115.0730	3115.0564	0.0166	0.01
RR 4,30	3115.7190	3115.6986	0.0204	0.01
RR 4,31	3116.3690	3116.3409	0.0281	0.02
RR 4,32	3117.0090	3116.9832	0.0258	0.02
RR 5, 5	3108.3330	3108.3439	-0.0109	0.07
RR 5, 6	3108.9720	3108.9826	-0.0106	1.00
RR 5, 7	3109.6160	3109.6214	-0.0054	1.00
RR 5, 8	3110.2520	3110.2605	-0.0085	1.00
RR 5, 9	3110.8950	3110.8997	-0.0047	0.40
RR 5,10	3111.5340	3111.5392	-0.0052	0.40
RR 5,11	3112.1750	3112.1788	-0.0038	0.14
RR 5,12	3112.8200	3112.8186	0.0014	0.12
RR 5,14	3114.1000	3114.0987	0.0013	0.05
RR 5,15	3114.7380	3114.7390	-0.0010	0.01

ASSIGN.	OBS. FREQ.	CALC. FREQ.	RESID.	WHT.
RR 5,17	3116.0190	3116.0200	-0.0010	0.01
RR 5,18	3116.6600	3116.6607	-0.0007	0.01
RR 5,19	3117.2900	3117.3016	-0.0116	0.00
RR 5,20	3117.9340	3117.9425	-0.0085	0.00
RR 5,21	3118.5760	3118.5835	-0.0075	0.01
RR 5,22	3119.2110	3119.2247	-0.0137	0.01
RR 5,23	3119.8480	3119.8659	-0.0179	0.00
RR 5,24	3120.4780	3120.5072	-0.0292	0.00
RR 5,25	3121.1160	3121.1486	-0.0326	0.00
RR 6, 6	3117.5850	3117.5801	0.0049	1.00
RR 6, 7	3118.2220	3118.2187	0.0033	0.40
RR 6, 8	3118.8610	3118.8575	0.0035	0.40
RR 6, 9	3119.5010	3119.4965	0.0045	0.40
RR 6,10	3120.1420	3120.1357	0.0063	0.40
RR 6,11	3120.7780	3120.7750	0.0030	0.40
RR 6,12	3121.4160	3121.4145	0.0015	0.40
RR 6,13	3122.0550	3122.0542	0.0008	0.40
RR 6,14	3122.6970	3122.6940	0.0030	1.00
RR 6,15	3123.3360	3123.3339	0.0021	0.40
RR 6,16	3123.9730	3123.9739	-0.0009	0.25
RR 6,17	3124.6150	3124.6141	0.0009	0.14
RR 6,18	3125.2560	3125.2544	0.0016	0.14
RR 6,19	3125.9000	3125.8948	0.0052	0.07
RR 6,20	3126.5410	3126.5353	0.0057	0.05
RR 6,21	3127.1860	3127.1758	0.0102	0.02
RR 6,22	3127.8200	3127.8165	0.0035	0.02
RR 6,23	3128.4640	3128.4572	0.0068	0.02
RR 6,24	3129.1010	3129.0980	0.0030	0.02
RR 6,25	3129.7450	3129.7388	0.0062	0.01
RR 6,27	3131.0300	3131.0206	0.0094	0.01
RR 6,28	3131.6700	3131.6616	0.0084	0.01
RR 6,29	3132.3110	3132.3026	0.0084	0.01
RR 6,30	3132.9580	3132.9436	0.0144	0.00
RR 6,31	3133.5960	3133.5846	0.0114	0.00
RR 6,32	3134.2270	3134.2256	0.0014	0.01
RR 6,33	3134.8730	3134.8666	0.0064	0.00
RR 6,34	3135.5230	3135.5076	0.0154	0.00
RR 6,35	3136.1570	3136.1485	0.0085	0.01
RR 6,36	3136.7960	3136.7895	0.0065	0.01
RR 6,37	3137.4410	3137.4303	0.0107	0.01
RR 6,38	3138.0800	3138.0712	0.0088	0.00
RR 6,40	3139.3630	3139.3527	0.0103	0.01
RR 6,41	3140.0050	3139.9933	0.0117	0.01
RR 7, 7	3126.7420	3126.7436	-0.0016	0.07
RR 7, 8	3127.3770	3127.3822	-0.0052	0.03
RR 7, 9	3128.0190	3128.0209	-0.0019	0.30
RR 7,10	3128.6580	3128.6597	-0.0017	0.10
RR 7,12	3129.9380	3129.9379	0.0001	0.14
RR 7,13	3130.5750	3130.5772	-0.0022	0.12
RR 7,14	3131.2200	3131.2166	0.0034	0.04
RR 7,15	3131.8600	3131.8562	0.0038	0.07
RR 7,16	3132.4990	3132.4958	0.0032	0.04

ASSIGN.	OBS. FREQ.	CALC. FREQ.	RESID.	WHT.
RR 7,17	3133.1360	3133,1356	0,0004	0.01
RR 7,18	3133.7820	3133,7754	0,0066	0.02
RR 7,19	3134.4210	3134,4154	0,0056	0.02
RR 7,20	3135.0600	3135,0554	0,0046	0.02
RR 7,21	3135.7070	3135,6955	0,0115	0.02
RR 7,22	3136.3460	3136,3356	0,0104	0.01
RR 7,23	3136.9890	3136,9758	0,0132	0.01
RR 7,24	3137.6290	3137,6161	0,0129	0.01
RR 7,25	3138.2780	3138,2563	0,0217	0.00
RR 7,26	3138.8970	3138,8967	0,0003	0.00
RR 7,27	3139.5570	3139,5370	0,0200	0.00
RR 8, 8	3135.8280	3135,8321	-0,0041	0.12
RR 8, 9	3136.4690	3136,4705	-0,0015	0.12
RR 8,10	3137.1070	3137,1091	-0,0021	0.07
RR 8,11	3137.7470	3137,7477	-0,0007	0.07
RR 8,12	3138.3900	3138,3866	0,0034	0.07
RR 8,13	3139.0260	3139,0255	0,0005	0.07
RR 8,14	3139.6650	3139,6645	0,0005	0.12
RR 8,15	3140.3080	3140,3037	0,0043	0.07
RR 8,16	3140.9450	3140,9429	0,0021	0.04
RR 8,17	3141.5840	3141,5822	0,0018	0.01
RR 8,18	3142.2270	3142,2216	0,0054	0.01
RR 8,19	3142.8630	3142,8611	0,0019	0.01
RR 8,20	3143.5010	3143,5006	0,0004	0.01
RR 8,21	3144.1420	3144,1402	0,0018	0.00
RR 9, 9	3144.8390	3144,8434	-0,0044	0.05
RR 9,10	3145.4770	3145,4816	-0,0046	0.10
RR 9,11	3146.1170	3146,1199	-0,0029	0.10
RR 9,13	3147.3950	3147,3969	-0,0019	0.25
RR 9,14	3148.0320	3148,0356	-0,0036	0.25
RR 9,15	3148.6710	3148,6743	-0,0033	0.14
RR 9,16	3149.3090	3149,3131	-0,0041	0.12
RR 9,17	3149.9490	3149,9519	-0,0029	0.12
RR 9,18	3150.5940	3150,5909	0,0031	0.12
RR 9,19	3151.2310	3151,2299	0,0011	0.12
RR 9,20	3151.8720	3151,8689	0,0031	0.12
RR 9,22	3153.1520	3153,1470	0,0050	0.05
RR 9,23	3153.7880	3153,7861	0,0019	0.05
RR 9,24	3154.4270	3154,4253	0,0017	0.05
RR 9,26	3155.7030	3155,7035	-0,0005	0.05
RR 9,27	3156.3470	3156,3426	0,0044	0.01
RR 9,28	3156.9840	3156,9817	0,0023	0.01
RR 9,29	3157.6190	3157,6208	-0,0018	0.01
RR 9,30	3158.3580	3158,2598	0,0982	0.00
RR11,11	3162.6410	3162,6273	0,0137	0.01
RR11,13	3163.9090	3163,9027	0,0063	0.01
RR11,14	3164.5440	3164,5405	0,0035	0.01
RR11,15	3165.1960	3165,1783	0,0177	0.00
RR11,16	3165.8280	3165,8162	0,0118	0.01
RR11,17	3166.4680	3166,4541	0,0139	0.00
RR12,12	3171.3920	3171,3975	-0,0055	0.02
RR12,13	3172.0380	3172,0348	0,0032	0.02

ASSIGN.	OBS. FREQ.	CALC. FREQ.	RESID.	WHT.
RR12,14	3172.6740	3172,6722	0,0018	0.02
RR12,15	3173.3110	3173.3095	0,0015	0.01
RR12,16	3173.9470	3173,9469	0,0001	0.02
RR12,17	3174.5900	3174,5843	0,0057	0.01
RR12,18	3175.2260	3175,2217	0,0043	0.00
RR12,19	3175.8630	3175,8592	0,0038	0.00
QP 3, 4	6043.0770	6043,0655	0,0115	0.07
QP 3, 6	6041.8130	6041,7982	0,0148	0.07
QP 3, 7	6041.1840	6041,1658	0,0182	0.17
QP 3, 8	6040.5660	6040,5341	0,0319	0.07
QP 3, 9	6039.9120	6039,9032	0,0088	0,67
QP 3,10	6039.2780	6039,2731	0,0049	0.40
QP 3,11	6038.6410	6038,6439	-0,0029	0,67
QP 3,12	6038.0220	6038,0154	0,0066	0,03
QP 3,13	6037.3800	6037,3878	-0,0078	0.67
QP 3,14	6037.7400	6036,7610	0,9790	0,00
QP 3,14	6036.7470	6036,7610	-0,0140	0.17
QP 3,15	6036.1210	6036,1351	-0,0141	0,00
QP 3,16	6035.4950	6035.5100	-0,0150	0,00
QP 2, 5	6042.7490	6042,7202	0,0288	0,07
QP 2, 6	6042.1020	6042,0870	0,0150	0,07
QP 2, 7	6041.4820	6041,4544	0,0276	0,07
QP 2, 8	6040.8350	6040,8227	0,0123	0,07
QP 2, 9	6040.2040	6040,1918	0,0122	0,07
QP 2,10	6039.5660	6039,5617	0,0043	0,07
QP 2,11	6038.9390	6038,9324	0,0066	0,07
QP 2,12	6038.3140	6038,3039	0,0101	0,03
QP 2,13	6037.6750	6037,6762	-0,0012	0,07
QP 2,14	6037.0470	6037,0494	-0,0024	0,07
QR 3, 3	6048.1670	6048,1645	0,0025	0,03
QR 3, 4	6048.8200	6048,8051	0,0149	0,01
QR 3, 5	6049.4580	6049,4464	0,0116	0,03
QR 3, 6	6050.0980	6050,0884	0,0096	0,07
QR 3, 7	6050,7280	6050,7311	-0,0031	0,07
QR 3, 8	6051.3800	6051,3744	0,0056	0,17
QR 3, 9	6052.0220	6052,0184	0,0036	0,17
QR 3,10	6052,6600	6052,6631	-0,0031	0,67
QR 3,11	6053,3040	6053,3084	-0,0044	0,67
QR 3,12	6053,9410	6053,9543	-0,0133	0,67
QR 3,13	6054,5980	6054,6008	-0,0028	0,67
PP 1, 3	6088,6610	6088,6590	0,0020	0,01
PP 1, 4	6088,0160	6088,0242	-0,0082	0,05
PP 1, 5	6087,3800	6087,3902	-0,0102	0,01
PP 1, 6	6086,7450	6086,7569	-0,0119	0,00
PP 1, 7	6086,1180	6086,1244	-0,0064	0,00
PP 1, 8	6085,4730	6085,4927	-0,0197	0,00
PP 1, 9	6084,8450	6084,8618	-0,0168	0,01
PP 1,11	6083,5880	6083,6025	-0,0145	0,00
PP 1,12	6082,9650	6082,9741	-0,0091	0,01
PP 1,13	6082,3520	6082,3465	0,0055	0,05
PP 1,14	6081,7050	6081,7198	-0,0148	0,05
PP 1,15	6081.0910	6081,0939	-0,0029	0,01

ASSIGN.	OBS. FREQ.	CALC. FREQ.	RESID.	WHT.
PP 1,19	6078.5730	6078,5991	-0,0261	0.00
PP 1,20	6077.9730	6077,9776	-0,0046	0.10
PP 1,21	6077.3530	6077,3570	-0,0040	0.10
PP 1,25	6074.8820	6074,8838	-0,0018	0.00
PP 1,26	6074.1830	6074,2679	-0,0849	0.00
PP 1,27	6073.5430	6073,6528	-0,1098	0.00
RP 0, 1	6100.6890	6100,7148	-0,0258	0.00
RP 0, 2	6100.0590	6100,0784	-0,0194	0.00
RP 0, 3	6099.4450	6099,4428	0,0022	0.01
RP 0, 4	6098.8090	6098,8079	0,0011	0.01
RP 0, 5	6098.1780	6098,1738	0,0042	0.01
RP 0, 6	6097.5640	6097,5404	0,0236	0.00
RP 0, 7	6096.9310	6096,9078	0,0232	0.00
RP 0, 8	6096.3040	6096,2760	0,0280	0.00
RP 0, 9	6095.6560	6095,6450	0,0110	0.01
RP 0,10	6095.0250	6095,0147	0,0103	0.05
RP 0,11	6094.3950	6094,3853	0,0097	0.05
RP 0,12	6093.7660	6093,7567	0,0093	0.05
RP 0,13	6093.1400	6093,1289	0,0111	0.05
RP 0,14	6092.5170	6092,5019	0,0151	0.10
RP 0,15	6091.8860	6091,8758	0,0102	0.10
RP 0,16	6091.2520	6091,2505	0,0015	0.05
RP 0,18	6090.0000	6090,0025	-0,0025	0.10
RP 0,19	6089.3850	6089,3798	0,0052	0.01
RP 0,20	6088.7590	6088,7580	0,0010	0.05
RP 0,21	6088.1290	6088,1371	-0,0081	0.05
RP 0,22	6087.5190	6087,5170	0,0020	0.01
RP 0,23	6086.9030	6086,8979	0,0051	0.01
RP 0,24	6086.2810	6086,2796	0,0014	0.05
RP 0,25	6085.6740	6085,6623	0,0117	0.05
RP 0,26	6085.0590	6085,0459	0,0131	0.01
RP 0,27	6084.4370	6084,4304	0,0066	0.01
RR 0, 1	6102.5750	6102,6283	-0,0533	0.00
RR 0, 2	6103.2530	6103,2675	-0,0145	0.00
RR 0, 3	6103.9030	6103,9075	-0,0045	0.01
RR 0, 4	6104.5470	6104,5481	-0,0011	0.01
RR 0, 5	6105.1870	6105,1895	-0,0025	0.05
RR 0, 6	6105.8290	6105,8315	-0,0025	0.05
RR 0, 7	6106.4770	6106,4741	0,0029	0.25
RR 0, 8	6107.1170	6107,1175	-0,0005	0.10
RR 0, 9	6107.7590	6107,7615	-0,0025	0.05
RR 0,10	6108.4030	6108,4061	-0,0031	0.10
RR 0,11	6109.0490	6109,0514	-0,0024	0.10
RR 0,12	6109.6980	6109,6973	0,0007	0.10
RR 0,13	6110.3520	6110,3438	0,0082	0.10
RR 0,14	6110.9960	6110,9909	0,0051	0.10
RR 0,15	6111.6540	6111,6387	0,0153	0.00
RR 0,17	6112.9460	6112,9359	0,0101	0.01
RR 0,18	6113.5970	6113,5854	0,0116	0.00
RR 0,19	6114.2430	6114,2355	0,0075	0.00
RR 0,20	6114.8950	6114,8861	0,0089	0.00
RR 0,23	6116.8560	6116,8413	0,0147	0.01

ASSIGN.	OBS. FREQ.	CALC. FREQ.	RESID.	WHT.
RR 0,24	6117.5100	6117,4941	0,0159	0,01
RR 0,25	6118.1630	6118,1475	0,0155	0,01
RR 0,26	6118.8100	6118,8013	0,0087	0,01
RR 0,27	6119.4760	6119,4557	0,0203	0,00
PR 1,18	6102,7830	6102,8047	-0,0217	0,05
PR 1,19	6103,4290	6103,4551	-0,0261	0,01
PR 1,20	6104,0990	6104,1061	-0,0071	0,00
PR 1,21	6104.7630	6104,7576	0,0054	0,01
RR 1, 1	6113,2980	6113,2974	0,0006	0,10
RR 1, 2	6113.9400	6113,9366	0,0034	0,05
RR 1, 3	6114.5850	6114,5764	0,0086	0,00
RR 1, 4	6115,2250	6115,2170	0,0080	0,00
RR 1, 5	6115.8530	6115,8582	-0,0052	0,01
RR 1, 6	6116.5020	6116,5001	0,0019	0,01
RR 1, 7	6117.1460	6117,1426	0,0034	0,10
RR 1, 8	6117,7920	6117,7858	0,0062	0,10
RR 1,10	6119.1150	6119,0740	0,0410	0,00
RR 1,11	6119,7480	6119,7191	0,0289	0,00
RR 1,12	6120.3850	6120,3648	0,0202	0,00
RR 1,13	6121,0210	6121,0110	0,0100	0,10
RR 1,14	6121.6540	6121,6579	-0,0039	0,10
RR 1,15	6122.2980	6122,3054	-0,0074	0,10
RP 3, 9	6127.3180	6127,3028	0,0152	0,05
RP 3,10	6126.6900	6126,6721	0,0179	0,01
RP 3,11	6126,0310	6126,0423	-0,0113	0,01
RP 3,13	6124.7820	6124,7849	-0,0029	0,00
RP 3,14	6124.1450	6124,1573	-0,0123	0,01
RR 2, 2	6124.4900	6124,4899	0,0001	0,10
RR 2, 3	6125.1330	6125,1297	0,0033	0,10
RR 2, 4	6125.7710	6125,7701	0,0009	0,05
RR 2, 5	6126.4050	6126,4112	-0,0062	0,05
RR 2, 6	6127,0450	6127,0530	-0,0080	0,10
RR 2, 7	6127.6890	6127,6953	-0,0063	0,05
RR 2, 8	6128.3340	6128,3383	-0,0043	0,10
RR 2, 9	6128.9810	6128,9819	-0,0009	0,05
RR 2,10	6129.6250	6129,6262	-0,0012	0,10
RR 2,11	6130.2720	6130,2710	0,0010	0,05
RR 2,12	6130.9110	6130,9164	-0,0054	0,05
RR 2,13	6131.5600	6131,5624	-0,0024	0,10
RR 2,14	6132.2030	6132,2090	-0,0060	0,05
RR 2,15	6132.8540	6132,8562	-0,0022	0,01
RR 2,17	6134.1440	6134,1521	-0,0081	0,01
RR 2,18	6134.7810	6134.8010	-0,0200	0,01
RR 2,19	6135,4410	6135,4503	-0,0093	0,01
RR 2,20	6136,0850	6136,1002	-0,0152	0,01
RR 3, 3	6135.5720	6135,5656	0,0064	1,00
RR 3, 4	6136,2070	6136,2059	0,0011	1,00
RR 3, 5	6136.8440	6136,8469	-0,0029	1,00
RR 3, 6	6137,4920	6137,4884	0,0036	1,00
RR 3, 7	6138.1340	6138,1306	0,0034	1,00
RR 3, 8	6138,7710	6138,7734	-0,0024	1,00
RR 3, 9	6139,4110	6139,4168	-0,0058	1,00

ASSIGN.	OBS. FREQ.	CALC. FREQ.	RESID.	WHT.
RR 3,10	6140.0570	6140,0608	-0,0038	1,00
RR 3,11	6140.6930	6140,7054	-0,0124	0,25
RR 3,12	6141.3490	6141,3505	-0,0015	1,00
RR 3,13	6141.9990	6141,9963	0,0027	1,00
RR 3,14	6142.6410	6142,6426	-0,0016	1,00
RR 3,16	6143.9250	6143,9368	-0,0118	0,01
RR 3,17	6144.5850	6144,5847	0,0003	0,05
RR 3,18	6145.2350	6145,2331	0,0019	0,05
RR 3,19	6145.8740	6145,8821	-0,0081	0,05
RR 3,20	6146.5310	6146,5316	-0,0006	0,05
RR 3,21	6147.1770	6147,1816	-0,0046	0,05
RR 3,22	6147.8200	6147,8321	-0,0121	0,05
RR 3,23	6148.4690	6148,4831	-0,0141	0,05
RR 3,24	6149.1340	6149,1345	-0,0005	0,01
RR 3,25	6149.7780	6149,7864	-0,0084	0,01
RR 3,26	6150.4100	6150,4388	-0,0288	0,01
RR 3,27	6151.0960	6151,0917	0,0043	0,01
RR 3,28	6151.7600	6151,7450	0,0150	0,01
RR 3,29	6152.3950	6152,3987	-0,0037	0,01
RR 3,30	6153.0600	6153,0529	0,0071	0,01
RR 3,32	6154.3800	6154,3625	0,0175	0,01
RR 3,33	6155.0240	6155,0180	0,0060	0,01
RR 4,10	6150.3840	6150,3757	0,0083	0,01
RR 4,11	6151.0260	6151,0201	0,0059	0,01
RR 4,12	6151.6840	6151,6649	0,0191	0,01
RR 4,13	6152.3120	6152,3104	0,0016	0,01
RR 4,14	6152.9750	6152,9563	0,0187	0,01
RR 4,17	6154.9090	6154,8974	0,0116	0,01
RR 4,18	6155.5470	6155,5455	0,0015	0,01
RR 4,19	6156.1880	6156,1940	-0,0060	0,01
RR 4,20	6156.8260	6156,8431	-0,0171	0,01
RR 5, 5	6157.3550	6157,3565	-0,0015	0,25
RR 5, 6	6157.9960	6157,9977	-0,0017	0,25
RR 5, 7	6158.6360	6158,6395	-0,0035	0,25
RR 5, 8	6159.2790	6159,2818	-0,0028	0,05
RR 5, 9	6159.9260	6159,9248	0,0012	0,10
RR 5,10	6160.5610	6160,5682	-0,0072	0,10
RR 5,11	6161.2110	6161,2123	-0,0013	0,10
RR 5,12	6161.8530	6161,8568	-0,0038	0,10
RR 5,13	6162.4990	6162,5019	-0,0029	0,05
RR 5,14	6163.1460	6163,1476	-0,0016	0,01
RR 5,16	6164.4280	6164,4404	-0,0124	0,05
RR 5,17	6165.0840	6165,0876	-0,0036	0,05
RR 5,18	6165.7270	6165,7352	-0,0082	0,01
RR 5,19	6166.3730	6166,3834	-0,0104	0,01
RR 5,20	6167.0200	6167,0320	-0,0120	0,01
RR 5,23	6168.9670	6168,9807	-0,0137	0,00
RR 6, 6	6168.0820	6168,0656	0,0164	0,01
RR 6, 7	6168.7190	6168,7072	0,0118	1,00
RR 6, 8	6169.3600	6169,3493	0,0107	0,10
RR 6, 9	6169.9960	6169,9920	0,0040	0,25
RR 6,10	6170.6350	6170,6351	-0,0001	1,00

ASSIGN.	OBS. FREQ.	CALC. FREQ.	RESID.	WHT.
RR 6,11	6171.2820	6171.2789	0.0031	1.00
RR 6,12	6171.9230	6171.9231	-0.0001	1.00
RR 6,13	6172.5630	6172.5679	-0.0049	0.10
RR 6,14	6173.2240	6173.2132	0.0108	0.25
RR 6,16	6174.4930	6174.5053	-0.0123	0.25
RR 6,17	6175.1270	6175.1520	-0.0250	0.10
RR 6,18	6175.8050	6175.7993	0.0057	0.05
RR 6,19	6176.4450	6176.4470	-0.0020	0.05
RR 6,20	6177.0950	6177.0952	-0.0002	0.05
RR 6,21	6177.7370	6177.7438	-0.0068	0.05
RR 6,22	6178.3940	6178.3929	0.0011	0.05
RR 6,23	6179.0420	6179.0424	-0.0004	0.05
RR 6,24	6179.6890	6179.6923	-0.0033	0.05
RR 6,25	6180.3220	6180.3427	-0.0207	0.01
RR 6,26	6180.9920	6180.9935	-0.0015	0.01
RR 6,29	6182.9360	6182.9482	-0.0122	0.01
RR 8, 8	6189.0700	6189.0935	-0.0235	0.10
RR 8, 9	6189.7100	6189.7355	-0.0255	0.05
RR 8,10	6190.3530	6190.3781	-0.0251	0.05
RR 8,11	6191.0020	6191.0212	-0.0192	0.05
RR 8,12	6191.6400	6191.6648	-0.0248	0.05
RR 8,13	6192.2790	6192.3088	-0.0298	0.01
RR 8,14	6192.9380	6192.9534	-0.0154	0.01
RR 8,16	6194.2320	6194.2438	-0.0118	0.01
RR 8,17	6194.8760	6194.8897	-0.0137	0.01
RR 8,18	6195.5080	6195.5361	-0.0281	0.01
RR 8,19	6196.1630	6196.1829	-0.0199	0.01
RR 8,20	6196.8090	6196.8301	-0.0211	0.01
RR 8,21	6197.4490	6197.4778	-0.0288	0.01
RR 8,22	6198.1020	6198.1258	-0.0238	0.01
RR 8,23	6198.7270	6198.7743	-0.0473	0.00
RR 9, 9	6199.4110	6199.4043	0.0067	0.25
RR 9,10	6200.0520	6200.0466	0.0054	0.10
RR 9,11	6200.6930	6200.6893	0.0037	0.10
RR 9,12	6201.3410	6201.3325	0.0085	0.05
RR 9,13	6201.9810	6201.9762	0.0048	0.05
RR 9,15	6203.2680	6203.2649	0.0031	0.05
RR 9,16	6203.9110	6203.9099	0.0011	0.05
RR 9,17	6204.5600	6204.5554	0.0046	0.05
RR 9,18	6205.1990	6205.2013	-0.0023	0.05
RR 9,19	6205.8510	6205.8476	0.0034	0.01
RR 9,20	6206.4990	6206.4943	0.0047	0.01
PP 9, 9	5994.9450	5994.3129	0.6321	0.00
PP 9,10	5994.3140	5993.6847	0.6293	0.00
PP 9,11	5993.6520	5993.0575	0.5945	0.00
PP 9,14	5991.7920	5991.1818	0.6102	0.00
PP 9,15	5991.1400	5990.5585	0.5815	0.00
PP 8, 8	6007.0770	6006.7114	0.3656	0.00
PP 8, 9	6006.5160	6006.0820	0.4340	0.00
PP 8,10	6005.8850	6005.4536	0.4314	0.00
PP 8,11	6005.2980	6004.8261	0.4719	0.00
PP 8,12	6004.6420	6004.1995	0.4425	0.00